Ontario

We are committed to providing accessible customer service.
If you need accessible formats or communications supports, please contact us.

Nous tenons à améliorer l’accessibilité des services à la clientèle.
Si vous avez besoin de formats accessibles ou d’aide à la communication, veuillez nous contacter.

2022 Jean Property Prospecting Report

Jean Township, Thunder Bay District,

Ontario Canada NTS 52B/08SE

(UTM Nad83 Zone 15)

714874E, 5349254N

Prepared by: Andrew Tims PGeo,

September 15, 2022

Table of Contents

List of Figures

List of Tables

1.0 Summary

Andrew Tims was retained by Mantra Exploration Inc. (“the Company”) to commission an airborne magnetic survey on the Jean Property (“the Property”) and to ground-truth any anomalous magnetic trends on the claim cells staked in early 2022.

The Jean Property consists of 95 claim cells covering 2,058 hectares located in Thunder Bay Mining District of Northwestern Ontario, Canada. The Property is located about 65 kilometers to the southwest of Thunder Bay and can be accessed by secondary highways from the Trans-Canada Highway 11/17. A network of gravel roads and trails traverse the mineral claims and areas of rock exposures.

The Jean Property area is underlain by an Archean granitic basement, which is unconformably overlain by gently southerly-dipping sedimentary rocks of the Aphebian (lower Proterozoic) Animikie group. These sediments are capped by a Helikian (1.0 Ga) Keweenawan diabase sill. Gunflint Iron formation of Animikie Group is part of extensive Lake Superior-type iron formation (LSTIF) ranges developed along the margins of cratons or epicontinental platforms between 2.4 Ga and 1.9 Ga. It is banded iron formation (BIF) mainly comprised of taconite rocks, and is characterized by unusually high iron content.

During the month of December 2021 Mantra expanded the property by acquiring 31 additional claim cells along the property’s northern and eastern boundary. Mantra completed a high-resolution aeromagnetic gradiometer- digital VLF-EM survey over the claim block in July of 2022. The fixed wing survey covered 246 line-km focusing primarily on the new claims but overlapping onto the western claims that were worked by Great Lake Resources in 2012.

Prospecting activities collected a total of 11 rock samples. Mapping indicates that the new claim cells along the northern boundary are underlain by an Archean granitic basement with substantial fluvial-glacial cover. Algal chert and jasper outcrops are found to be more resistant to weathering and exposed at places along road cuts were also helpful in locating Taconite and shale outcrops. The work verified historical results as well as evaluated the iron potential of the newly acquired cells. Assay on the new claim cells produced iron content between 19 and 31% indicating good potential to develop a resource.

2.0 Introduction

This report presents and summarizes the results of and airborne geophysical survey and follow-on outcrop mapping and sampling on the Jean property between July 20 and August 5th, 2022. .

3.0 Property Description and Location

The Jean Property has good year-round road access from the town of Thunder Bay, Ontario. Highway 588, located immediately to the south of the Property is a paved all-season road (Figure 1). The Property can be accessed via the Trans-Canada Highway 11/17, about 20 km west from the Highway 61 junction to Highway 588 (Stanley access), and then a further 45 km southwest along Highway 588. Travel time by road from Thunder Bay to the Property is approximately one hour. A network of gravel roads and trails traverse the mineral claims and provide access to various areas of the Property. The approximate UTM co-ordinates for the centre of the property is 714874E, 5349254N (NAD83 Zone 15) on NTS map sheets 52B/08SE.

The maximum relief in the area is about 110 metres (from 470 m to 580 m above sea level). Topography is generally flat with the exception of hills located in the southern part of the Property and were formed due to the presence of diabase sill rocks that has resisted erosion and now stands above the surrounding flat lying terrain in the form of large round mesas such as Mink Mountain and Sun Hill (Figures 2 and 4).

Exposures of iron-bearing rocks are scarce in the low-lying country adjoining streams and lakes because of drift cover. Beneath the diabase capping of hills and ridges, however, the rocks are well exposed. The property has an active MNDM exploration permit: PR-20-000085

4.0 Claims and Ownership

The Jean Property consists of 95 claim cells covering 2,058 hectares land located in Thunder Bay Mining District of Northwestern Ontario, Canada (Figure 1 and 2).

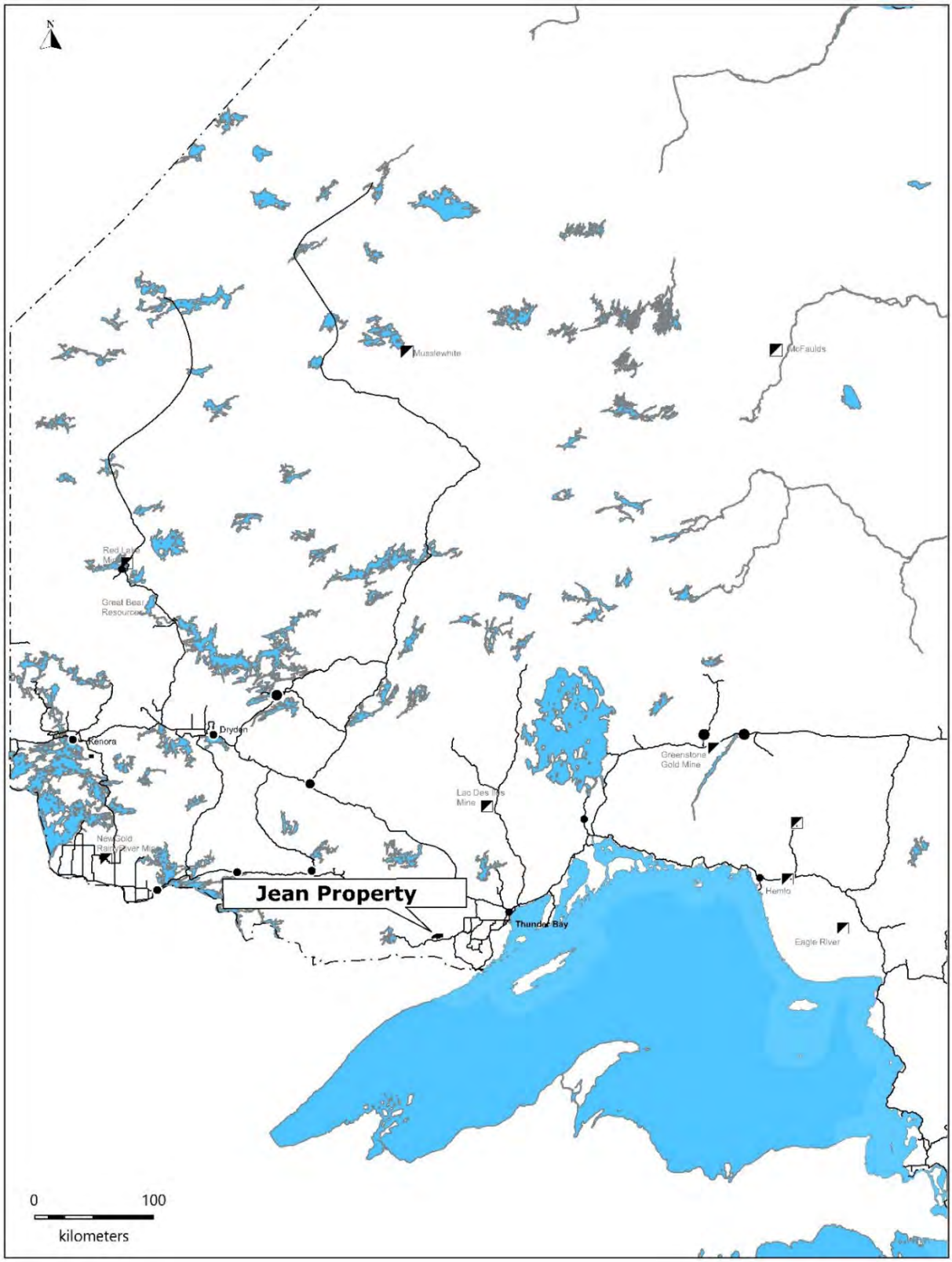

Figure 1. Jean property location

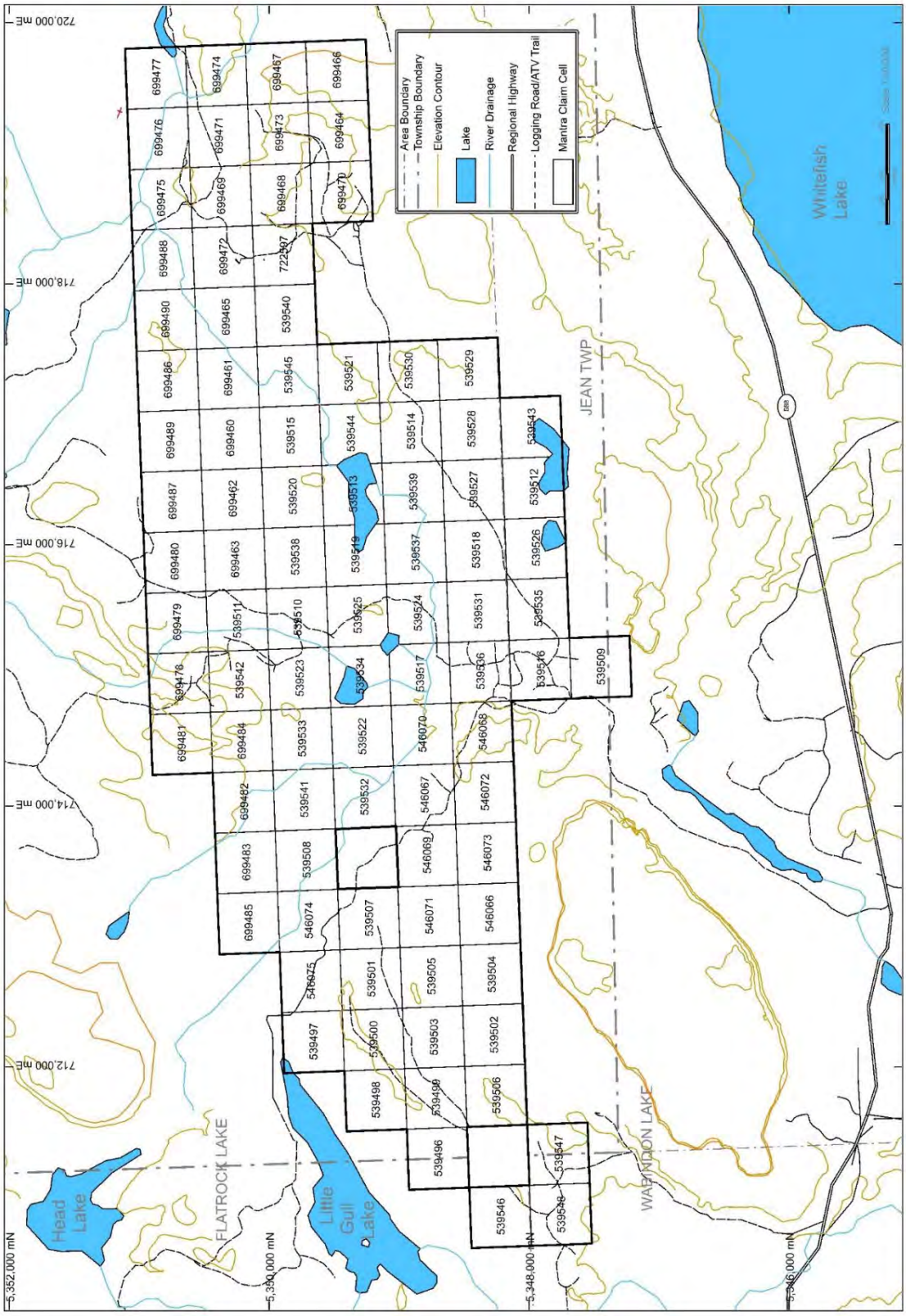

Figure 2. Jean property claim map.

The Property is located about 65 kilometers to the southwest of Thunder Bay, approximately 2 kilometers north of the Whitefish Lake on Highway 588. Mantra Exploration Inc. which changed its name to Great Lakes Resources Ltd. (“Great Lakes”) owns 100 % of the Mineral Claims.

The original 18 claims covered by the 2016 technical report were converted to 53 claim cells in April of 2018 under the Mining Lands Information System through the Ontario governments’ Modernizing the Mining Act endeavour. The new claim cells were transferred from AsiaBaseMetals Inc. to Mantra Exploration Inc in September of 2020. The property was enlarged by 41 additional claim cells in March of 2020. A single cell was added to the property in May of 2022.

Table 1. Jean property claim list

Tenure ID	Township	Tenure Type	Anniversary Date	Tenure Status	Tenure %	Work Required	Work Applied	Available Consultation Reserve	Total Reserve
539496	FLATROCK LAKE ,JEAN	Single Cell	2022-01-18	Active	100	400	0	0	0
539497	JEAN	Single Cell	2022-01-18	Active	100	400	0	0	0
539498	JEAN	Single Cell	2022-01-18	Active	100	400	0	0	0
539499	JEAN	Single Cell	2022-01-18	Active	100	400	0	0	0
539500	JEAN	Single Cell	2022-01-18	Active	100	400	0	0	0
539501	JEAN	Single Cell	2022-01-18	Active	100	400	0	0	0
539502	JEAN	Single Cell	2022-01-18	Active	100	400	0	0	0
539503	JEAN	Single Cell	2022-01-18	Active	100	400	0	0	0
539504	JEAN	Single Cell	2022-01-18	Active	100	400	0	0	0
539505	JEAN	Single Cell	2022-01-18	Active	100	400	0	0	0
539506	JEAN	Single Cell	2022-01-18	Active	100	400	0	0	0
539507	JEAN	Single Cell	2022-01-18	Active	100	400	0	0	0
539508	JEAN	Single Cell	2022-01-18	Active	100	400	0	0	0
539509	JEAN	Single Cell	2022-01-18	Active	100	400	0	0	0
539510	JEAN	Single Cell	2022-01-18	Active	100	400	0	0	0
539511	JEAN	Single Cell	2022-01-18	Active	100	400	0	0	0
539512	JEAN	Single Cell	2022-01-18	Active	100	400	0	0	0
539513	JEAN	Single Cell	2022-01-18	Active	100	400	0	0	0
539514	JEAN	Single Cell	2022-01-18	Active	100	400	0	0	0
539515	JEAN	Single Cell	2022-01-18	Active	100	400	0	0	0
539516	JEAN	Single Cell	2022-01-18	Active	100	400	0	0	0
539517	JEAN	Single Cell	2022-01-18	Active	100	400	0	0	0
539518	JEAN	Single Cell	2022-01-18	Active	100	400	0	0	0
539519	JEAN	Single Cell	2022-01-18	Active	100	400	0	0	0
539520	JEAN	Single Cell	2022-01-18	Active	100	400	0	0	0
539521	JEAN	Single Cell	2022-01-18	Active	100	400	0	0	0

Tenure ID	Township	Tenure Type	Anniversary Date	Tenure Status	Tenure %	Work Required	Work Applied	Available Consultation Reserve	Total Reserve
539522	JEAN	Single Cell	2022-01-18	Active	100	400	0	0	0
539523	JEAN	Single Cell	2022-01-18	Active	100	400	0	0	0
539524	JEAN	Single Cell	2022-01-18	Active	100	400	0	0	0
539525	JEAN	Single Cell	2022-01-18	Active	100	400	0	0	0
539526	JEAN	Single Cell	2022-01-18	Active	100	400	0	0	0
539527	JEAN	Single Cell	2022-01-18	Active	100	400	0	0	0
539528	JEAN	Single Cell	2022-01-18	Active	100	400	0	0	0
539529	JEAN	Single Cell	2022-01-18	Active	100	400	0	0	0
539530	JEAN	Single Cell	2022-01-18	Active	100	400	0	0	0
539531	JEAN	Single Cell	2022-01-18	Active	100	400	0	0	0
539532	JEAN	Single Cell	2022-01-18	Active	100	400	0	0	0
539533	JEAN	Single Cell	2022-01-18	Active	100	400	0	0	0
539534	JEAN	Single Cell	2022-01-18	Active	100	400	0	0	0
539535	JEAN	Single Cell	2022-01-18	Active	100	400	0	0	0
539536	JEAN	Single Cell	2022-01-18	Active	100	400	0	0	0
539537	JEAN	Single Cell	2022-01-18	Active	100	400	0	0	0
539538	JEAN	Single Cell	2022-01-18	Active	100	400	0	0	0
539539	JEAN	Single Cell	2022-01-18	Active	100	400	0	0	0
539540	JEAN	Single Cell	2022-01-18	Active	100	400	0	0	0
539541	JEAN	Single Cell	2022-01-18	Active	100	400	0	0	0
539542	JEAN	Single Cell	2022-01-18	Active	100	400	0	0	0
539543	JEAN	Single Cell	2022-01-18	Active	100	400	0	0	0
539544	JEAN	Single Cell	2022-01-18	Active	100	400	0	0	0
539545	JEAN	Single Cell	2022-01-18	Active	100	400	0	0	0
539546	FLATROCK LAKE , WABINDON LAKE	Single Cell	2022-01-18	Active	100	400	0	0	0
539547	FLATROCK LAKE , JEAN,WABINDON LAKE	Single Cell	2022-01-18	Active	100	400	0	0	0
539548	FLATROCK LAKE , WABINDON LAKE	Single Cell	2022-01-18	Active	100	400	0	0	0
546066	JEAN	Single Cell	2022-03-22	Active	100	400	0	0	0
546067	JEAN	Single Cell	2022-03-22	Active	100	400	0	0	0
546068	JEAN	Single Cell	2022-03-22	Active	100	400	0	0	0
546069	JEAN	Single Cell	2022-03-22	Active	100	400	0	0	0
546070	JEAN	Single Cell	2022-03-22	Active	100	400	0	0	0
546071	JEAN	Single Cell	2022-03-22	Active	100	400	0	0	0
546072	JEAN	Single Cell	2022-03-22	Active	100	400	0	0	0
546073	JEAN	Single Cell	2022-03-22	Active	100	400	0	0	0
546074	JEAN	Single Cell	2022-03-22	Active	100	400	0	0	0
546075	JEAN	Single Cell	2022-03-22	Active	100	400	0	0	0

Tenure ID	Township	Tenure Type	Anniversary Date	Tenure Status	Tenure %	Work Required	Work Applied	Available Consultation Reserve	Total Reserve
699460	JEAN	Single Cell	2023-12-24	Active	100	400	0	0	0
699461	JEAN	Single Cell	2023-12-24	Active	100	400	0	0	0
699462	JEAN	Single Cell	2023-12-24	Active	100	400	0	0	0
699463	JEAN	Single Cell	2023-12-24	Active	100	400	0	0	0
699464	JEAN	Single Cell	2023-12-24	Active	100	400	0	0	0
699465	JEAN	Single Cell	2023-12-24	Active	100	400	0	0	0
699466	JEAN	Single Cell	2023-12-24	Active	100	400	0	0	0
699467	JEAN	Single Cell	2023-12-24	Active	100	400	0	0	0
699468	JEAN	Single Cell	2023-12-24	Active	100	400	0	0	0
699469	JEAN	Single Cell	2023-12-24	Active	100	400	0	0	0
699470	JEAN	Single Cell	2023-12-24	Active	100	400	0	0	0
699471	JEAN	Single Cell	2023-12-24	Active	100	400	0	0	0
699472	JEAN	Single Cell	2023-12-24	Active	100	400	0	0	0
699473	JEAN	Single Cell	2023-12-24	Active	100	400	0	0	0
699474	JEAN	Single Cell	2023-12-24	Active	100	400	0	0	0
699475	JEAN	Single Cell	2023-12-24	Active	100	400	0	0	0
699476	JEAN	Single Cell	2023-12-24	Active	100	400	0	0	0
699477	JEAN	Single Cell	2023-12-24	Active	100	400	0	0	0
699478	JEAN	Single Cell	2023-12-24	Active	100	400	0	0	0
699479	JEAN	Single Cell	2023-12-24	Active	100	400	0	0	0
699480	JEAN	Single Cell	2023-12-24	Active	100	400	0	0	0
699481	JEAN	Single Cell	2023-12-24	Active	100	400	0	0	0
699482	JEAN	Single Cell	2023-12-24	Active	100	400	0	0	0
699483	JEAN	Single Cell	2023-12-24	Active	100	400	0	0	0
699484	JEAN	Single Cell	2023-12-24	Active	100	400	0	0	0
699485	JEAN	Single Cell	2023-12-24	Active	100	400	0	0	0
699486	JEAN	Single Cell	2023-12-24	Active	100	400	0	0	0
699487	JEAN	Single Cell	2023-12-24	Active	100	400	0	0	0
699488	JEAN	Single Cell	2023-12-24	Active	100	400	0	0	0
699489	JEAN	Single Cell	2023-12-24	Active	100	400	0	0	0
699490	JEAN	Single Cell	2023-12-24	Active	100	400	0	0	0
722597	JEAN	Single Cell	2024-05-06	Active	100	400	0	0	0

5.0 History

The Jean Property is underlain by Gunflint Iron Formation (GIF) which was first discovered in 1850. The earliest recorded geological investigation of the Gunflint was conducted by E. O. Ingall in 1887 who briefly described the iron-bearing strata near Silver Mountain and Whitefish Lake. Other early accounts were made by Smith (1905)

and Silver (1906). Van Hise and Leith in 1911 presented a general overview of the iron bearing rocks in the Thunder Bay district. In 1924 J. E. Gill was the first to describe the Gunflint Iron Formation in detail, and in 1926, its stratigraphy northeast of Silver Mountain. T. L. Tanton described the iron prospects at Mink Mountain in 1923, and in 1931 gave an overview of the general geology in the vicinity of Thunder Bay (Pufahl 1996). The Property was part of historical exploration work carried out by various operators in this area. The historical exploration and geological work documented on the Property area is summarized in the following sections, and the work on adjoining properties is summarized in Section 23 of this report.

Gunflint Iron Mines Ltd. (1943)

Gunflint Iron Mines Ltd. (GIML) in 1943 staked and explored southern portion of Mink Mountain which is south of Jean Property with 10-hole diamond drilling program. In 1960, Moorehouse and Goodwin re-interpreted five (No. 1, No. 3, No. 4, No. 5 and No.7) of six drill logs of completed holes using their adopted stratigraphic classification and nomenclature system and included in their Ontario Department of Mines (ODM)-Report ORV 69.

In 1952, ODM collected four drill core samples belonging to Lower Taconite by their interpretation, from one hole located west of Mink Mountain and Lloyd K. Johnson Exploration conducted minus 100- and minus 200-mesh magnetic tube test for determining total iron content (Fe%).The total Fe% obtained range from 22.18% to 26.86% for feed, 34.68% to 52.26% for minus 100-mesh and 50.08% to 62.26% for minus 200-mesh, and was published as representative for Lower Taconite in ODM-Report 69.

Great Lakes Resources Ltd. (2011-12)

Great Lakes Resources Ltd. (GLR) staked the Jean Iron Property in 2009 and started exploration work in 2011 with two-phase geologic exploration and surface sampling programs, one in May 2011 and the other in August 2011. A diamond drill program consisting of eight vertical NQ-size diamond drillholes totaling 492.88m was completed in May-June 2012.

6.0 Geology

6.1 Regional Geology

The Paleoproterozoic iron formations in the seven iron ranges of the Lake Superior region crop out in in northwestern Ontario, east-central and northern Minnesota, northern Wisconsin, and the Upper Peninsula of Michigan as an oval shaped region encompassing 220,000 km2. Iron formation strata in the Lake Superior region were the first to be mined on a large scale in North America and to have their geology described in detail (Figure 5). Iron formations in other parts of the world were compared to the Lake Superior ranges and genetic concepts were developed with direct reference to the sedimentary basins in this classical area. Similar iron formation lithofacies and stratigraphic- tectonic settings have been reported on all continents. The iron ranges of the Lake Superior region have provided an excellent type-area for reference and study of iron formation and other stratafer sediments in continental shelf and platform settings (Gross 2009).

Extensive Lake Superior-type iron formation (LSTIF) ranges were developed along the margins of cratons or epicontinental platforms between 2.4 Ga and 1.9 Ga (Figure 5). Thicker iron formations were deposited in shallow basins on continental shelves and platforms in neritic environments, interbedded with mature dolostone, quartz arenite, black shale and argillite. Iron formation units in the Animikie basin were the first examples of LSTIF to be described in detail and remain as the principal type area for reference (area around L. Superior and L. Michigan on Figure 5).

The Paleoproterozoic sedimentary rocks deposited in the Animikie Basin form: a southward-thickening wedge covering the southern margin of the Superior province, which is truncated in east-central Minnesota and northern Wisconsin by: the 'Penokean" magmatic terranes". The nature of the sediment varies from volcanic and clastic to the chemical precipitates which form the thick successions of iron formation. The termination of the Penokeani orogeny marked the onset of an intrusive igneous phase which emplaced subduction related tonalitic and granitic plutons into the Anirnikie sediments and the arc related volcanics of the Wisconsin magmatic terranes. The present form of the basin was achieved around 1 Ga ago when a north-northwest

trending branch of the-Midcontinental Rift System separated the Animikie sediments into a northwestern and southeastern segment. The northwestern segment of the Anirnikie Group unconformably overlays the Superior Province and consists of a basal sandstone-siltstone (Pokegama Quartzite, Mahnomen Formation), iron formation (Gunflint, Biwabik, Trommald iron formations), and a thick, upper, shale-siltstone sequence (Rove, Virginia and Rabbit Lake Formations) (Gross 2009).

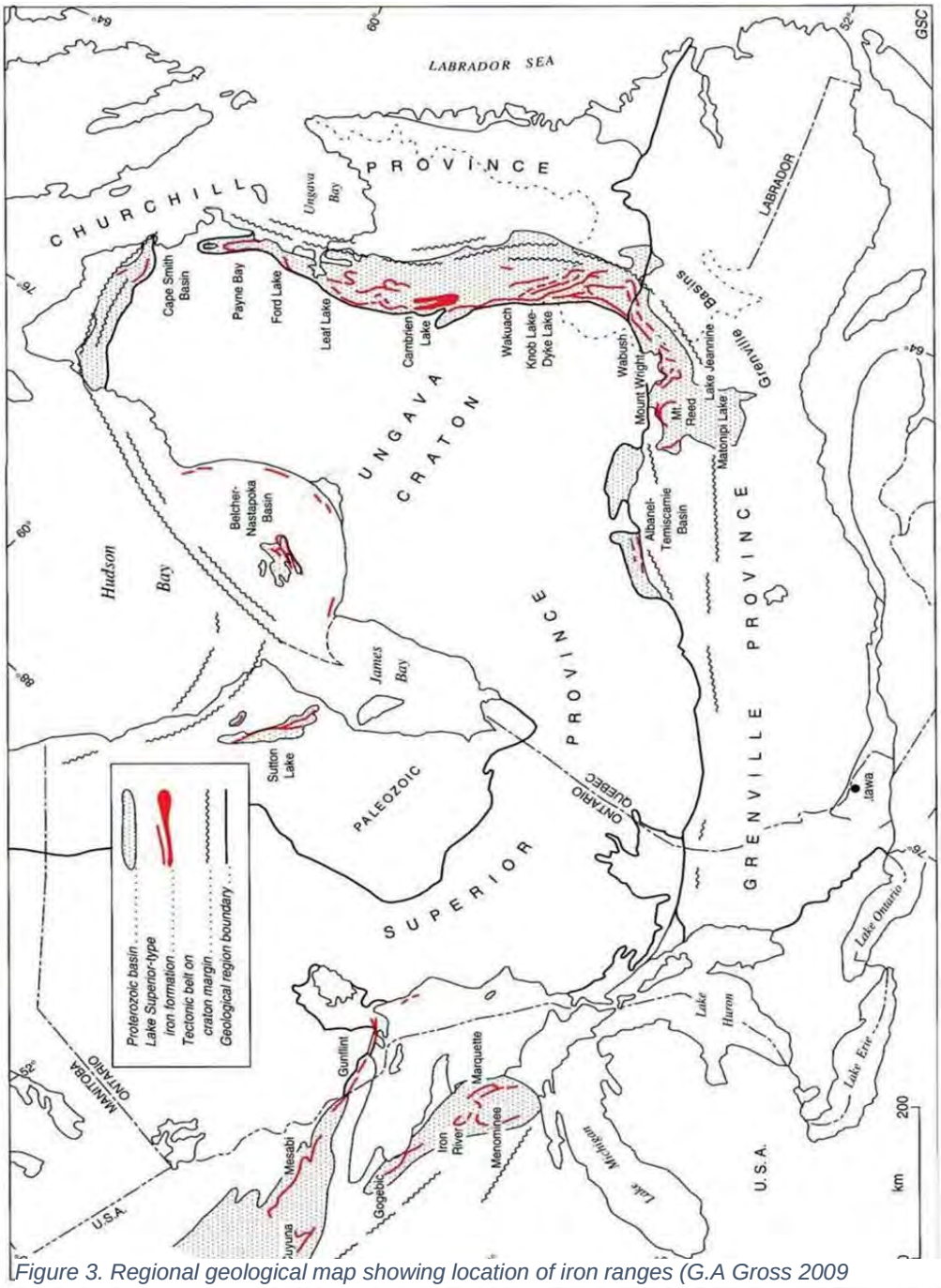

Figure 3. Regional geological map showing location of iron ranges (G.A Gross 2009

6.2 Property Geology

The Jean Iron Property, except in the marginal north which is in unconformity-contact with Archean Basement, is underlain by flat to 5-10° south dipping Upper Gunflint and Lower Gunflint Formation (Map 1, in pocket).

Archean Basement consists predominantly of pink granite and granite gneiss. The texture ranges from conspicuously gneissic to coarsely pegmatitic. Numerous inclusions of chloritic and micaceous schist, and gneiss of various shapes and sizes, occur within the granite.

Lower Gunflint Formation overlying Archean Basement with unconformity contains 4 members. They are, in ascending stratigraphic order as follows:

-Lower Taconite: The lower taconite is approximately 60 m thick and contains roughly 26% iron 46% silica. The upper unit is 40-50m thick and averages 31% iron with 43% silica (Goodwin). Weathered rocks of the member are characterized by a shingly appearance due to numerous closely spaced parting planes, rusty color, and finely granular texture. The iron oxide is commonly an intimate mixture of hematite and magnetite, or near the weathered surfaces, the hydrated equivalents.

-Lower Shale: The shale is soft, black and typically fissile. Thin-section examination reveals much fine-grained clastic material together with carbonaceous matter. Bands of grey to black chert, commonly flecked with pyrite, are present near the top of the member.

-Lower Algal Chert: The algal chert is commonly in the form of reef-like mounds, which are roughly elliptical in plan and average 3m long, 1.2m wide, and 1m thick. The chert forming the mounds is finely contorted in the manner typical of algal structures. Small brown, white, and red granules are often closely associated. The algal chert typically grades upwards into green and white banded chert with massive texture.

-Basal Conglomerate: A basal conglomerate horizon marks the unconformity between overlying Lower Gunflint Formation and underlying Archean Basement. The pebbles of the conglomerate are well-rounded and composed mainly of white vein quartz, milky

white chert, and occasionally jasper. Most pebbles are approximately 2-3cm in diameter, although up to 10-15cm are observed. The matrix consists of sandy quartz grains with considerable amount of chloritic material.

Upper Gunflint Formation is in conformable contact with Lower Gunflint Formation and defmed to the southern portion of the Property. It is subdivided into 5 members and they are in ascending order as follows.

-Upper Limestone Member: The limestone of this member is typically dark-grey to black and very fine grained. It is easily confused with the finer-grained phases of diabase. There are usually thin interbandings of grey-to-black massive chert up to *Scm* thick.

-Upper Taconite Member: The rocks of this member consist of thick-bedded granular chert with shaly partings. The chert layers are commonly green in colour, due to abundant greenalite granules. The thickness of the chert layers ranges from 0.1 to 0.6m. The shaly partings that separate chert beds range in thickness from 2.5 to 33cm, most commonly about l0 cm. The partings are dark-brown to black and very fine grained. They consist of an intermixture of ferruginous carbonate, magnetite, and occasional fragmental grains.

-Upper Shale Member: The member consists largely of black, fissile shale. Locally, small concretions are present; they are generally 1-2 cm in diameter and composed of black sideritic carbonate. A prominent feature of the Shale member, and a good horizon marker, is the presence of a pisolite layer near the top of the member. The layer is 22-45 cm thick. It consists of pisolites averaging 0.5cm in diameter that are somewhat flattened along the bedding plane.

-Upper Jasper Member: The rocks of this member grade upwards by increase in shaly material to shale of the overlying member. The jasper lenses consist of abundant, close packed, small red granules in a chert matrix having a granular texture. Not all granules are red; occasionally a lens has a local concentration of green granules or a general intermixture of red and green. There is an increase of green granules relative to red granules towards the top of the member, and the uppermost lenses are predominantly green. The lower beds of the member are characterized by granules and small lenticles,

or beads, of jaspery chert; this grades upwards into beds consisting of thick lenses of granular jaspery chert with shaly partings.

-Upper Algae Chert: This member can be further divided into three parts based on the mode of occurrence of chert which include from bottom to top: i) Granular chert with jasper veinlets (0.6m - 3m thick); ii) Algal-oolitic chert, lava flow locally (1.2m - 15m thick); and iii) Coarse granular ferrugineous chert (0.6m - 2m thick). This member also contains mafic lava locally. Structurally, the Gunflint Formation is generally monotonously flat to 4-5° dipping south. Younger diabase sills, up to 30m thick are common intruding into Animikie Series. No major structural deformation, effect of metamorphism and significant supergene enrichment to form direct shipping ores were recorded in the area. Beyond the southern boundary, a sheet of diabase sill about 30m in thickness intruded upper portion of Rove Formation and formed as resistant cappings as Mink Mountain and Sun Hill Mountain after erosion. Lower Taconite Member of Lower Gunflint Formation is the most exposed lithologic unit covering approximately 85-90% and is the main economically-interested stratigraphic horizon of the Property.

Table 2. Stratigraphy of Gunflint Iron Formation

Cycle	Member	Thickness (metres)
Upper Gunflint	Upper Limestone	1.5 – 6
	Upper Taconite	45 – 55
	Upper Shale	1.5 – 5
	Upper Jasper	12 – 20
	Upper Algal Chert	2.5 – 6.5
	Lava Flow Locally	0 – 12
	Total Upper Gunflint	**62.5 – 104.5**
Lower Gunflint	Lower Taconite	46 – 64
	Lower Shale	1 – 6
	Lower Algal Chert	0.6 – 4.5
	Basal Conglomerate	0 – 0.3
	Total Lower Gunflint	**47.6 – 74.8**
Total Thickness of Gunflint Iron Formation		**110.1 – 179.3**

Source: Goodwin (1952)

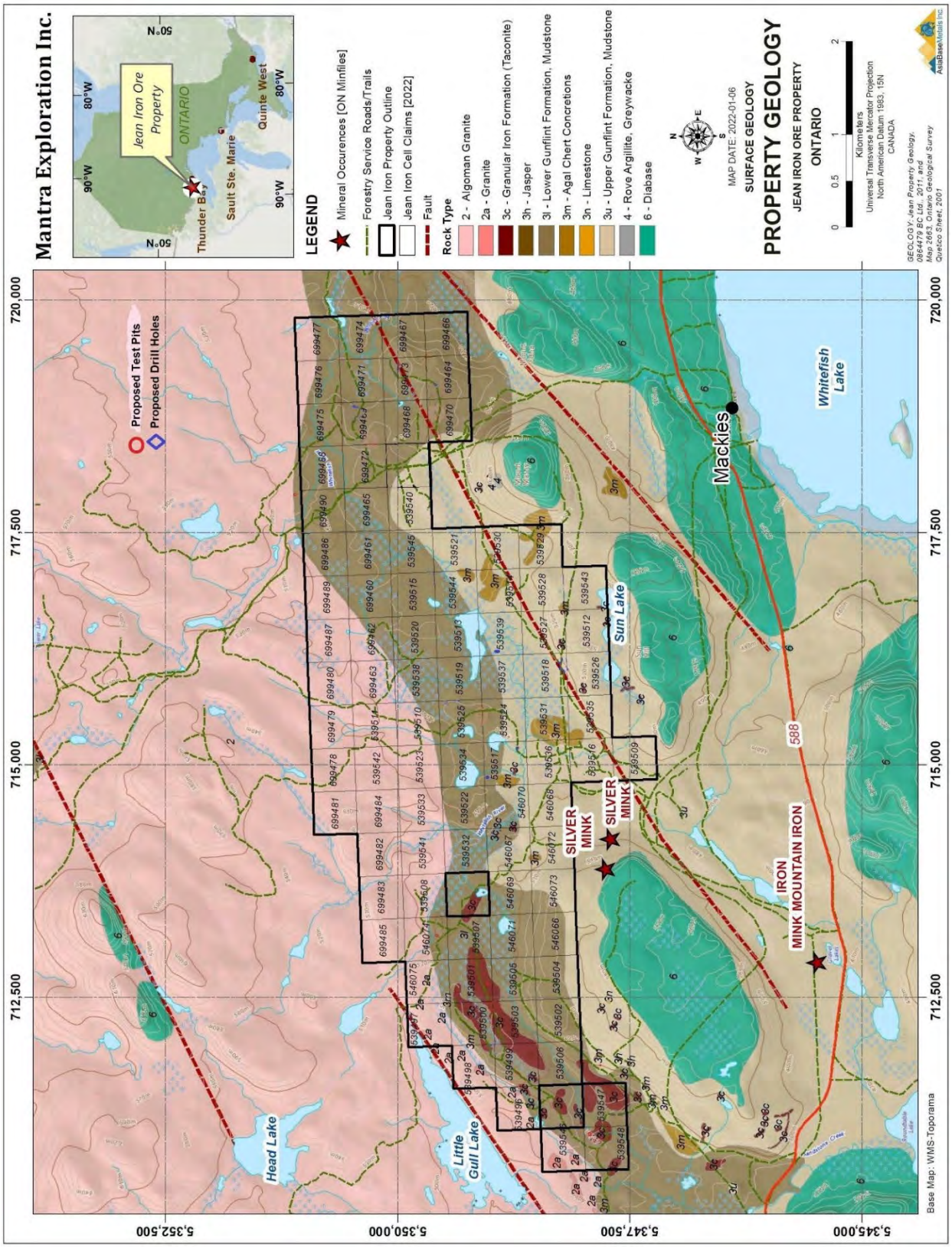

Figure 4. Jean property geology

6.2.1 Mineralization

The iron formations of Gunflint Formation is typical Lake Superior-type Banded Iron Formation developed along the margins of cratons or epicontinental platforms between 2.4 Ga and 1.9 Ga. This deposit type is consists of banded sedimentary rocks composed principally of bands of magnetite and hematite within quartz (chert)-rich rock, with variable amounts of silicate, carbonate and sulphide lithofacies. Such iron formations have been the principal sources of iron throughout the world. Based on compilation made by ODM (1952-60) based on historical chemical analyses, it is known that Lower Taconite Member of Lower Gunflint Formation, and Upper Jasper Member and the Upper Taconite Member of Upper Gunflint Formation are of particular economic interest for iron.

7.0 Work Program

A high-resolution aeromagnetic gradiometer- digital VLF-EM survey over the Jean claim block was undertaken between July 19th and the 21st. The fixed-wing survey covered 246 line-km. The detailed report from Terraquest with maps can be found in Appendix 1. The author undertook 4 days of prospecting and mapping using the Terraquest data from July 19th to August 5th, 2022. An outcrop/sample map can be found in Appendix 2 with assay certificates located in Appendix 3.

The property was accessed from east to west by a newly constructed forestry access road. Traverses were pre-determined the day before using satellite imagery and compiled historic data. Many new outcrops were exposed due the road construction and forestry equipment activities, which helped to better observe the geology of the property (Photo x; Photo x).

Geotools were used where necessary to strip moss from outcrop and hammer and chisel to collect grab samples. Field observations were made and recorded in field a rugged tablet computer.

A total of 11 samples were gathered and sent for geochemical analysis Activation Laboratories (Actlabs) in Thunder Bay. Samples were crushed to -10 mesh followed by

pulverizing a 250-gram split to -150 mesh (95%). Each sample was analyzed for iron content via their Davis Tube Recovery process with a via XRF finish – package Code 8.

Figure 5. Sample 18959 with pervious undocumented channel sample. Hammer handle points north.

Figure 6. Typical soil-bedrock profile at historical trench 15-2 in the Lower Shale Member.

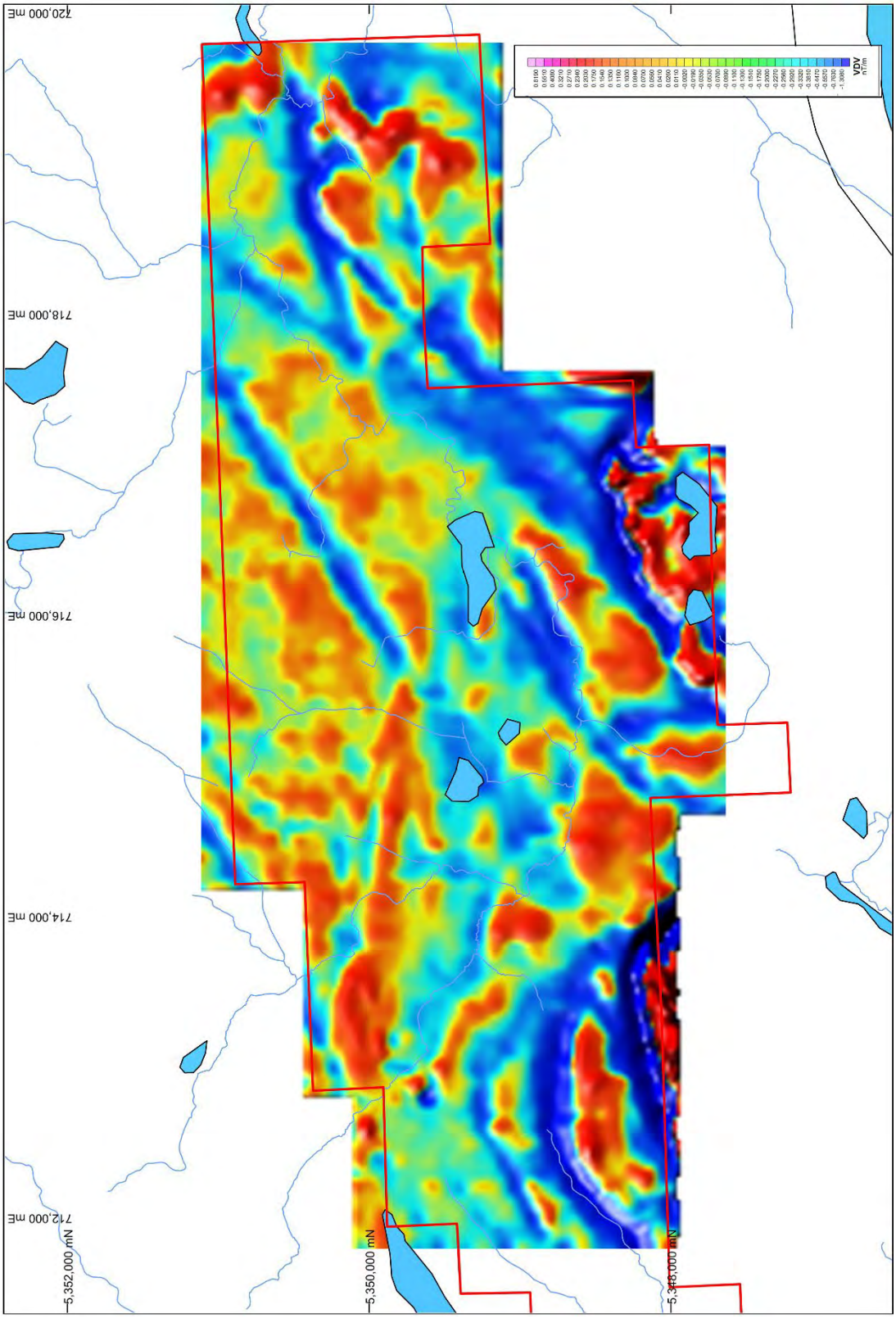

Figure 7. Terraquest Ltd. reconstructed total field (RTF) magnetics for Jean Property

7.1 Daily Log

July 19, 2022

Sunny, windy in afternoon, averaging 24°C Terraquest undertakes training and orientation flight. The author drives to the property to evaluate access to search for drill core from 2012 drill program. Drill core located at Maki Resort along shore of Whitefish Lake.

July 20, 2022

Sunny, very strong winds, averaging 24°C. Terraquest completed a 4-hour flight.

July21, 2022

Sun/cloud, averaging 26°C. Terraquest completes airborne survey.

July 25,2022

Sun and cloud, 24°C. Traversed the property from south to north looking or outcrop. One sample was taken from possible sub-crop on cell 539511. A second sample was taken from a jasper bearing unit on cell 546068.

August 3, 2022

Sunny clouding over and light rain, 22°C. Accessed the western portion of the property to compare outcrop and sampling from 2012 work program with new geophysical data. Sample 18959 was collected on flat outcrop beside historical channel sample on cell 539547. A bedrock outcrop beside the access trail was sampled, 18960, on cell 539546. A pyritic shale unit was sampled, 18961, on cell 539496. Sample 18962 was collected on cell 539503, sample 18963 weas collected on cell 539501 and sample 18964 was collected on cell 539499.

August 3, 2022

Sunny, 26°C. Accessed the new cells to the northeast along an old logging road. The northernmost sample, 18965, was shale with a granular groundmass adjacent to strong magnetic high which did not outcrop. Sample 18966 was taken from a flat outcrop with 10-15% specular hematite in a granular groundmass on cell 699464 in the middle of a magnetic high adjacent VLF conductor. Sample 18967 was take to the west of 18966

Table 3. Table of Samples and Iron Assays

Sample ID	Easting	Northing	Claim Cell	Type	Fe203(T)	Description
18957	715521	5350185	539511	Grab, outcrop/ subcrop	14.38	TACONITE: Dark grey, fine to medium grained, granular texture, brown weathered surface due to hematite, siliceous, 20% magnetite.
18958	714434	5348514	546068	Grab, outcrop/ subcrop	8.03	TACONITE: dark grey, fine to medium grained, medium bedded, brown weathered patches and layers due to hematite, siliceous, 25% magnetite.
18959	711124	5347797	539547	Grab, outcrop	48.84	TACONITE: Dark grey to brown, hematite staining and patches, not magnetic, fine grained, green clayey parts.
18960	711037	5348134	539546	Grab, outcrop/ subcrop	33.11	TACONITE: Greenish grey to dark grey, brown haematitic weathering, reddish jasper at places, shingly to massive.
18961	711390	5348394	539496	Grab outcrop	30.58	TACONITE: Dark grey, slatey, hematite along fractures and bedding planes, not magnetic, locally pyrite nodules and zinc oxide staining.
18962	712238	5348914	539503	Grab outcrop	23.7	TACONITE: Dark grey, fine to medium grained, medium bedded, brown weathered surface due to hematite, siliceous, not magnetitc.
18963	712529	5349036	539501	Grab outcrop	39.05	TACONITE: dark grey, fine to medium grained, medium bedded, brown weathered patches and layers due to hematite, siliceous, 25% magnetite.
18964	711869	5348867	539499	Grab, outcrop	26.02	TACONITE: Dark grey to brown, hematite staining and patches, reddish jasper at places, less magnetic (<20%), fine grained, green clayey parts.
18965	718493	5350525	699469	Grab, outcrop	28.63	TACONITE: Greenish grey to dark grey, brown hematitic weathering, reddish jasper at places, shingly to massive, <20% magnetite.
18966	718969	5349557	699464	Grab outcrop	31.8	TACONITE: Dark grey, massive, hematite in ground mass, granular.
18967	718773	5349551	699470	Grab outcrop	19.02	TACONITE: Dark grey, massive, hematite along fractures and bedding planes, less green minerals, not magnetic .

on cell 699470 along the edge of the magnetic high from and outcrop with trace hematite in the groundmass and rusty bedding planes.

8.0 Conclusions and Recommendations

The Jean Iron Property consists of 95 claim cells 2,058 hectares' land located in Thunder Bay Mining District of Northwestern Ontario, Canada. The Property is located about 65 kilometers to the southwest of Thunder Bay, approximately 2 kilometers north of the Whitefish Lake on Highway 588. It can be accessed via the Trans-Canada Highway 11/17, about 20 km west from the Highway 61 junction to Highway 588 (Stanley access), and then a further 45 km southwest along Highway 588. A network of gravel roads and trails traverse the mineral claims and provide access to various areas of the Property.

Mantra Exploration Inc. owns 100% of the Mineral Claims. The Company initiated exploration work on the property in 2022 after completion of an airborne magnetic and very low frequency survey to evaluated the iron potential of the newly staked claim cells. Mantra was issued a permit (PR22-000085) effective June 29th, 2022 to June 29th, 2025.

During the month of December 2021 Mantra expanded the property by acquiring 31 additional claim cells along the property's northern and eastern boundary. During the current exploration work carried out by Mantra in 2022, a total 11 rock samples were collected. The work verified historical results as well as evaluated the iron potential of the newly acquired cells.

Prospecting and mapping work indicated that the new claim cells along the northern boundary are underlain by an Archean granitic basement with substantial fluvial-glacial cover. Algal chert and jasper containing rocks are found to be more resistant to weathering and exposed at places; whereas, a few new road cuts were also helpful in locating Taconite and shale outcrops. Iron content of shales were observed to be generally low with rusty brown surface weathering due to disseminated hematite along fractures and bedding planes. Jasper and algal cherts are found to be rich in iron and are more magnetic than other units of Gunflint Iron Formation. Taconite unit visually contains 20% to 30% hematite.

Sampling of the lower taconite unit by the author on the eastern new claim cells yielded iron contents between 19 and 31% indicating good potential to develop a resource. Sampling of the Property by Pirzada in 2011 and 2013 in the west end of the property produced iron contents of 41.1% and 58.3% from 2011 drill core. These samples were from taconite member of Lower Gunflint Iron formation. These values were confirmed by authors sampling in Table 3 and Figure 4.

Outcrops centered on samples 1192091 and 1192095 from 2015 mapping require detailed stripping, geological mapping, and channel sampling to assess their potential. Likewise outcrops from samples collected by the author in the east end of the property, 18965 to 18967, likewise require similar follow-up work.

Table 4. Phase 1 Proposed Budget

Item	Unit	Number of Units	Unit Rate($)	Total($)
Prospecting and Sampling	day	14	1100	15400
Geological work and sampling	day	10	1100	11000
Excavator for trenching	hrs	24	450	10800
Equipment rentals - pump/saws	lump sum	1	10000	10000
Assays - Davis Tube + magnetic sep	sample	200	142	28400
Travel	km	4000	0.55	2,200
Field Supplies	lumpsum	1	5000	5000
Room & Board	day	24	375	9000
Project Management, Report & Filing	day	6	650	3900
			10% Contingency	9,570
			Total	$105,270

If results from the first phase are positive, then a step-out and infill drilling program would be warranted in Phase 2. This work will help to define the trends and continuity of the favourable taconite units of Gunflint Iron formation within and adjacent to the past exploratory drilling area. This drilling program, if successful will provide basis of iron resource estimation. The metallurgical testing will help in defining the potential for economic concentration of iron in taconite. The scope of work and location of drill holes would be determined based on the findings of Phase 1a investigations. Initially a 5,000 metre diamond drilling program is proposed involving 20-25 drill holes.

Estimated cost of this program is $549,000.

Table 5. Phase 2 Proposed Budget

Item	Unit	Number of Units	Unit Rate($)	Total($)
Diamond drilling contractor	meters	1000	280	280000
Core logging geologist	day	15	650	9750
Core Technician	day	15	400	6000
Assays	sample	600	142	85200
Travel	km	5333	0.55	2,933
Field Supplies	lumpsum	1	3443	3443
Room & Board	day	30	375	11250
Project Management, Report & Filing	day	7	650	4550
			10% Contingency	40,313
			Total	$443,439

9.0 References

Aung Myint Thein, 2011; Assessment Report on the Jean Iron Property, Jean Township, Thunder Bay South Mining Division, Ontario, Claims 4252101, 4252102, 4252103, 4252104, 4252105, 4252106, 4252107, 4252108, 4252109, 4252110, 4252111, 4252112, 4252113, 4252114, 4252115, 4252116 and 4252117, October 26, 2011.

Aung Myint Thein, 2012; Assessment Report on the Jean Iron Property, Jean Township, Thunder Bay South Mining Division, Ontario, Claims 4252101, 4252102, 4252103, 4252104, 4252105, 4252106, 4252107, 4252108, 4252109, 4252110, 4252111, 4252112, 4252113, 4252114, 4252115, 4252116 and 4252117, August 30, 2012.

Flint Rock Mines Limited, 1962; Drill Hole Logs Whitefish Lake Property; Port Arthur Mining Division, May 07, 1962.

G.A. Gross, 2009; Iron Formation in Canada, Genesis and Geochemistry; Geological Survey of Canada Open File 5987.

Goodwin, A.M. (1961), Gunflint Iron Formation of the Whitefish Lake Area, District of Thunder Bay, Ontario, Ontario Department of Mines report ORV 69.

Gordon J. Allen, 2008; Assessment Report on Geological Mapping, Rock Sampling, and Radiometric Survey on Gunflint (Mt.Edna) Property, Thunder Bay Mining Division, Ontario; for Raytech Metals Corp., Dec 31, 2008.

Gunter Faure and Jack Kovach, 1969; Age of Gunflint Iron Formation of Animikie Series in Ontario, Canada; PP Geological Society of America.

J.F. Wright, 1952; Concentration Tests on Cores from Gunflint Range Exploration Drilling, November 27, 1952.

Kelly, T.J., 1961; Statistical review of mineral industry 1959, Annual report of the Department of Mines, Ontario, published 1961 (ORV 69).

Pier Kenneth Pufahl, 1996; Stratigraphic Architecture of a Paleoproterozoic Iron Formation Depositional System: the Gunflint, Mesabi and Cyyuna Iron Ranges; Master of Science Thesis, Lakehead University, Thunder Bay, Ontario.

Pirzada, Afzaal, 2014; Technical Report On the Jean Property Thunder Bay Mining District Northwestern Ontario, Canada Prepared for: AsiaBaseMetals Inc., 75 pg, SEDAR.

Pirzada, Afzaal, 2016; Technical Report On the Jean Property Thunder Bay Mining District Northwestern Ontario, Canada Prepared for: AsiaBaseMetals Inc., 89 pg, SEDAR.

Roman Shklanka, 1968; Iron Deposits of Ontario; Department of Mines, Mineral Circular No. 11, 1968.

Sharpe George C., 2011; Technical report on Gunflint Property, Thunder Bay Mining District, Ontario; prepared for Canada Iron Inc., dated August 10, 2011.

Zago Neal, and Gutta Blair, 2012; Whitefish River assessment report, prepared for Lakehead Region Conservation Authority; August 2012.

Appendix 1. Terraquest Airborne Survey Report

OPERATIONS REPORT:

High Resolution, Horizontal Magnetic Gradient & VLF-EM + Resistivity Airborne Survey

for

MANTRA EXPLORATION INC.

Jean Project
Thunder Bay, Ontario

Contract Number B551
November 5, 2022

Requested By:
Andrew Tims (P.Geo), Consulting Geologist
Northern Mineral Exploration Services

Prepared By:
Charles Barrie, Managing Partner
Terraquest Ltd.

Table of Contents

1 INTRODUCTION

1.1 ABSTRACT

This report covers a High Resolution, Fixed-Wing Geophysical Survey recording Horizontal Magnetic Gradient and VLF-EM over the Jean Project area located in the Thunder Bay, Ontario area on behalf of Mantra Exploration Inc.. To obtain this data, the area was systematically traversed by an aircraft carrying geophysical equipment along a series of parallel flight lines. The Jean survey has been designed so that the traverse lines intersect the geology and structure to acquire optimum geophysical data. For the Jean survey area a total of 81 traverse lines was flown at 100 metre intervals. A total of 4 tie lines was flown at an interval of 1000 metres totalling 218.54 total line-kilometres. The mean terrain clearance was 108.1 metres with an average velocity of 60.0 metres per second such that the data sampled at 10Hz have an average of 6 metres sample density along line.

Final deliverables are contained in a digital Archive and include Geosoft databases, Geosoft grid files, Geosoft Voxels GeoTIFF files, digital high-resolution and low-resolution map images, one copy of rolled high quality film maps and a final Operations Report which includes survey parameters, equipment specifications, summary of operations, description of processing techniques, and page size images of all the final products.

1.2 EXECUTIVE SUMMARY

This report describes the specifications and parameters of an airborne geophysical survey contracted by:

Mantra Exploration Inc.,
6153 Glendalough Place
Vancouver, BC V6N 1S5
Attn: Raj J. Chowdry, CEO Tel: 604-765-2030 Email: rchowdry@futuracapitalltd.com

Represented by,

Andrew Tims (PGeo) Consulting Geologist
Northern Mineral Exploration Services
Tel: 807-474-3242 Email: pgeo_tims@shaw.ca

The survey was performed by:

Terraquest Ltd., 301-2900 John Street
Markham, ON, L3R 5G3
Attn: Charles Barrie, VP Terraquest Tel: 905-477-2800 Email: cb@teraquest.ca

1.3 LOCATION

The Jean Project is in the Thunder Bay Mining District, Ontario, approximately 60 kilometres southwest of the city of Thunder Bay. It can be accessed by Route 588 from Thunder Bay, proceeding just past Whitefish Lake; the southern edge of the survey area is 0.4 km north of the highway. The survey block is generally rectangular with a few minor blocks removed in the northwest and southeast corners. This survey area covers approximately 21.6 square kilometers and its perimeter is approximately 22.95 kilometres. The centre of the area is approximately 90° 5' 34.827" W and 48° 15' 37.701" N.


ONTARIO
JEAN PROJECT

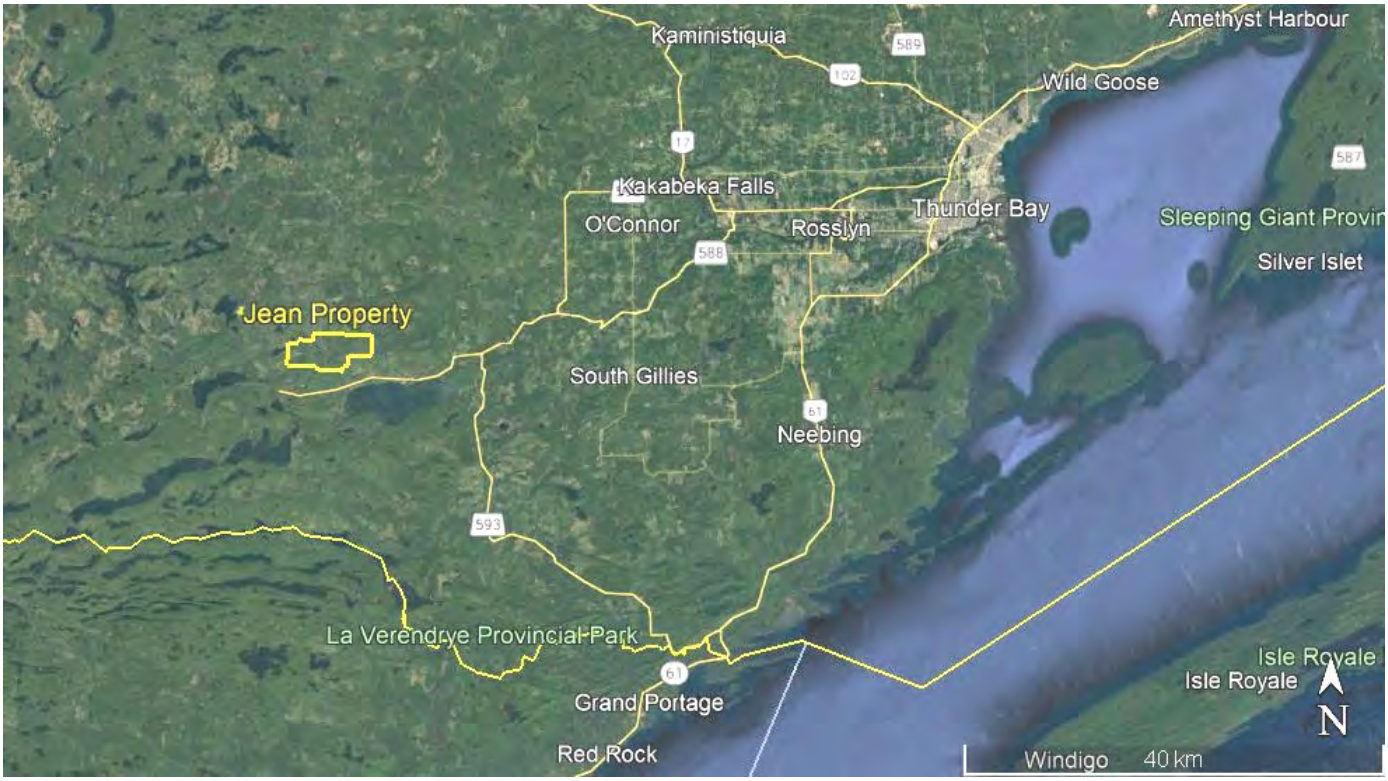
Kaminstiquia
Amethyst Harbour
Wild Goose
Kakabeka Falls
O'Connor
Rossl yn
Thunder Bay
Sleeping Giant Provin
Silver Islet
Jean Property
South Gillies
Neebing
La Verendrye Provincial Park
Grand Portage
Red Rock
Isle Royale
Isle Royale
N
Windigo
40 km

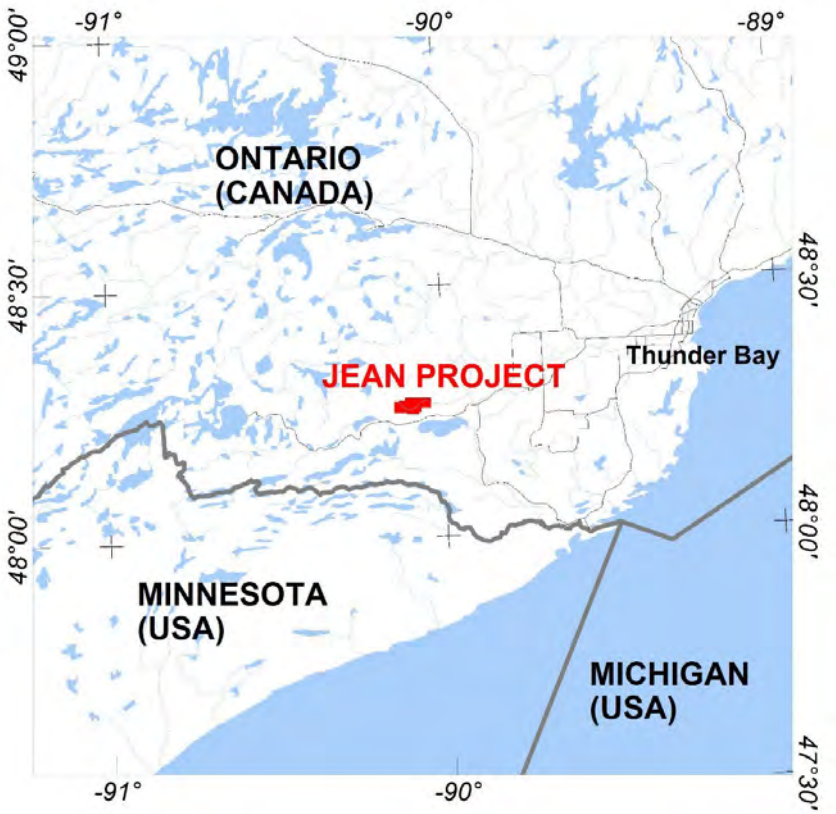
-91°
-90°
-89°
49°00'
48°30'
48°00'
47°30'
ONTARIO
(CANADA)
JEAN PROJECT
Thunder Bay
MINNESOTA
(USA)
MICHIGAN
(USA)

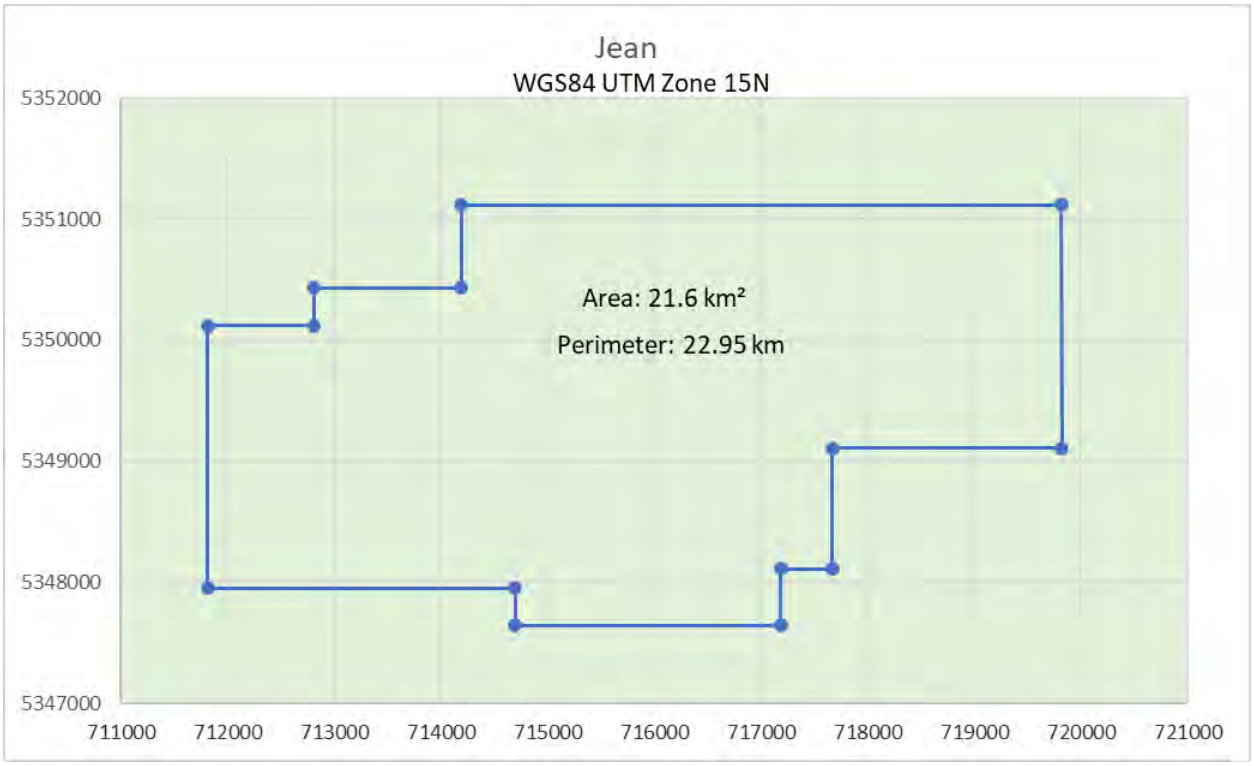
Jean
WGS84 UTM Zone 15N
Area: 21.6 km²
Perimeter: 22.95 km
5352000
5351000
5350000
5349000
5348000
5347000
711000
712000
713000
714000
715000
716000
717000
718000
719000
720000
721000

2 SURVEY SPECIFICATIONS

2.1 SURVEY TRANSVERSE AND CONTROL LINES

Traverse Line Spacing (m)	100
Traverse Line Orientation (degrees)	000°-180°
Number of Traverse Lines	81
Traverse Line Total Distance (km)	218.54
Tie Line Spacing (m)	1000
Tie Line Orientation (degrees)	090°-270°
Number of Tie Lines	4
Tie Line Total Distance (km)	27.48
Planned Total Line Distance (km)	246.02
Average Speed (m/s)	60.0
Average Terrain Clearance (m)	108.1
Drape Surface Height (m)	100
Total Line Distance Flown (km)	245.61

2.2 SURVEY STATISTICS

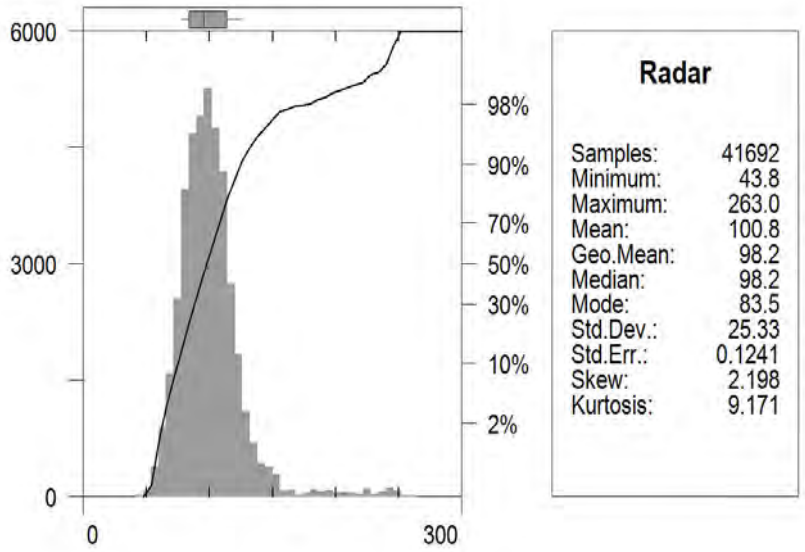

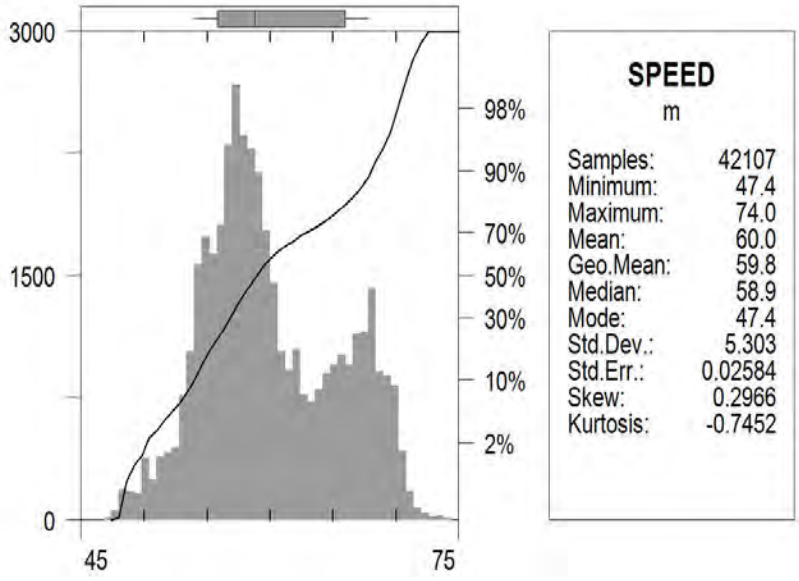

2.3 SURVEY LINE NAVIGATION

The survey area is defined by coordinates supplied by the client and were used to establish the survey boundaries and the flight lines. All survey planning is completed using the WGS84 projection system, although alternative coordinate systems may be used in final processing. Survey planning for the positions of the transverse lines and tie lines is completed using either AgNav or Geosoft software. In either case, the key inputs to the software include the line spacing and line direction. Survey lines are not usually coincident with the survey boundaries unless necessary. The traverse line spacing and orientation is usually consistent across the entire area but tie line spacing and orientation may vary slightly to better accommodate oddly shaped survey boundaries. The navigation file is provided in Appendix II.

The onboard satellite navigation system was used to ferry to the survey site and to survey along each line. The flight path guidance accuracy is variable depending upon the number and condition (health) of the satellites employed; the uncorrected accuracy was for the most part better than 10 metres. Real-time GPS correction using the WAAS satellite broadcast services for North America improves the navigational accuracy to about 3 metres or less in the horizontal plane and 4-5 metres in the vertical direction.

2.4 Pre-Survey Navigational Flight Surface

A pre-planned, digital drape surface is critical to ensuring properly collected airborne magnetic data in variable or rough terrain by reducing the altitude differences between the traverse and control lines. The drape surface is integrated into the aircraft survey guidance system where a differential GPS provides real-time corrected position information with reference to the horizontal and vertical survey plan.

The flight drape surface for this survey was generated by taking into consideration the local terrain, the aircraft's climb/descent performance and the survey height requested by the client. The computed drape surface establishes the altitude profile that best suites the terrain and the aircraft's capability. During the final data processing stage, the levelled magnetic product benefits significantly from traverse and control line intersections that are very close in altitude. In areas of steep terrain and high magnetic gradient, just a small difference in altitude can introduce significant levelling error. The drape surface reduces this error, and the result is a superior magnetic product. Terraquest generated pre-planned drape surface for this airborne survey is based on an industry standard climb rate of 5%. A safe and optimal terrain clearance is determined once the planned drape surface has been calculated.

2.5 Tolerances And Re-Flights

2.5.1 Traverse Line Separation

Re-flights (if any) are flown if the traverse line separation of the final corrected flight path exceeds 1.2 times the planned line separation over a distance greater than 3 times the planned traverse line separation.

2.5.2 Terrain Clearance:

As specified in the contract, the survey is flown with a tight drape fashion with as low a nominal terrain clearance as safety permits, targeting a minimum of 70 metres drape above the highest obstacle with typical excursions to 100 metres, best efforts, to optimize the magnetic data. Re-flights (if any) are flown if the final differentially corrected altitude deviated from the planned flight surface by +/-15 m over a distance of 2 kilometres along a line.

2.5.3 Diurnal Variation:

Diurnal activity in the survey was limited to 4 nT for a 1-minute chord.

2.5.4 GPS Data:

GPS data included at least 4 satellites 15 degrees over horizon for navigation and flight path recovery.

2.5.5 Radio Transmission:

The aircraft pilot made no radio transmission that interfered with magnetic response unless mandated by airport or air traffic safety situations.

2.5.6 Sample Density:

A re-flight is required if the sample density along one or more of the survey lines exceeds 8 metres over a cumulative total of 1000 metres for the magnetic data.

2.5.7 Magnetic Noise:

As specified in the contract, the fourth difference noise envelope for the tail sensor data does not exceed +/- 0.10 nT.

2.5.8 Measurement Gaps:

There were no significant gaps in any of the digital data.

3 SURVEY EQUIPMENT

3.1 SURVEY AIRCRAFT

The Cessna U206, registration C-GGLS, owned and operated by Terraquest Ltd. was the survey aircraft used for B551. This aircraft is approved by the Canadian Ministry of transport and has a certification for specialty flying that includes airborne geophysical surveys. This aircraft is maintained by a regulatory AMO facility, Enterprise Air Ltd. in Oshawa, ON.

The aircraft has been specifically modified with long-range fuel cells to provide up to 7 hours of range, outboard tanks, tundra tires, cargo door, and avionics as well as an array of sensors to carry out airborne geophysical surveys.

The magnetic sensors are in wing tip pods that extend approximately 1.2 metres beyond each wing tip and in a tail stinger pod which extends approximately 3 metres beyond the tail. The separation of the magnetic sensors are as follows:

Transverse (wingtip to wingtip sensors) = 17.63 metres
Longitudinal (wing centre to tail sensor) = 10.86 metres

The GPS antenna is located on the cabin roof near the centre line of the wing spar.

3.2 GEOPHYSICAL EQUIPMENT AND SPECIFICATIONS

3.2.1 High Sensitivity Magnetometer:

One high-resolution cesium vapour magnetometer is mounted in the tail stinger pod and two are mounted in wing tip pods. A fluxgate tri-axial magnetometer is mounted in the middle of the tail stinger to monitor aircraft manoeuvre and magnetic interference; these data are used post-flight to compensate the high sensitivity magnetic data for aircraft manoeuvre noise.

Type of Magnetometer Sensor	Cesium Vapour
Model	CS-3, CS-L
Manufacturer	Scintrex
Resolution	0.001 nT counting at 0.1 per second

Sensitivity	+/- 0.005 nT
Dynamic Range	15,000 to 100,000 nT
Fourth Difference	0.02 nT
Recorded Sample Rate	0.1 seconds
Noise Envelope	0.10nT (Tail Sensor)

3.2.2 Tri-Axial Fluxgate Magnetic Sensor

Tri-Axial Fluxgate Magnetic Sensor	Used for compensation, mounted in mid-section of tail stinger
Model	W/FM100G2-1F
Manufacturer	Billingsley Magnetics
Description	Low noise miniature triaxial fluxgate magnetometer
Axial Alignment	> Orthogonality > +/- 1 degree
Accuracy	< +/- 0.75% of full scale (0.5% typical)
Field Measurement	+/- 100,000 nanotesla
Linearity	< +/- 0.015% of full scale
Sensitivity	100 microvolt/nanotesla
Noise	< 12 picoTesla RMS/–Hz @ 1 Hz

3.2.3 VLF-EM System

VLF-EM data were captured using a Magenta Inc. Matrix-Plus Digital VLF receiver. The Matrix-Plus frequency specific, digital VLF-EM System was recently developed for Terraquest Ltd. and was deployed on this survey. It employs 3 orthogonal, air-core coils mounted near the front of the nose boom, and coupled with a receiver-console, tuned to receive independently up to eight frequencies. This instrument is capable of simultaneously monitoring up to eight (8) VLF frequencies, recording the full parameterization of the VLF signal (useful for advanced processing including inversion modelling including the following parameters:

- Accelerometer: x, z, and y
- Gyro: x, y, and z
- Magnetic field: x, y, and z
- Raw Amplitude (secondary field)
- Raw Apparent Station Azimuth (relative to instrument orientation)
- Raw Planar Ellipticity
- Raw Vertical Ellipticity
- Raw Field Tilt Angle
- In Phase

Typical frequencies for North America include Cutler, Maine, NAA frequency: 24.0 kHz, LaMoure, North Dakota NML frequency 25.2 kHz, and Seattle WA NLK frequency 24.8 kHz.

VLF - EM	Stand-alone module
Model	Matrix-Plus
Manufacturer	Magenta Ltd.
Primary Source	Magnetic field component radiated from government VLF radio transmitters
Parameters Measured	Total Field Amplitude, Vertical and Planar Ellipticities, Azimuth to transmitter & Field Tilt Angles
Frequency Range	Up to eight independent frequencies
Gain	Constant gain setting
Filtering	No filtering
Recorded Sample Rate	0.05 seconds
Recording	Internally with USB access, externally to DAS for redundancy

3.2.4 Data Acquisition System

DAS & Compensation	Combined
Model	DAARC 500
Manufacturer	RMS Instruments
Operating System	QNX 6.3 or greater
Time	104 MHz temperature compensated crystal clock
Front End Magnetic Processing	Resolution 0.32pT; system noise <0.1pT; sample rate 160, 640, 800m or 1280 Hz
Front End - Fluxgate	I/F module; oversampling, self-calibrating 16 bit A/D converter
Compensation	Improvement Ratio (total field) 10-20 typical
Input Serial	8 isolated RS232 channels; ASCII & Binary formats
Input Analog	16-bit, self-calibrating A/D conv.
Input Events	Four latched event inputs
Raw Data Logging	At front end sampling rate, 1 MB buffer
Output/Recording	Rate 10 (used), 20 or 40 Hz; Serial up to 115.2 kbps; Recording media 1 GB Flash; 80 GB Hard Drive; Flash disk via USB; Display
Front Panel Indicators	8 LEDs for mag input; 2 LEDs for Front End status

3.3 Aircraft Ancillary Equipment

3.3.1 Radar Altimeter

Altimeter	Radar
Model	KRA-10A
Manufacturer	King
Serial Number	071-1114-00
Accuracy	5% up to 2,500 feet
Calibrate Accuracy	1%
Output	Analog for pilot, converted to digital for data acquisition

3.3.2 Barometric Sensor

Sensors	Pressure (mB)
Model	PPT0020AWN2VA-C
Manufacturer	Honeywell
Source	coupled to aircraft barometric (pitot static) system
Output	Serial output to DAARC 500 channels 3 & 4 respectively

3.4 Ground Base Station Equipment Specifications

Base station data were provided by two GEM Systems, GSM-19's which are a high sensitivity Overhauser magnetometer with a built-in magnetometer counter and GPS system used for time synchronization with the aircraft data.

4 TESTS AND CALIBRATIONS

4.1 MAGNETIC COMPENSATION (FIGURE OF MERIT)

Compensation calibration tests were performed to determine the magnetic influence of aircraft maneuvers and the effectiveness of the aircraft compensation method. It is important to select an area near the survey project but with a uniform magnetic background. The aircraft flew a square pattern in the four cardinal directions at a high altitude over a magnetically quiet area and performed pitches (± 5°), rolls (± 10°) and yaws (± 5°). The sum of the maximum peak-to-peak residual noise amplitudes in the total compensated signal resulting from the twelve maneuvers is referred to as the FOM.

The FOM was flown on July 17th 2022 and the results for this survey were FOM 1.95 nT, FOM 1.82 nT and FOM 0.96 nT for the Left, Right and Tail sensors respectively (see Appendix III).

4.2 MAGNETIC LAG

Evaluation of the magnetic lag factor was accomplished by adjusting the lag on a line-to-line basis over the survey area to obtain the most suitable lag. The established lags were 0.5 seconds for the left and right wingtip sensors, and 0.7 seconds for the tail sensor.

4.3 RADAR ALTIMETER CALIBRATION

Verification of the altimeter calibration are completed up to several times a year. This involves flying the aircraft at appropriate intervals above the base airstrip or some other suitable location with known elevation and flat terrain. The radar data is compared against the GPS height of the aircraft minus the known elevation of the airstrip at each height. This calibration was done on a previous survey on 29 June 2021. (see Appendix IV).

5 LOGISTICS

5.1 PERSONNEL

Terraquest Ltd. supplied the following properly qualified and experienced personnel to carry out the survey and to reduce, compile and report on the data:

Planning	John Currie/Allen Duffy
Pilot	Vince Ou
Operator	Alexander Louie
QA/QC Processing	Russell Imrie/Allen Duffy
Magnetics Processing	Shane Hefford
VLF Processing	Shane Hefford
Resistivity Processing	Fernando Santos/Allen Duffy
Operations Manager	Charles Barrie

5.2 BASE OF OPERATIONS

Decisions regarding the base of base depend on a variety of factors such as availability of accommodations, accessibility to airstrip, availability of fuel, proximity to the survey area, etc. Terraquest assumes discretion and responsibility for such decisions. The crew's accommodations were the responsibility and cost of Terraquest.

For the Jean Project, the base of operations was Thunder Bay, Ontario. For redundancy, two GSM-19 base stations (combined high sensitivity magnetic and GPS, see section 3.4) were set up at a secure and magnetically quiet location at the local airport (see below).

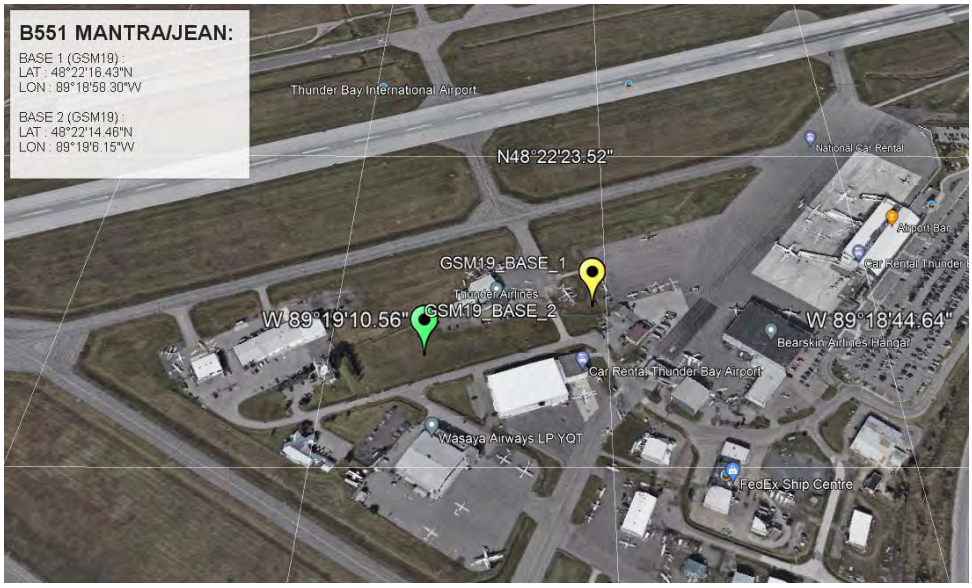

5.3 Operations Reporting

During survey flying, the pilot and operator maintain daily reports, a pre-flight safety report, and aircraft journey log. The base station magnetic data and airborne data are monitored throughout the duration of the survey and a record of all notes acquired by the operator are relayed to the data processor. At the end of a day of survey flying, the flight reports and data are uploaded to the project geophysicist who completes quality control inspection on the raw and compensated survey data. Additionally, the geophysicist transcribes the operator and quality control notes into a proprietary QA/AC assessment log.

All survey personnel crew adopted and worked under the Terraquest Ltd. Health, Safety and Environmental Protection Manual (which include Site Specific Safety Plan and Emergency Response Plan) along with guidelines from the IAGSA safety and security standards.

The survey was flown between the 16th and 21st of July, 2022. All the survey line data were collected in a single flight on July 21st, flight number 2145. There were 2 weather days, 1 mob day, 1 calibration day, and 1 set-up day. The geophysicist reviewed the data, created daily status reports, field flight path and total magnetic field preliminaries, and declared the data satisfactory.

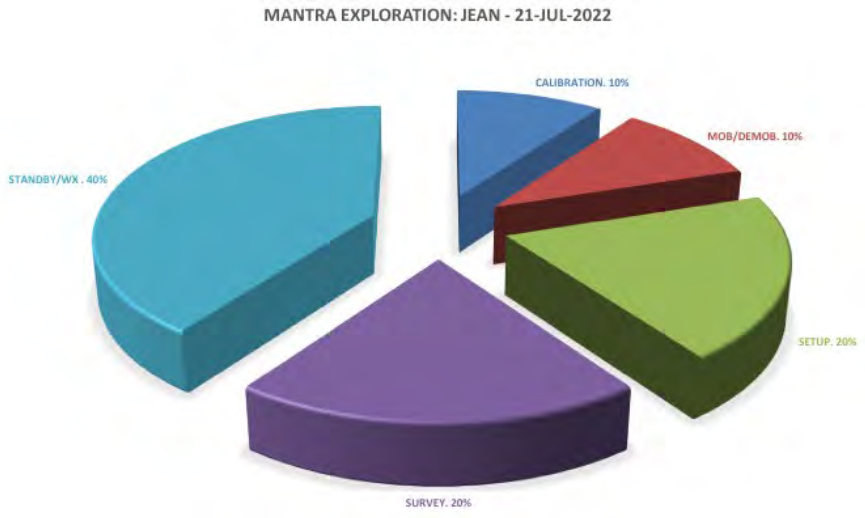

6 DATA PROCESSING

6.1 DATA QUALITY CONTROL

All field data are examined as soon as possible after a survey flight by the Processing Geophysicist to inspect the data for quality control and tolerances. All efforts are made to inspect the data prior to a subsequent survey flight to ensure the highest standard of data integrity. All accepted data have been inspected for continuity and integrity, and approved by the Processing Geophysicist.

6.2 PRE-PROCESSING OF POSITIONAL DATA (GPS)

Raw GPS data from the aircraft are recovered as binary files. The latitude, longitude and altitude data are recorded in WGS84 spheroid by default and is converted into the appropriate local coordinate system (as required). A point-to-point speed calculation is completed from the final X, Y co-ordinates and reviewed as part of the quality control. All flight data are trimmed to the survey boundary and a preliminary plot of the flight path is completed and compared to the theoretical pre-planned flight path to verify positional accuracy.

6.3 DIGITAL TERRAIN MODEL (DTM)

The radar altimeter data were subtracted from the GPS altitude to produce a Digital Terrain Model (DTM). The resulting data were micro-leveled to remove line-to-line imperfections in the data. The final grids were created using bi-directional Akima spline interpolation at a cell size of 25 metres.

6.4 FINAL MAGNETIC DATA PROCESSING

6.4.1 Magnetic Data Grids

All magnetic data grids were created using bi-directional data interpolation (Akima) at a cell size of 25 metres.

6.4.2 Lag Correction of Total Magnetic Field

The evaluation of the magnetic lag factor was accomplished by adjusting the lag across the survey area to achieve the most effective lag. The established lag values were 0.7 seconds for the tail Mag and 0.5 seconds for the wing tips.

6.4.3 Diurnal Data and Diurnal Corrections of the Total Magnetic Field

Magnetic data from the diurnal base station were scrutinized for spurious readings (data spikes) and any obvious cultural interference. Any such features were manually removed and the data re-interpolated (Akima spline) to maintain a continuous record. A low-pass filter (60 fid cut-off wavelength) was applied to the edited diurnal record. The resulting data were used to pre-level (diurnally correct) the measured TMI data for the Tie and Traverse lines prior to implementing Tie-Traverse intersection leveling.

6.4.4 Total Magnetic Field Tie-Traverse Line Intersection Levelling

The lag-corrected, pre-treated (altitude correction) data were refined using tie-line levelling. Using the Geosoft Oasis implementation of this procedure, an initial table of tie-traverse line intersection differences is compiled (together with supporting ancillary parameters such as local gradient, etc.) and intersection data is loaded into the processing databases. In a series of iterative levelling passes, outlier intersection values are either disabled or modified to refine and finalize the overall result.

6.4.5 Total Magnetic Field Micro-Levelling

Minor levelling imperfections may still exist in the gradient enhanced intersection levelled data, most likely due to incomplete removal of diurnal influences in sections of lines between intersection points. These errors are removed by application of mild micro-levelling procedure whereby highly directional filtering identifies and removes residual noise correlated with the line direction. The resulting corrections are limited to the maximum amplitude of +/- 8 nT to avoid “damaging” valid, geologic responses to achieve the Total Magnetic Intensity.

6.4.6 Anomalous Total Magnetic Field

To achieve the *Anomalous Total Magnetic Intensity* for this survey, the International Geomagnetic Reference Field (IGRF) was obtained from the 2020 model year and extrapolated to July 21 2022 at an effective mean survey elevation of 508 metres above sea level, these were removed from the processed values to create the Anomalous Total Magnetic Field.

6.4.7 Calculated Magnetic Vertical Derivative

The first *Vertical Derivative* was calculated using a 2D FFT operator on the Total Field data grid. Unwanted, high frequency "ringing" in the resulting 1VD grid was minimized by concurrent application of an 8th order Butterworth low pass filter with a cut-off keyed to the line spacing.

6.4.8 Calculated Magnetic Analytic Signal

The angle of the earth's magnetic field at this survey latitude is flattened to some degree, affecting the apparent location of magnetic sources in the Total Magnetic Intensity map. The resulting interpretational complexity may be simplified by calculation and display of the magnetic *Analytic Signal*. It is derived from the three orthogonal magnetic gradients using the Geosoft module. This feature has the advantage of producing body centric anomalies - regardless of magnetic inclination - with source edges mapped out by the function's maxima. Additionally, approximate source depth may be estimated by measuring individual anomaly widths at half amplitude

6.4.9 Measured Magnetic Horizontal Gradients

Terraquest solves the spatial mathematical relationship of the three total field measurements (left, right and tail) by using the accurate location of the three magnetic sensors in space to directly calculate the East-West and North-South gradients, referenced to geographic north, at each point along the survey line.

Both *Horizontal Gradients* were then median leveled to remove bias, followed by mild micro-leveling to remove any remaining imperfections. Following this, the transverse and longitudinal gradients were gridded using a bi-directional Akima algorithm and a cell size of 25 metres. The measured transverse and longitudinal gradients provide an improved rendition of the shorter wavelengths in magnetic field than the residual magnetic field measured by the tail sensor alone. This is because the direction and amplitude of the field's total horizontal gradient can be determined using the 2 measured gradients, providing information regarding the behavior of the magnetic field in-between traverse lines. Thus, it is useful to incorporate the gradient data in the preparation of the residual magnetic field grid.

6.4.10 Magnetic Reconstructed Total Field (RTF)

Data grids of the measured horizontal gradients (HX, HY) were used to generate the Reconstructed Total Magnetic Field using the 2D FFT process described by J. B. Nelson*. This product (RTF) has the advantage of being un-affected by magnetic diurnal activity, though longer magnetic spatial wavelengths are not represented due to measurement resolution limitations in the magnetometers. The resulting data units (expressed as pseudo nanoTesla) are not true nT: approximate conversion to true nT may be accomplished by application of scaling factor if required. Using the calculated Reconstructed Total Field data grid, an "RTF" Geosoft database channel is created by performing a grid look-up ("grid sample") for each data point in the production database. Only grids were produced for the Total Reconstructed Field.

(Reference: Nelson, J.B., 1994, Leveling total-field aeromagnetic data with measured horizontal gradients: Geophysics, 59, 1166-1170).

6.4.11 Final Magnetic Maps

B551_MAN_JEAN_M01_DTM: Flight Path with Digital Terrain Model

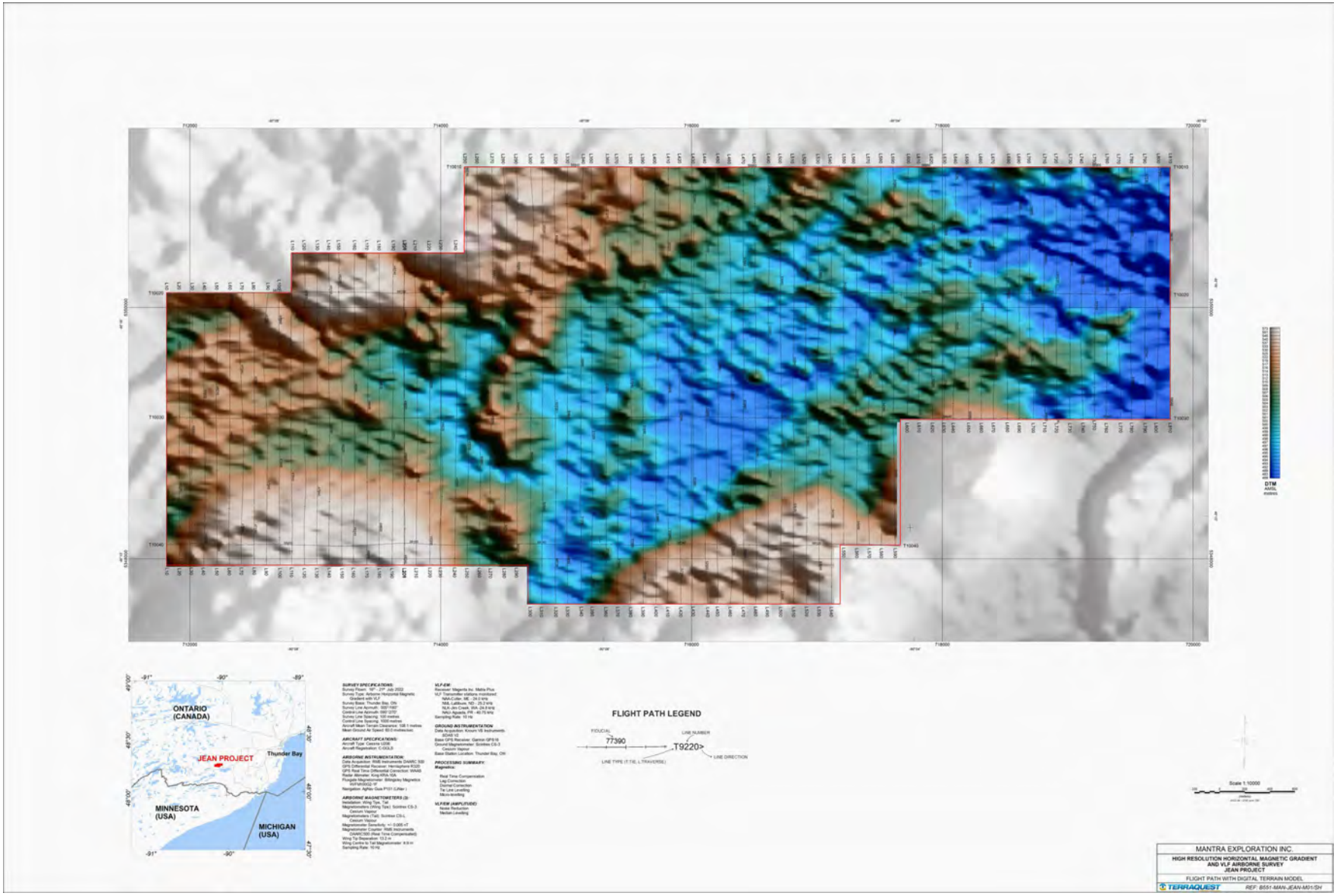

B551_MAN_JEAN_M02_TMI: Total Magnetic Intensity

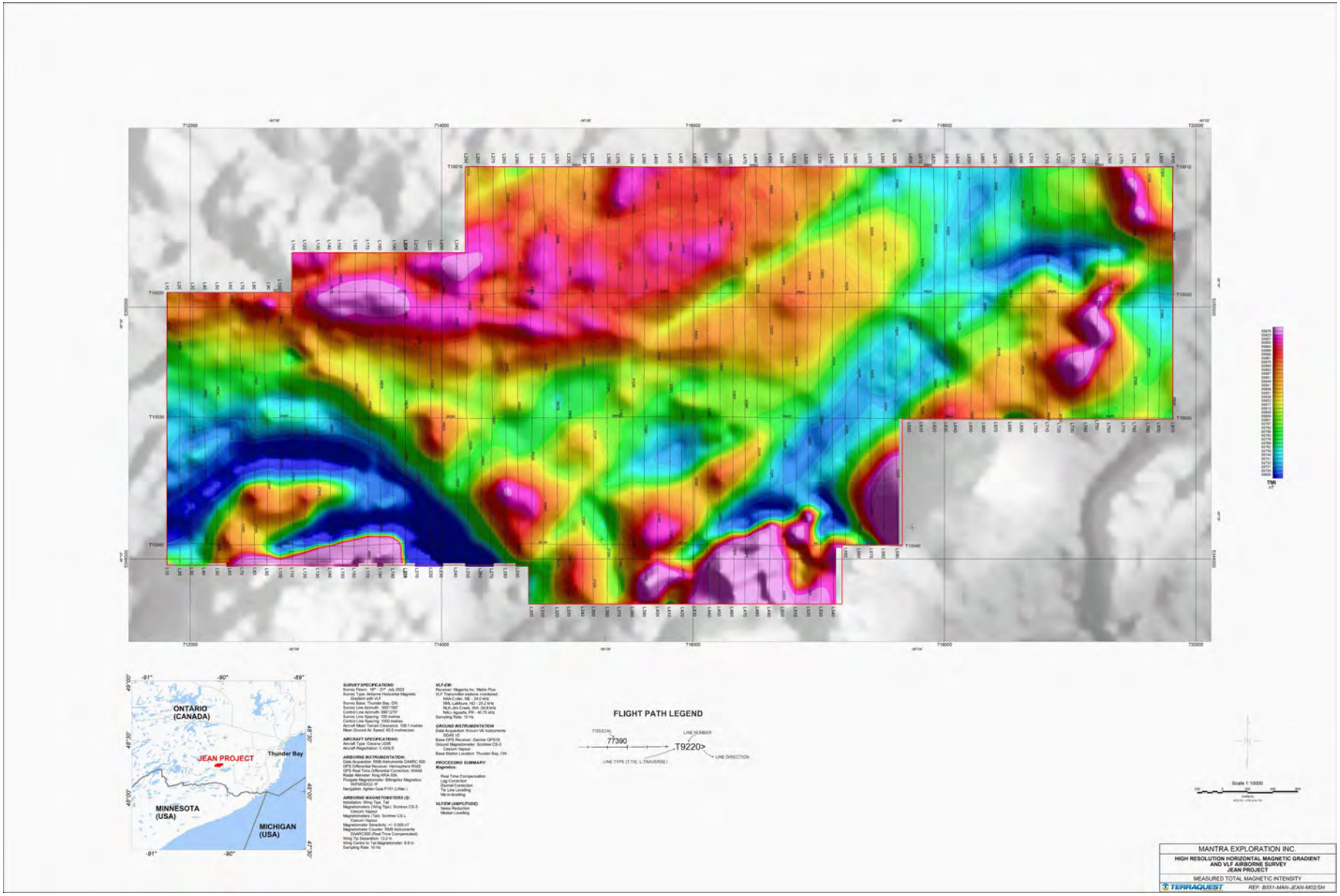

B551_MAN_JEAN_M03_TMIANM: Anomalous (IGRF corrected) Total Field with contours

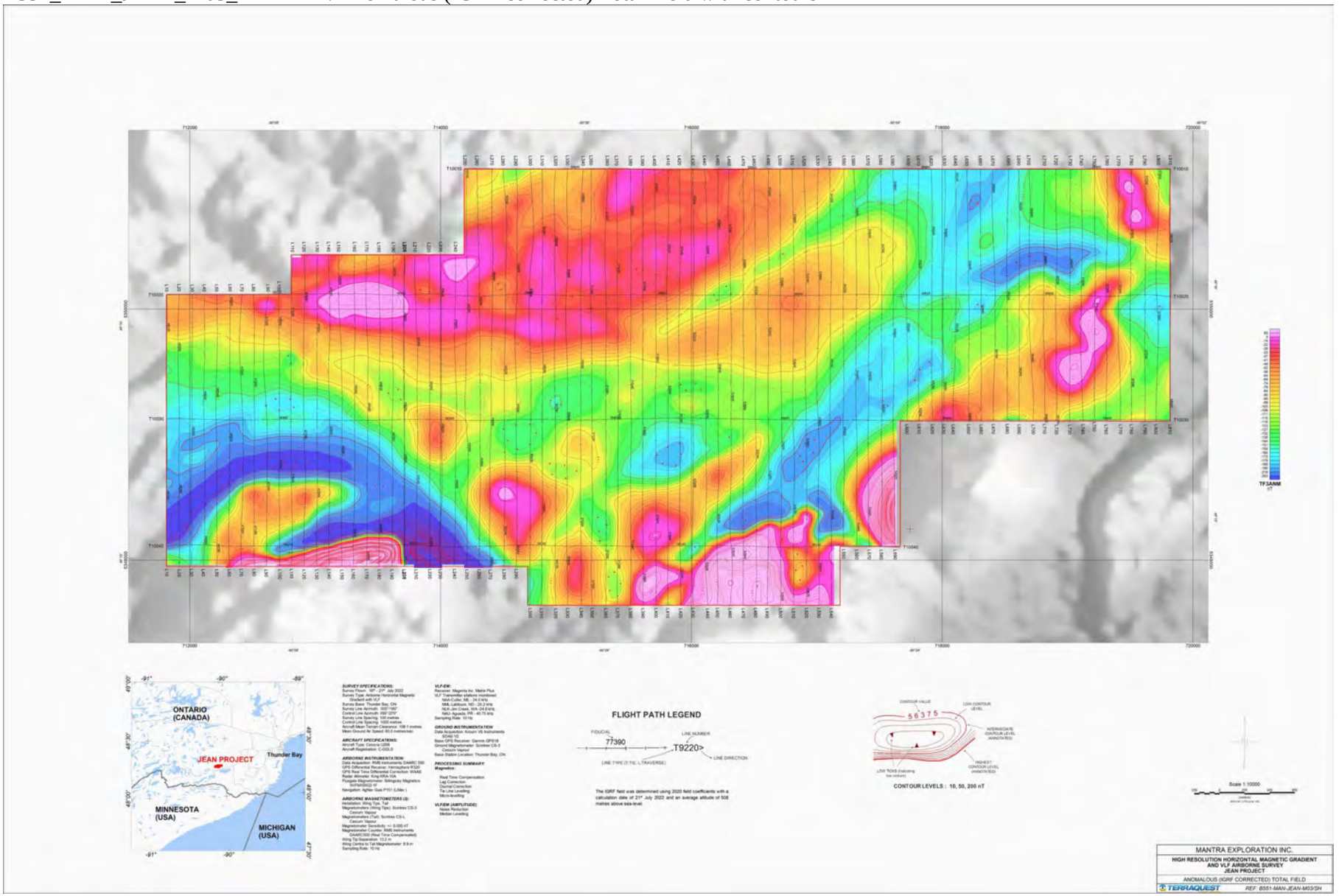

B551_MAN_JEAN_M04_TMIVD1: Calculated Vertical Magnetic Derivative

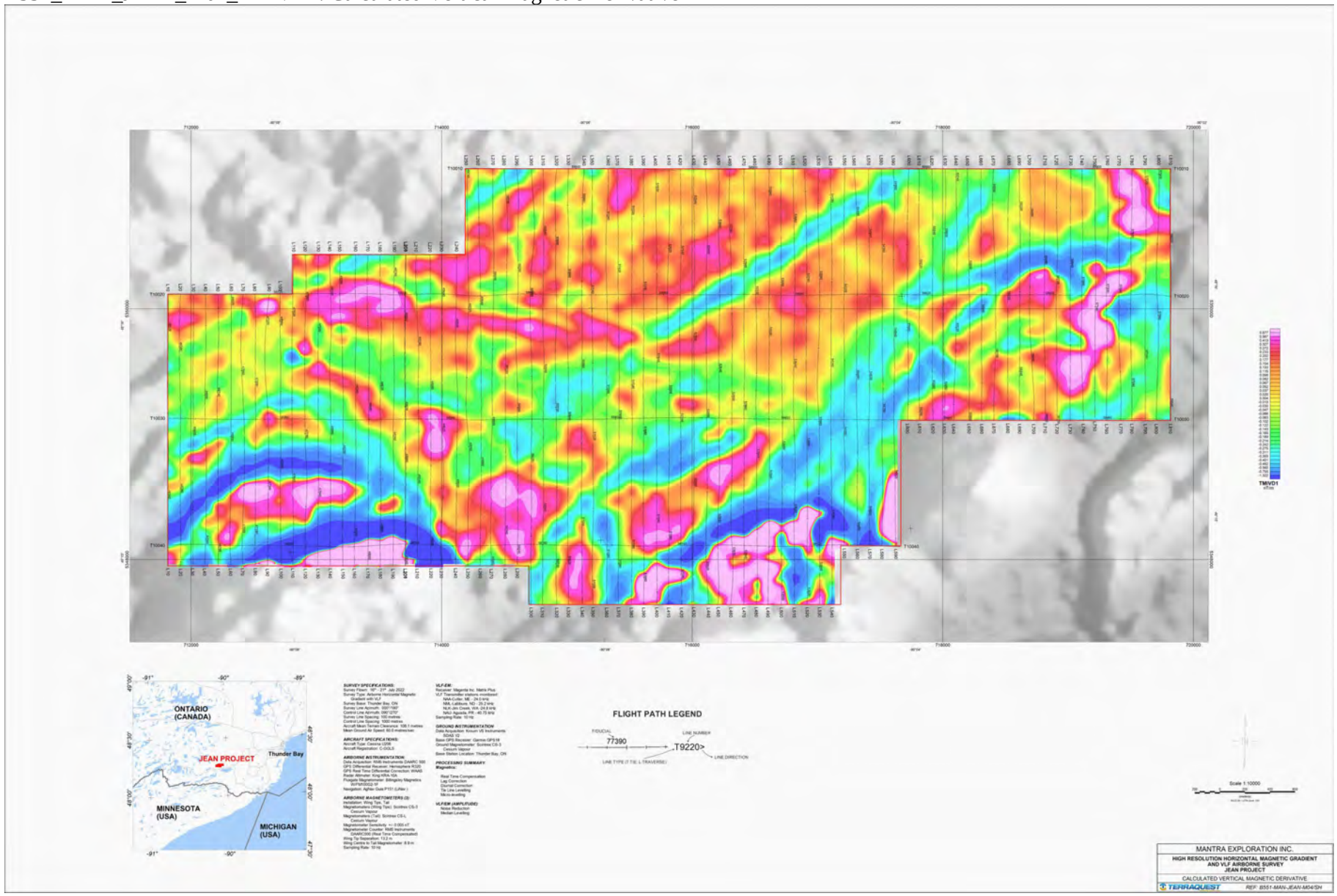

B551_MAN_JEAN_M05_ANSIG: Calculated Analytic Signal

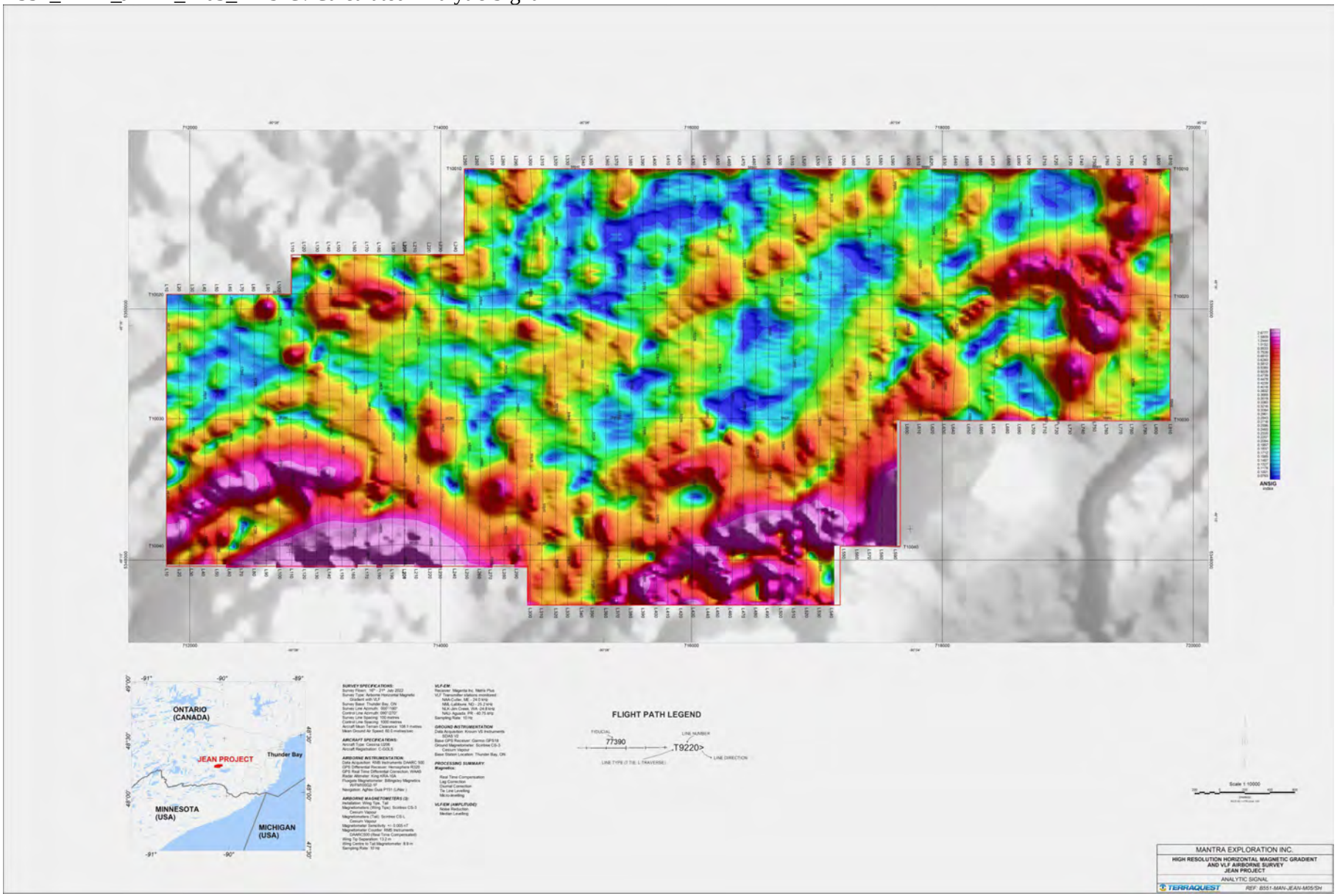

B551_MAN_JEAN_M06_HGEW: Measured East-West Magnetic Gradient

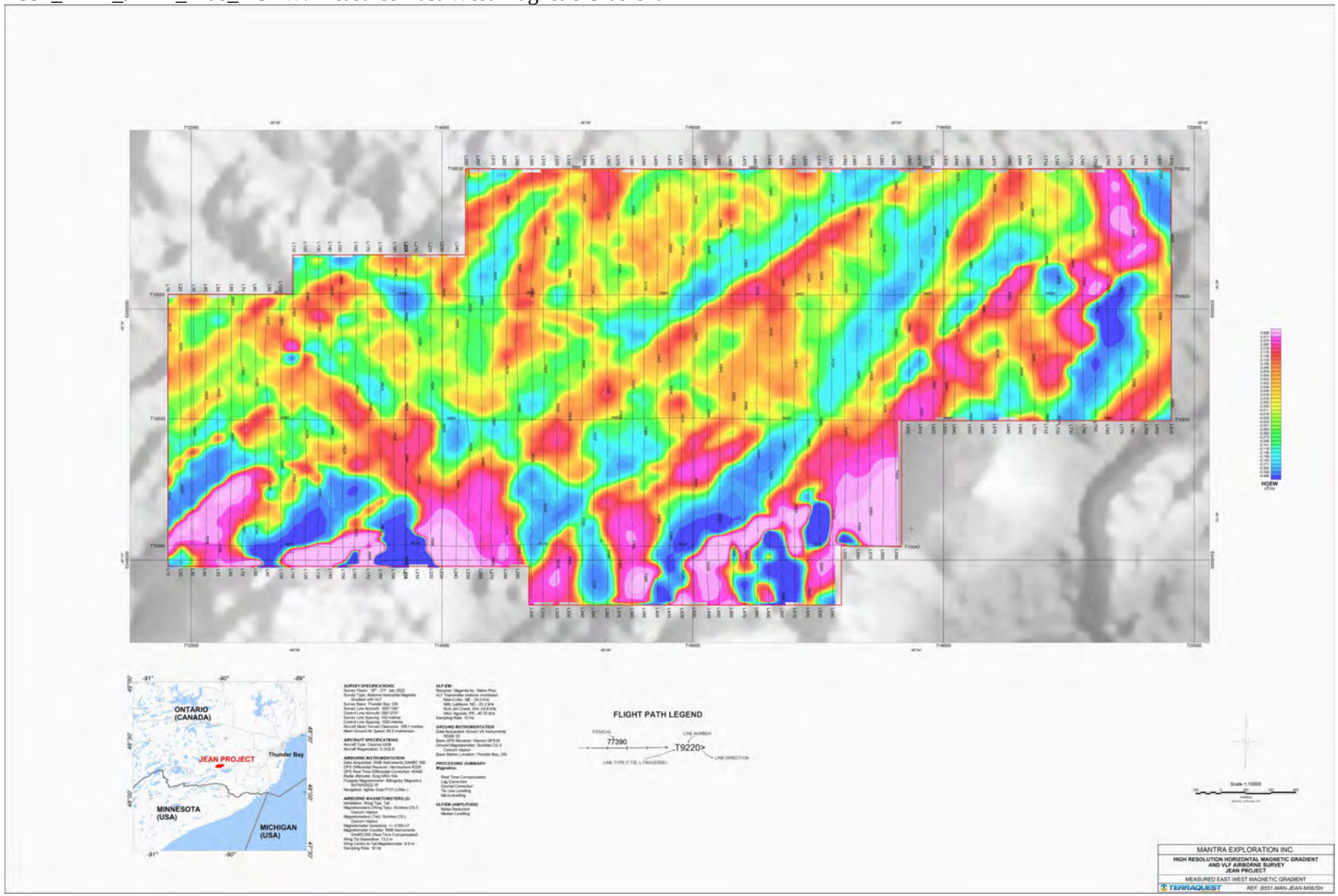

B551_MAN_JEAN_M07_HGNS: Measured North-South Magnetic Gradient

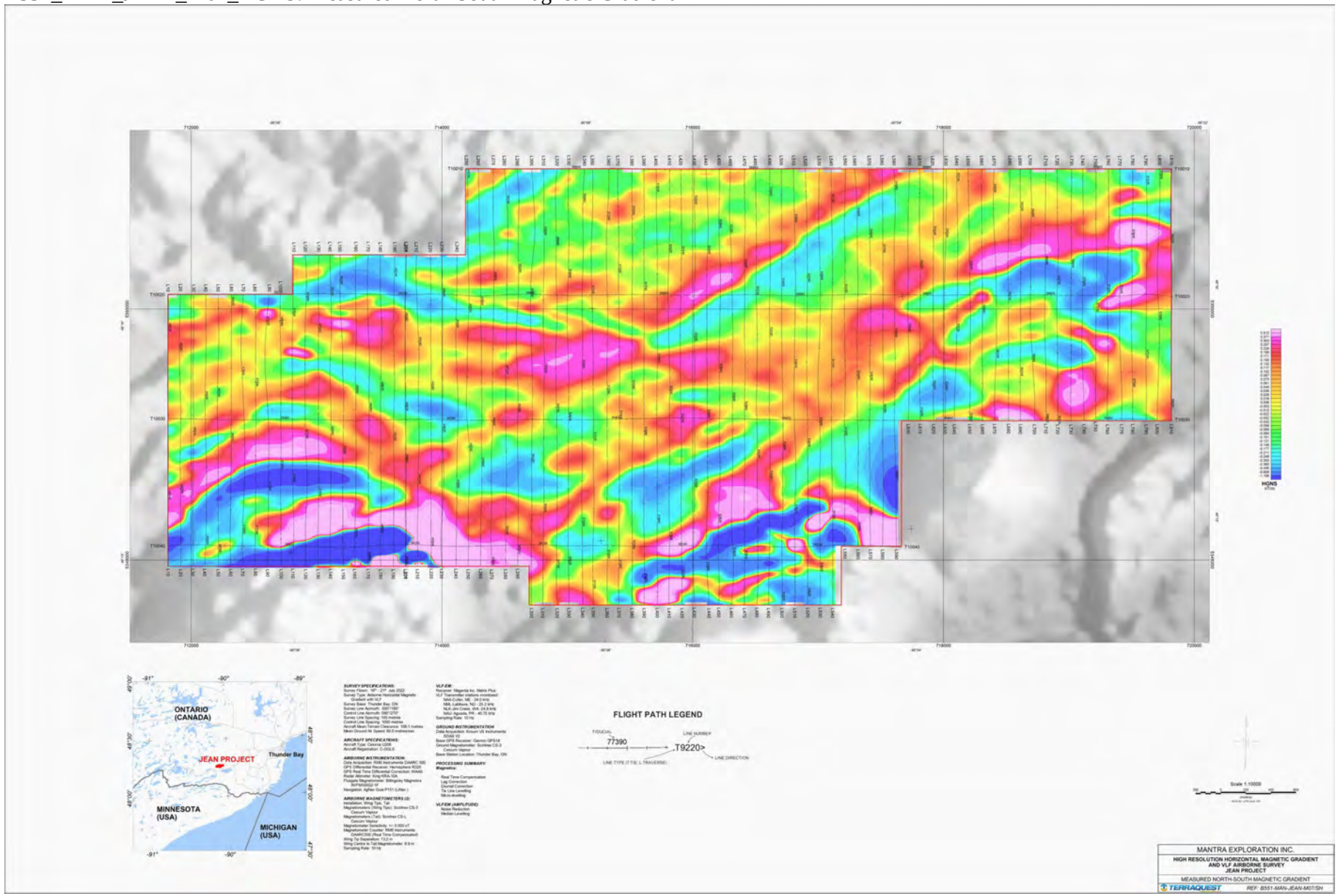

B551_MAN_JEAN_M08_RTF: Reconstructed Total Magnetic Field

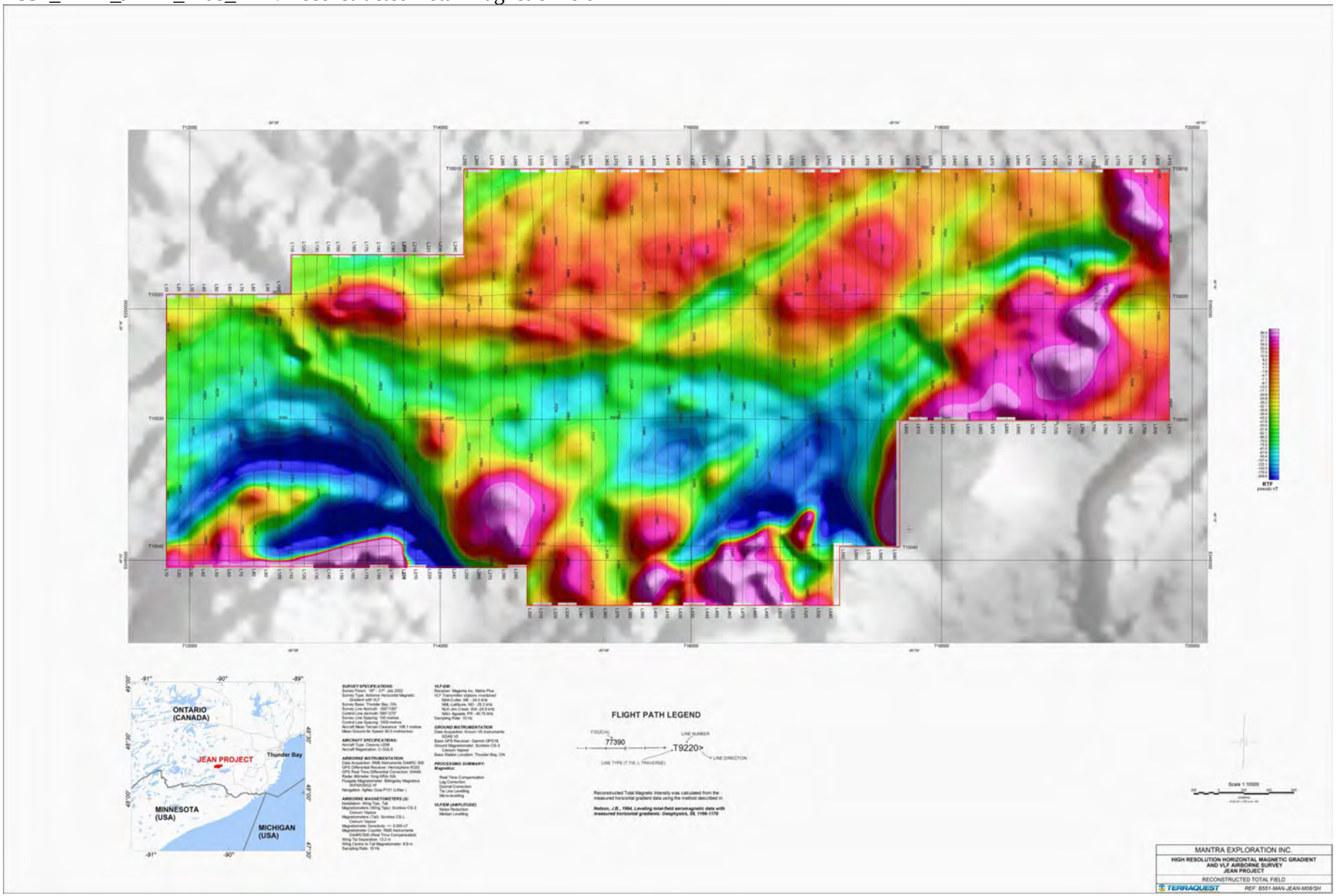

6.5 VLF-EM

6.5.1 VLF Station Signal Reception

Not all stations monitored provide usable signal. Generally, the quality of the signal is dictated by the transmitter source power and its distance from the survey area. Furthermore, as with all Electromagnetic (EM) wave propagation, the quality and/or power of the signal may also be degraded further with the natural earth features between the transmitter source and the receiver.

Most VLF stations have a scheduled maintenance cycle but transmitters may be down for other reasons from time to time. For example, NAA Cutler, Maine is typically down for maintenance for all (or part of) Monday; NML LaMoure, North Dakota on parts of Tuesdays; and NLK Seattle, Washington progressively throughout Wednesday. Unlike magnetic data, VLF-EM data have a relatively broad wavelength and do not require close line intervals. Data acquisition is conducted in a manner that ensures VLF signal is available at an appropriate line interval throughout the survey area. Usually this means that at VLF data is acquired for least every other survey line but generally depends on the survey line spacing and the availability of transmitter signal. Known VLF interruptions or transmitter unavailability is typically used to accomplish other duties that do not rely on VLF transmitter availability (i.e. fly survey control lines, perform aircraft maintenance, etc.).

A rare, brief outage on Cutler occurred on this survey on 4 short lines (6300,6400,6500 & 6600); at this survey location Cutler and Jim Creek are almost 180 degrees apart, such that their angle of energization is almost the same and therefore have similar results.

In general, the following VLF transmitters can be observed and monitored and recorded for this survey are as follows:

Name	Latitude	Longitude	Power	Location	Frequency (Hz)	Distance (km)	Azimuth (degrees)
NAA	44.64450	-67.28456	1000kW	Cutler, Maine (USA)	24.0Hz	1785	94.4
NML	46.36598	-98.33566	500kW	LaMoure, North Dakota (USA)	25.2 kHz	655	254.3
NLK	48.20363	-121.9168	192 kW	Jim Creek/Oso, Washington (USA)	24.8 kHz	2340	281.8
NAU	18.39877	-67.17748	100kW	Aguada, Puerto Rico, USA	40.75kH	3911	140.1

Transmitter power, distances and azimuths relative to the survey block are illustrated below and also on the associated Project maps.

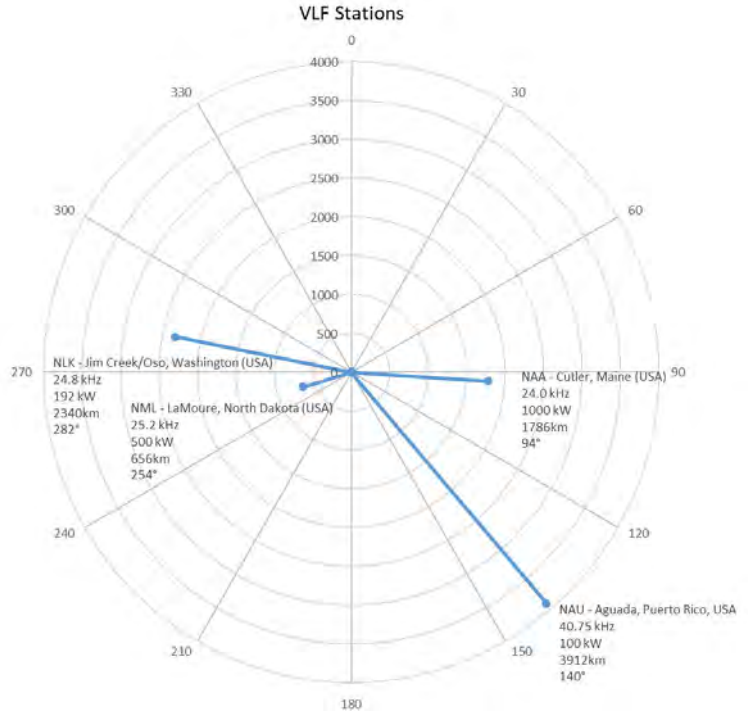

6.5.2 Matrix Plus VLF-EM Processing Total Field

The Total Field Amplitude data were processed from the strongest and clearest signals (Cutler-NAA, Jim Creek-NLK and LaMoure-NML) as follows:

1. Mask out any embedded "off-line" data.
2. Noise reduction filtering using non-linear Naudy filtering (5-point filter width), gridded with 25 metres grids.
3. Initial leveling (mean subtraction).
4. Fine leveling (micro-leveling).
5. Application of bias offsets such that finalized data ranged positive.

The finalised amplitude data are presented as a colour image of total field strength (amplitude). Conductor axes and other VLF anomalous features (topographic effects, conductive lake sediments, etc.) are mapped by "hot" colours (light brown -> white) as peak centric lineaments.

In order to improve the resolution of the conductor axes, the final corrected Amplitude data were high-pass filtered (30 fid cut-off) and used to create data grids which were analysed with a peak-detection algorithm (Blakely algorithm). The resulting peak locations were marked and superimposed on the amplitude images to emphasize conductor axes. The Peak Markers are also provided separately as a GeoTiff overlay (set white to transparent).

As additional products that may be useful in further interpretation, the *In-phase* and *Quadrature* have been calculated respectively from the Tilt and Vertical Ellipticity components from each of the three selected transmitters and included in the data ARCHIVE.

Raw data from NAU Aguada, Puerto Rico was also logged and available in the ARCHIVE.

6.5.3 Matrix Plus VLF-EM Total Field Maps

B551_MAN_JEAN_M09_NAA: VLF Amplitude (Station NAA, Cutler, Maine)

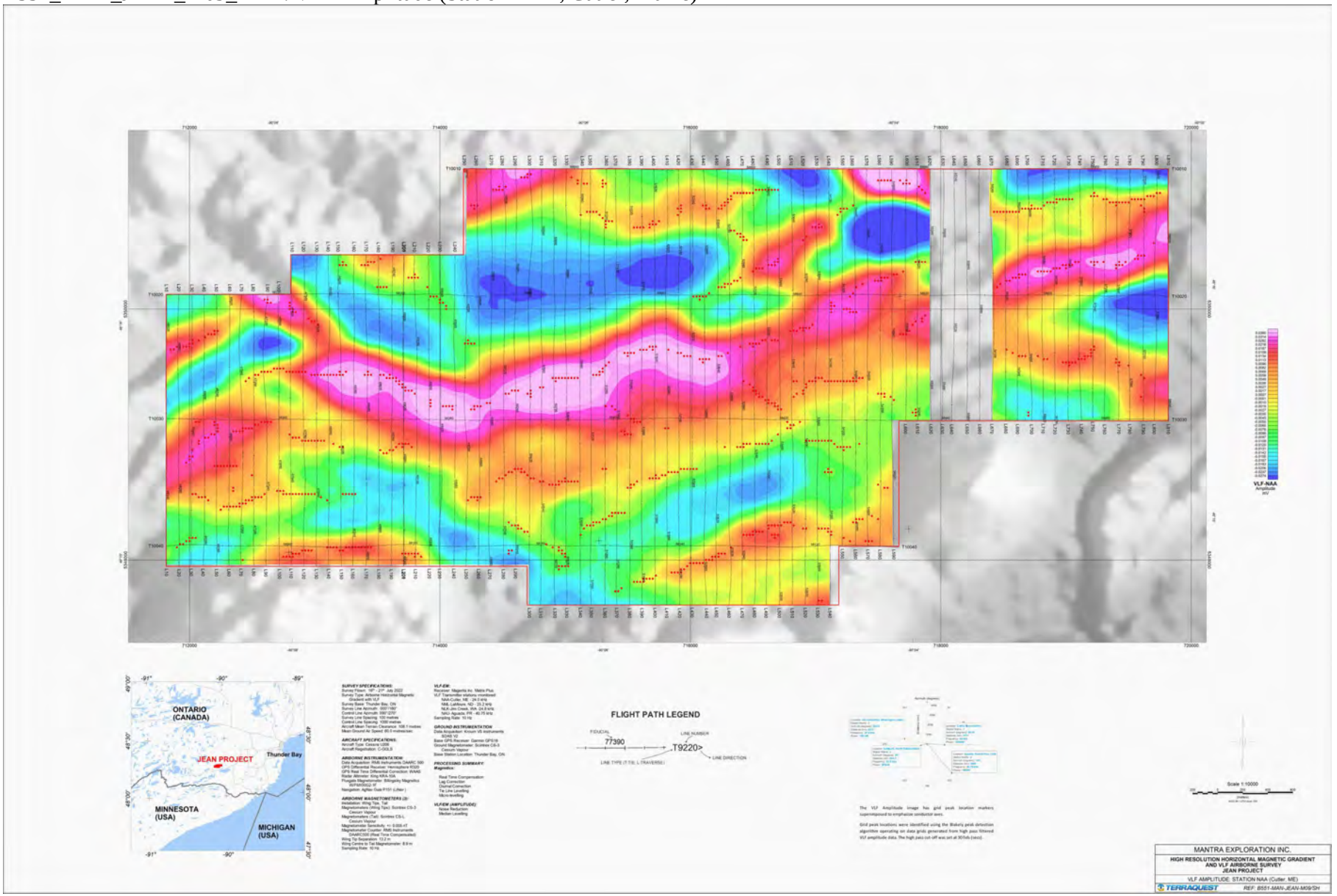

B551_MAN_JEAN_M10_NML: VLF Amplitude (Station NML, LaMoure, North Dakota)

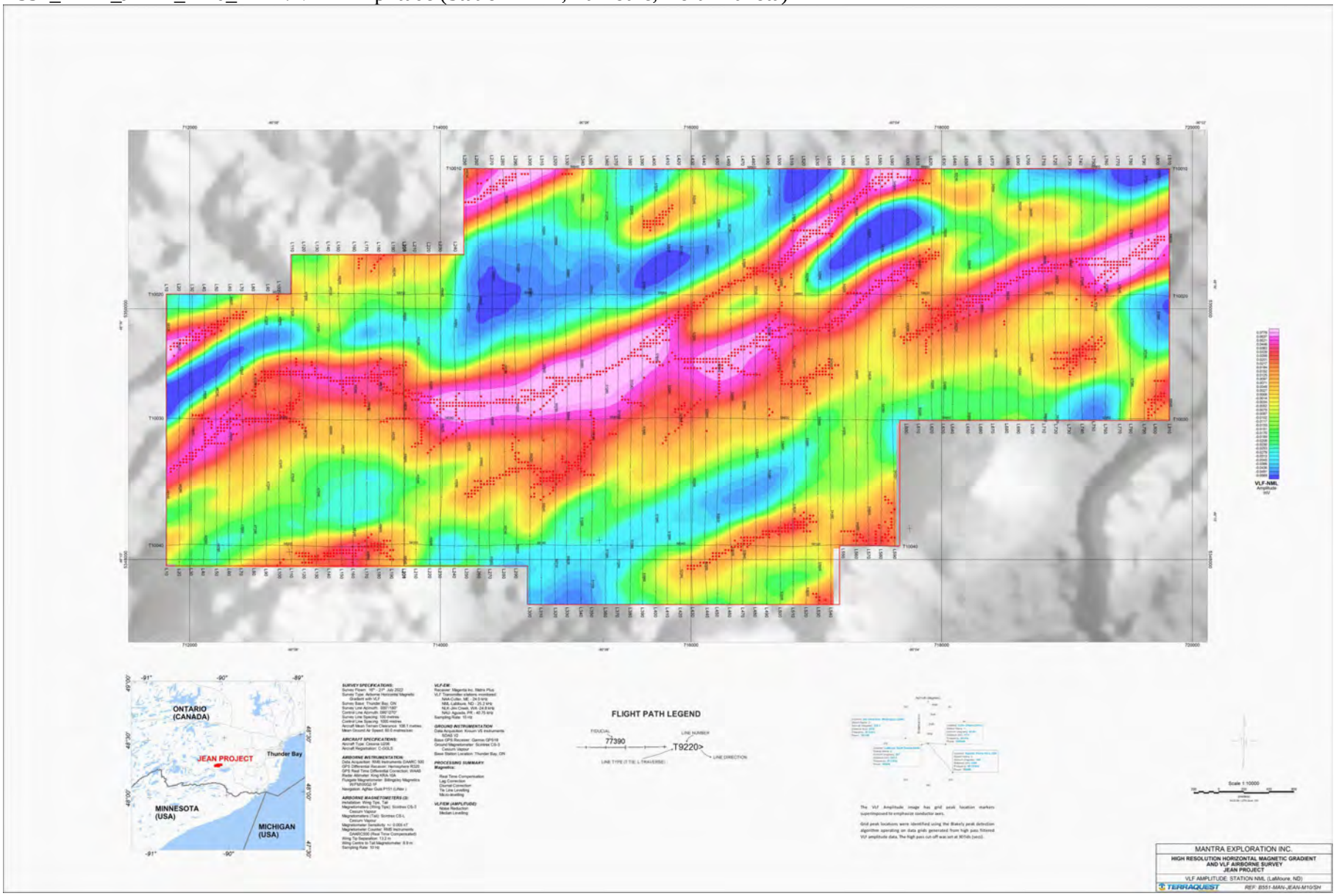

B551_MAN_JEAN_M11_NLK: VLF Amplitude (Station NLK, Jim Creek, Washington)

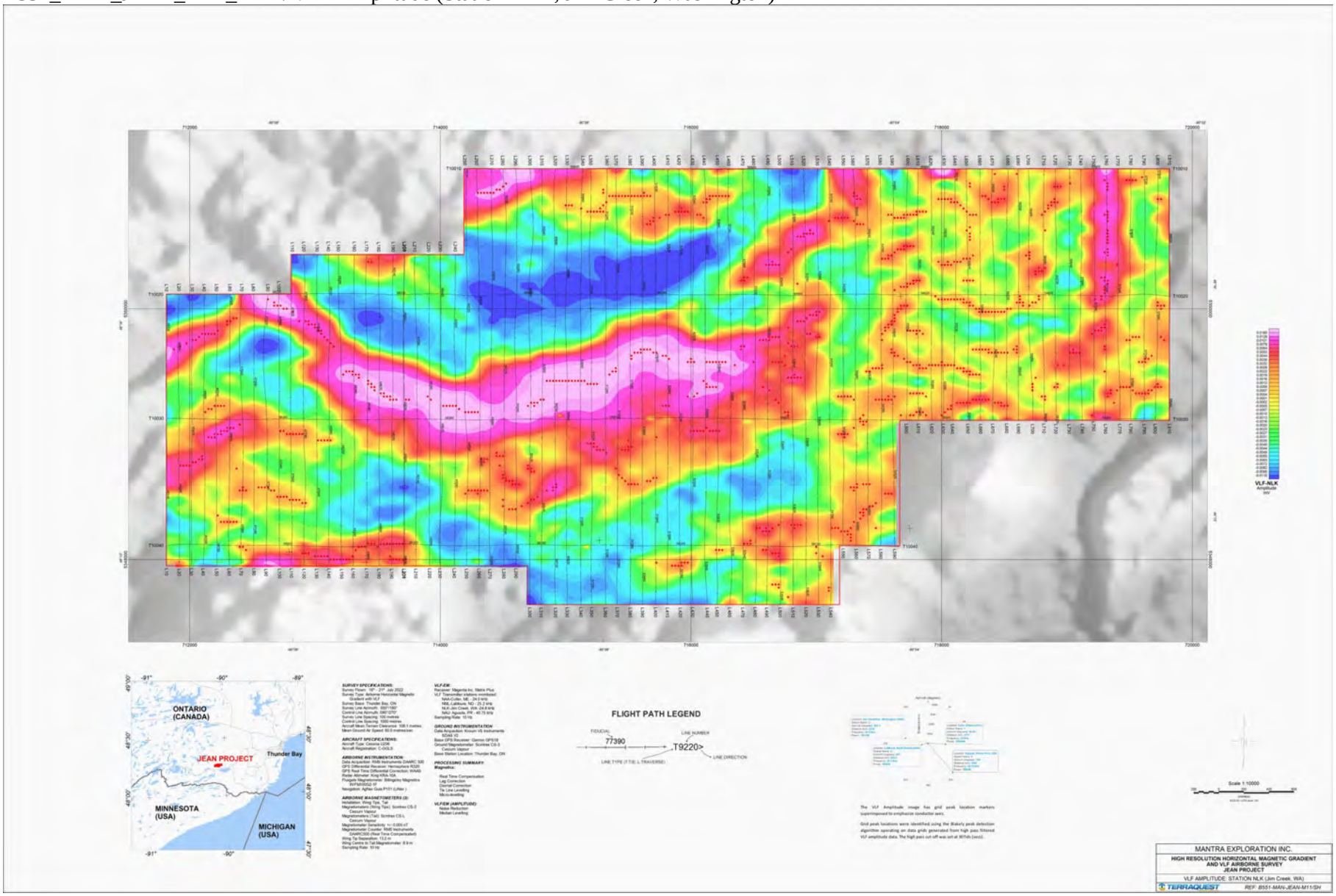

6.6 MATRIX-PLUS VLF-EM INVERSE MODELLING

6.6.1 Inversion Theory

The VLF signal used in prospection is generated by communication antennas working in the frequency range of 10 kHz to 40 kHz. These transmitter antennas behave like electric dipoles and its associated electromagnetic field (primary field) travels radially outward via two propagation mechanisms: along the earth's surface (wave guided) and by reflection at various charged layers in the ionosphere at altitudes of 60-400 km. The variable primary field induces electrical currents, mainly in conductive structures orientated parallel to the direction the electric field source (VLF transmitter). The induced currents generate an electromagnetic field (secondary field) that can be detected at surface or at some height by the receiver. Having a vertical component of the magnetic field, the following relationship exists between horizontal and vertical components:

$$H_z = T_{zy} H_y$$

where T_{zy} is the magnetic transference function or Tipper. In VLF-EM, the data are the In-phase and Quadrature, or the real and imaginary parts of the tipper (H_z^s/H_y, where H_z^s and H_y are the vertical component of the secondary field and the horizontal component of the total magnetic field.

The nonlinear, smoothness-constrained inversion algorithm (Sasaki, 1989, 2001; DeGroot and Constable, 1990) was adopted for VLF inversion (Monteiro Santos et al., 2006). The inversion is performed by an iterative process that allows the final model to be obtained, with its response fitting the data set in a least square sense. At each iteration, the optimization equations that must be solved to get the corrections of the parameters are represented as follows:

$$(J^T J + \lambda C^T C)\delta\vec{p} = J^T\vec{b}$$

Where $\delta\vec{p}$ is the vector containing the corrections applicable to the parameters (logarithm of block conductivity, σ_j) of an initial model, $\vec{b} = \overrightarrow{T^o} - T_i^c ist$ is the vector of the differences between the observed and calculated tipper components, **J** is the Jacobian matrix whose elements are given by $(\sigma_j)(\partial T_i^c/\partial\sigma_j)$, the superscript T denotes the transpose operation, and λ is a Lagrange multiplier (Damping factor) that controls the amplitude of the parameter corrections and whose best value is determined empirically. The elements of the matrix **C** are the coefficients of the values of the roughness in each parameter, which is defined in terms of the four neighbours' parameters.

DeGroot-Hedlin C. and Constable S.C., 1990. Occam's inversion to generate smooth, two-dimensional models from magnetotelluric data. Geophysics, 55, 1613-1624.

Monteiro Santos, F.A., António Mateus, Jorge Figueiras, Mário A. Gonçalves, 2006. Mapping groundwater contamination around a landfill facility using the VLF-EM method – a case study. Journal of Applied Geophysics.

Sasaki Y., 1989. Two-dimensional joint inversion of magnetotelluric and dipole-dipole resistivity data. Geophysics, 54, 254-262

6.6.2 Resistivity Processing

Based on the quality of the Matrix-Plus data on this survey and correlation with airborne magnetic data, the client requested to have the data inverted to calculate the resistivity. The final processed Total Field Strength and all recorded parameters were sent to EMTOMO to perform recently developed inversion procedures designed specifically for airborne VLF-EM data. The resulting Profile Geosoft databases include the modelled inversions calculated at 5, 10, 20, 40, 60, 80 and 100 metre depth planes (x, y, z format) for all three selected VLF stations.

Terraquest then final leveled and gridded each depth plane using Minimum Curvature gridding with 25 m grid cell size and stored in a Geosoft Grid format (Resistivity Grid Database) as a series of numerical lattices corresponding to each individual depth inversion which are useful for creating 3D data grids. These depth inversion planes have been stacked as pseudo three-dimensional montages and presented along with map images for each 2D map image.

Additionally, 3D grids (25x25x5m) in Geosoft VOXEL format of resistivity of all three VLF stations were created with voxel size 25x25x10 metres (x, y, z dimensions) and included in the final archive (refer to README file Appendix V – Readme file Part II); these are best visualized on a computer using 3D rotatable software to select desired parameters and views.

6.6.3 VLF-EM Resistivity Depth-Planes Maps

B551_MAN_JEAN_M12_VLF_RESISTIVITY_NAA

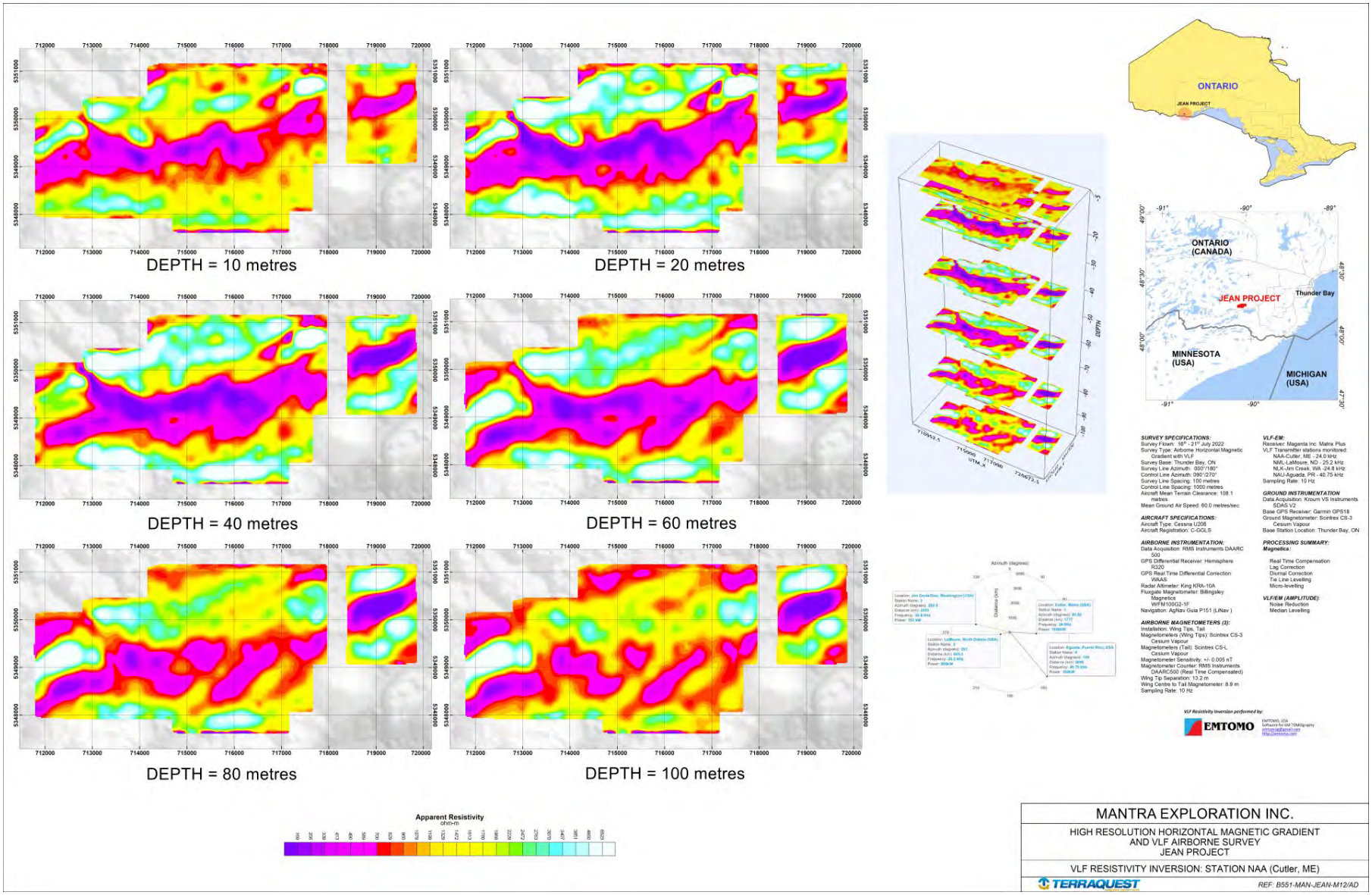

B551_MAN_JEAN_M13_VLF_RESISTIVITY_NML

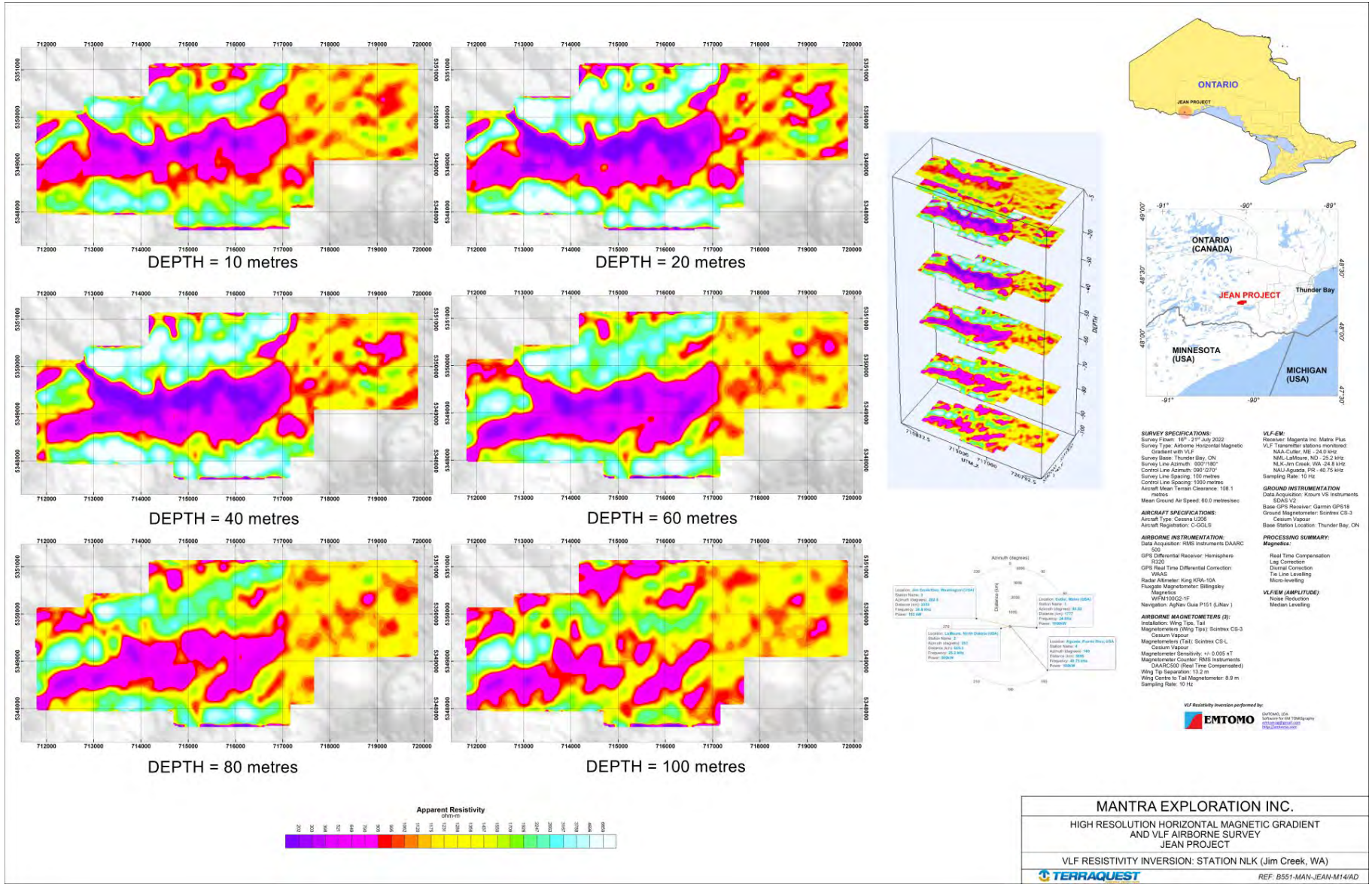

B551_MAN_JEAN_M14_VLF_RESISTIVITY_NLK

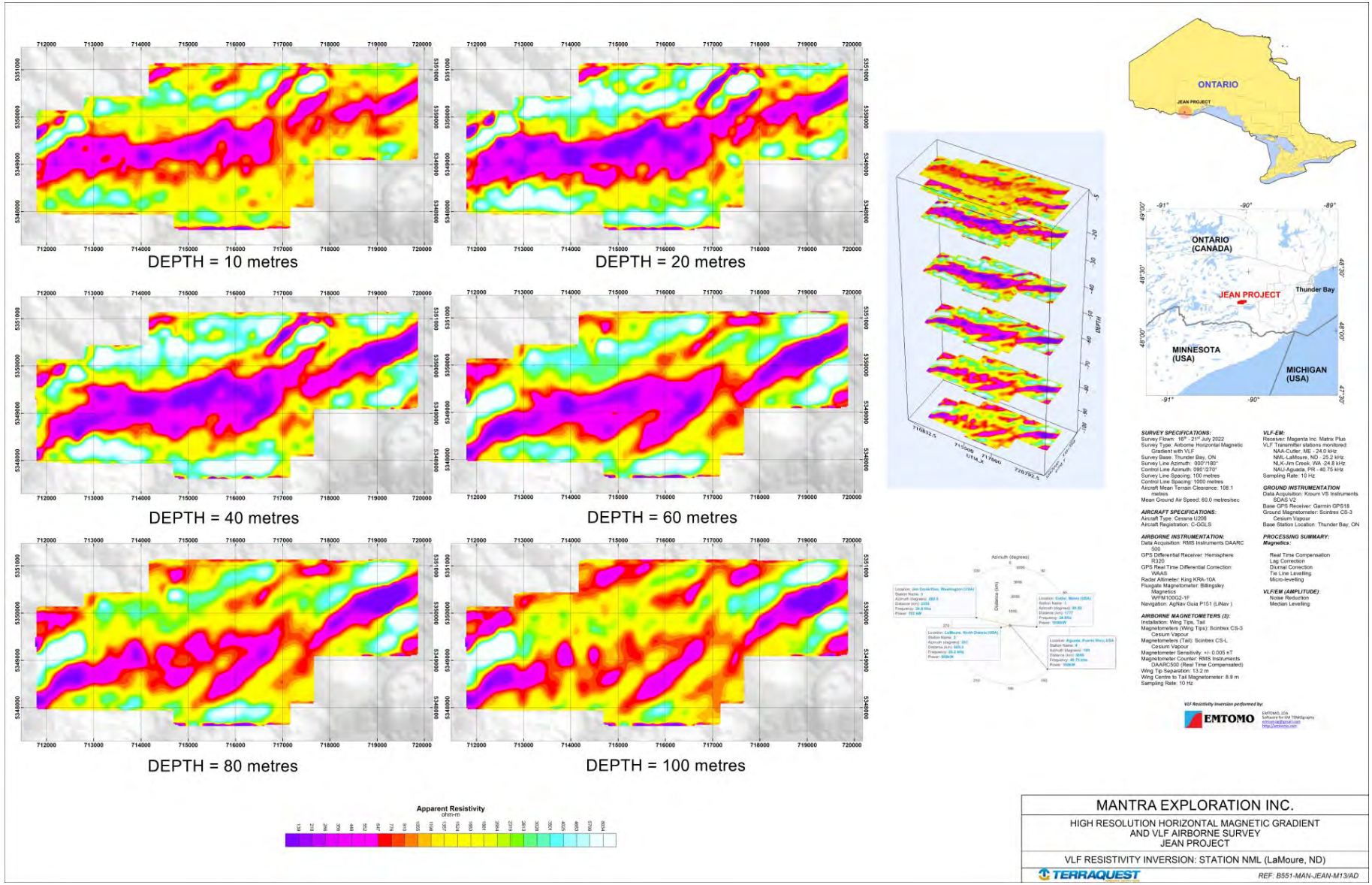

7 FINAL PRODUCTS

A complete list of all final products is listed in the ReadMe file Appendix V – Readme files Part I and II. All products including this Report are contained on an Archive USB stick in the back pocket of the Report

7.1 DATABASE

Final data are provided in a Geosoft Database (*.gdb) format compatible with 4.1 or higher. The Geosoft GDB (*.gdb) file is a binary file that can hold tables of various types of data. The column names and column data types are identical across all the tables. The database contains all the projection information necessary to properly position the data.

7.2 RASTER GRIDS

Raster representation of the final data is provided in Geosoft Grid format (*.grd). A Geosoft grid is a binary format for storing raster data commonly used for geophysical and elevation data. Two files describe each raster grid, a *.GRD and a *.GI). The *.GRD file contains the data while the accompanying *.GI file contains the spatial reference information. If the *.GI file is absent the projection information can be applied manually. Magnetic data grids are prepared using Bi-directional (Akima) spline interpolation, with a grid cell size typically one-quarter to one-fifth the average line spacing. VLF data grids are usually prepared using a Minimum Curvature interpolation with a grid cell size one-half to one-third the average line spacing due to the relative low frequency of the received signal.

7.3 VECTOR LAYERS

Spatially referenced vector data layers are provided in GeoTIFF format. GeoTIFF is a public domain metadata standard that enables georeferencing information to be embedded within a Tagged Image Format File (TIFF). The GeoTIFF format embeds geospatial metadata into image files such as VLF-EM Profile Peak Markers, survey flight path, and grid line contours so that they can be used spatially referenced data layers. These images are created using high resolution (300dpi) with the transparent layer set to white.

7.4 MAPS

The digital maps are provided at a scale of 1:10,000 in full resolution (300 DPI) in *.PNG format and low resolution (email-able, files in sub folder 'LORES') in *.JPG format. One set of the high resolution maps has been plotted on high quality drafting film. Page size versions of the LORES map images are provided in this report. List of maps is shown below:

```
B551_MAN_JEAN_M01_DTM      : Flight Path with DTM grid
B551_MAN_JEAN_M02_TMI      : Total Magnetic Intensity
B551_MAN_JEAN_M03_TMIANM   : Anomalous (IGRF corrected) Total Field with contours
B551_MAN_JEAN_M04_TMIVD1   : Calculated Vertical Magnetic Derivative
B551_MAN_JEAN_M05_ANSIG    : Calculated Analytic Signal
B551_MAN_JEAN_M06_HGEW     : Measured East-West Magnetic Gradient
B551_MAN_JEAN_M07_HGNS     : Measured North-South Magnetic Gradient
B551_MAN_JEAN_M08_RTF      : Reconstructed Total Field
B551_MAN_JEAN_M09_NAA      : VLF Amplitude (Station NAA, Cutler, Maine)
B551_MAN_JEAN_M10_NML      : VLF Amplitude (Station NML, LaMoure, North Dakota)
B551_MAN_JEAN_M11_NLK      : VLF Amplitude (Station NLK, Jim Creek, Washington)
B551_MAN_JEAN_M12_VLF_RESISTIVITY_NAA
B551_MAN_JEAN_M13_VLF_RESISTIVITY_NML
B551_MAN_JEAN_M14_VLF_RESISTIVITY_NLK
```

7.5 VOXELS

Inversion data is compiled into a 3-D representation called a Geosoft Voxel. Voxels are the common term for a “volume pixel” and are essentially a 3-D conceptual counterpart of the 2-D pixel. A voxel is the smallest distinguishable box-shaped element that represents a specific grid value in 3D space

7.6 REPORT

The operations report (this file) summarizes details for the execution and completion of this project. This includes pertinent details about each stage of the project including the survey planning, data acquisition, data processing and final deliverables.

8 SUMMARY

An airborne high sensitivity, Horizontal Magnetic Gradient and VLF-EM plus Inverted Resistivity Survey was performed for Mantra Exploration Inc. over the Jean Project located near Thunder Bay, Ontario. It was flown with a preplanned controlled drape mode based on 70 metres above the highest obstacle, with an average height of 108.1 metres above the ground taking into account narrow incised valleys. The combined traverse and control line kilometres flown for this project was 245.61 kilometres. At 10Hz and an average speed of 60.0 m/s the data sample point density along the lines is approximately 6 metres. The base of operations was located at Thunder Bay, Ontario.

This report and all digital products including a ReadMe file have been archived on a USB stick. Geosoft formats are used for the databases (GDB) including raw data, gridded data (GRD) and Resistivity Voxel.

Respectfully Submitted,

Charles Barrie, M.Sc., P.Geo.
Vice President
Terraquest Ltd.

9 APPENDICES

9.1 APPENDIX I - CERTIFICATE OF QUALIFICATION

I, Charles Barrie, certify that I:

1) am registered as a Fellow with the Geological Association of Canada, as a P.Geo. with the Association of Professional Geoscientists of Ontario (APGO) and work professionally as a geoscientist,
2) hold an Honours degree in Geology from McMaster University, Canada, obtained in 1977,
3) hold an M.Sc. in Geology from Dalhousie University, Canada, obtained in 1980,
4) am a member of the Prospectors and Developers Association of Canada,
5) am a member of the Canadian Institute of Mining, Metallurgy and Petroleum,
6) have worked as a geoscientist for over forty years,
7) am employed by and am an owner of Terraquest Ltd., specializing in high sensitivity airborne geophysical surveys, and
8) have prepared this operations and specifications report pertaining to airborne data collected by Terraquest Ltd.

Markham, Ontario, Canada Signed

9.2 APPENDIX II – FIELD REPORTS

Navigation File

```
0  B551 Mantra / Jean Property 100m SL
1  Z 15
2      719816     5351116       AREA CORNER 1
2      719817     5349108       AREA CORNER 2
2      717665     5349108       AREA CORNER 3
2      717665     5348109       AREA CORNER 4
2      717185     5348109       AREA CORNER 5
2      717185     5347641       AREA CORNER 6
2      714697     5347641       AREA CORNER 7
2      714697     5347950       AREA CORNER 8
2      711815     5347950       AREA CORNER 9
2      711815     5350117       AREA CORNER 10
2      712808     5350117       AREA CORNER 11
2      712808     5350432       AREA CORNER 12
2      714188     5350432       AREA CORNER 13
2      714188     5351117       AREA CORNER 14
2      719816     5351116       AREA CORNER 15
3      719816     5351116  COR1 WAYPOINT 1
4          81                   NUMBER OF LINES
5       100.0                   SPACING, m
8          75                   MAX CROSS TRACK, m
9    0  0  0                    DELTA X/Y/Z
10          1                   LOG FPR EVERY 1 SECS
11 0.9996000000       0.0       0.0 K0, X/Y SHIFT
14          0                   LINES EXTENDED BEYOND AREA
16         10                   FIRST LINE NUMBER
17   719816.0   5351116.0   0.0 MASTER POINT, HEADING
18   719816.0   5351116.0  90.0 TIE LINE MASTER POINT, HEADING
19     1000.0         0         TIE LINE SPACING, LINE EXTENSION, m
20 WGS-84      6378137.0   298.257223563 22       ELLIPSOID
21          1                   UTM VALUES RELATIVE TO N HEMISPHERE
30         20    9600  N  1  8  RS-232 PORT 2 INCOMING FORMAT
31         20    9600  N  1  8  RS-232 PORT OUTGOING FORMAT
38          0                   METRIC SYSTEM
41       0.00                   SYSTEM LAG, Secs.
80        0.00                  PLANNED ALTITUDE, m
83          0                   GPS ALTITUDE FOR VERTICAL BAR
84       1.00        0.00       ALTITUDE COEFFICIENT, OFFSET
85         100                   MAX VERTICAL BAR SCALE
102  UTM                        UTM X/Y SCALE
```

Daily Log

AC	DATE	COUNT	CLASS_AM	CLASS_PM	LKMS	ACCUM	COMMENT
C-GGLS	16-Jul-22	1					Vince Ou arrives onsite Thunder Bay with C-GGLS (flight GLS2143)
C-GGLS	17-Jul-22	2	MOB/DEMOB	CALIBRATION			FOM flown (flight GLS2144)
C-GGLS	18-Jul-22	3	SETUP	SETUP			Alexander Louie arrives on site with support vehicle. Base station set-up, etc.
C-GGLS	19-Jul-22	4	STANDBY/WX	STANDBY/WX			Continuous rain, low clouds.
C-GGLS	20-Jul-22	5	STANDBY/WX	STANDBY/WX			Below minimum conditions continue
C-GGLS	21-Jul-22	6	SURVEY	SURVEY	246.02	246.0	GLS2145: Production starts/ data acqusition complete

Flight List

AC	FLIGHT	DATE	TYPE	TIME UP	TIME DOWN	FLIGHT TIME	FROM	TO	CREW	PROD TIME	LKMS
C-GGLS	2143	16-Jul-22	FERRY	13:08:00	18:00:00	4:52:00	CYVO	CYQT	Ou		
C-GGLS	2144	17-Jul-22	CAL	14:15:00	15:39:00	1:24:00	CYQT	CYQT	Ou		
C-GGLS	2145	21-Jul-22	SURVEY	12:23:00	16:41:00	4:18:00	CYQT	CYQT	Ou, Louie	1:10:47	246.02

Survey Summary Status Chart

TERRAQUEST

PROJECT REF B551 /MANTRA EXPLORATION /JEAN: SUMMER, 2022

CURRENT STATUS:	21-Jul-22	C-GGLS					
TOTAL DAYS	INSTALL/ SET-UP	HIATUS	OPS DAYS	LKM/DAY	COMPL (%)	TOTAL FLT TIME	TOTAL PRD TIME
5	2		3	82.0	100.00%	10:34:00	1:10:47

OVERALL PRODUCTION SUMMARY:

	PLAN		FLOWN			
	NLIN	LKMS	NLIN	LKMS	REMAIN	COMPL (%)
TOTAL	85	246.0	85	246.0		100.00%
LINE	81	218.5	81	218.5		100.00%
TIE	4	27.5	4	27.5		100.00%
BORDER						

SURVEY STATS		
	DAY	PROJECT
FLIGHT HOURS	4:18:00	10:34:00
SURVEY HOURS	1:10:47	1:10:47
LKMS ACCEPT	246.02	246.02
LKMS REJECT		
LKMS % TOTAL	100.00%	100.00%

SUMMARY BY BLOCK:

NAME	CODE	PLAN		FLOWN		COMPL (%)
		NLIN	LKMS	NLIN	LKMS	
JEAN	JEA	85	246.02	85	246.02	100.00%

COMMENTS

GLS2145: Production starts/ data acqusition complete

C-GGLS

DAY CLASS SUMMARY	
CALIBRATION	0.5
EQUIPMENT	
INSTALL	
MAINT (SCHED)	
MAINT (UNSCHED)	
MOB/DEMOB	0.5
SETUP	1.0
SURVEY	1.0
TESTING	
STANDBY/WX	2.0
STANDBY/DIURNAL	
STANDBY/TQ	
STANDBY/CLIENT	
STANDBY/RESTRICT	
TRAINING	
TOTAL	5.0

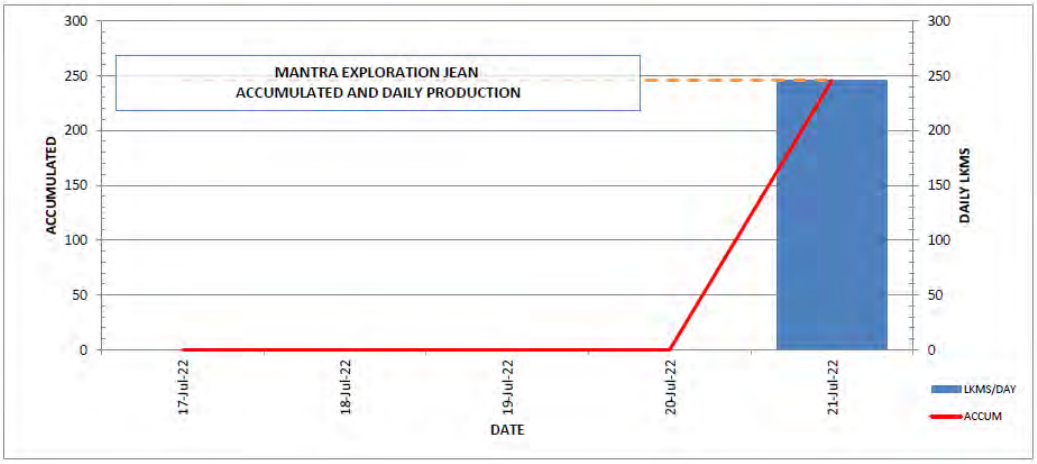

Line List

AC	BLK	LTYP	DATE	FLIGHT	FLINE	UTC_START	UTC_END	ACCEPT	IGNORE	REJECT	STATUS	PROD TIME
C-GGLS	JEA	LINE	21-Jul-22	2145	10	12:48:36	12:49:09	2.2			FULL	0:00:33
C-GGLS	JEA	LINE	21-Jul-22	2145	20	12:51:10	12:51:47	2.2			FULL	0:00:38
C-GGLS	JEA	LINE	21-Jul-22	2145	30	12:53:44	12:54:17	2.2			FULL	0:00:33
C-GGLS	JEA	LINE	21-Jul-22	2145	40	12:56:17	12:56:55	2.2			FULL	0:00:38
C-GGLS	JEA	LINE	21-Jul-22	2145	50	12:58:48	12:59:22	2.2			FULL	0:00:34
C-GGLS	JEA	LINE	21-Jul-22	2145	60	13:01:22	13:02:01	2.2			FULL	0:00:39
C-GGLS	JEA	LINE	21-Jul-22	2145	70	13:03:51	13:04:25	2.2			FULL	0:00:34
C-GGLS	JEA	LINE	21-Jul-22	2145	80	13:06:15	13:06:52	2.2			FULL	0:00:37
C-GGLS	JEA	LINE	21-Jul-22	2145	90	13:08:37	13:09:11	2.2			FULL	0:00:34
C-GGLS	JEA	LINE	21-Jul-22	2145	100	13:11:06	13:11:44	2.2			FULL	0:00:38
C-GGLS	JEA	LINE	21-Jul-22	2145	110	13:13:34	13:14:12	2.5			FULL	0:00:38
C-GGLS	JEA	LINE	21-Jul-22	2145	120	13:16:02	13:16:46	2.5			FULL	0:00:44
C-GGLS	JEA	LINE	21-Jul-22	2145	130	13:18:32	13:19:10	2.5			FULL	0:00:38
C-GGLS	JEA	LINE	21-Jul-22	2145	140	13:21:01	13:21:46	2.5			FULL	0:00:44
C-GGLS	JEA	LINE	21-Jul-22	2145	150	13:23:17	13:23:55	2.5			FULL	0:00:38
C-GGLS	JEA	LINE	21-Jul-22	2145	160	13:25:35	13:26:19	2.5			FULL	0:00:44
C-GGLS	JEA	LINE	21-Jul-22	2145	170	13:27:41	13:28:21	2.5			FULL	0:00:40
C-GGLS	JEA	LINE	21-Jul-22	2145	180	13:29:55	13:30:39	2.5			FULL	0:00:44
C-GGLS	JEA	LINE	21-Jul-22	2145	190	13:32:18	13:32:57	2.5			FULL	0:00:39
C-GGLS	JEA	LINE	21-Jul-22	2145	200	13:34:25	13:35:09	2.5			FULL	0:00:44
C-GGLS	JEA	LINE	21-Jul-22	2145	201	13:36:42	13:37:21		2.5		IGNORE	0:00:38
C-GGLS	JEA	LINE	21-Jul-22	2145	210	13:38:48	13:39:33	2.5			FULL	0:00:45
C-GGLS	JEA	LINE	21-Jul-22	2145	220	13:41:05	13:41:43	2.5			FULL	0:00:38
C-GGLS	JEA	LINE	21-Jul-22	2145	230	13:43:20	13:44:05	2.5			FULL	0:00:45
C-GGLS	JEA	LINE	21-Jul-22	2145	240	13:45:52	13:46:31	2.5			FULL	0:00:39
C-GGLS	JEA	LINE	21-Jul-22	2145	250	13:48:03	13:49:01	3.2			FULL	0:00:58
C-GGLS	JEA	LINE	21-Jul-22	2145	260	13:50:24	13:51:14	3.2			FULL	0:00:50
C-GGLS	JEA	LINE	21-Jul-22	2145	270	13:52:39	13:53:36	3.2			FULL	0:00:57
C-GGLS	JEA	LINE	21-Jul-22	2145	280	13:54:56	13:55:45	3.2			FULL	0:00:48
C-GGLS	JEA	LINE	21-Jul-22	2145	290	13:57:18	13:58:15	3.2			FULL	0:00:57
C-GGLS	JEA	LINE	21-Jul-22	2145	300	13:59:45	14:00:39	3.5			FULL	0:00:54
C-GGLS	JEA	LINE	21-Jul-22	2145	310	14:02:06	14:03:09	3.5			FULL	0:01:03
C-GGLS	JEA	LINE	21-Jul-22	2145	320	14:04:32	14:05:26	3.5			FULL	0:00:54
C-GGLS	JEA	LINE	21-Jul-22	2145	330	14:06:54	14:07:55	3.5			FULL	0:01:02
C-GGLS	JEA	LINE	21-Jul-22	2145	340	14:09:17	14:10:11	3.5			FULL	0:00:54
C-GGLS	JEA	LINE	21-Jul-22	2145	350	14:11:37	14:12:37	3.5			FULL	0:01:00
C-GGLS	JEA	LINE	21-Jul-22	2145	360	14:13:55	14:14:47	3.5			FULL	0:00:52
C-GGLS	JEA	LINE	21-Jul-22	2145	370	14:16:15	14:17:14	3.5			FULL	0:01:00
C-GGLS	JEA	LINE	21-Jul-22	2145	380	14:18:35	14:19:28	3.5			FULL	0:00:53
C-GGLS	JEA	LINE	21-Jul-22	2145	390	14:20:56	14:21:57	3.5			FULL	0:01:01
C-GGLS	JEA	LINE	21-Jul-22	2145	400	14:23:38	14:24:32	3.5			FULL	0:00:54
C-GGLS	JEA	LINE	21-Jul-22	2145	410	14:26:10	14:27:12	3.5			FULL	0:01:01
C-GGLS	JEA	LINE	21-Jul-22	2145	420	14:28:50	14:29:44	3.5			FULL	0:00:54
C-GGLS	JEA	LINE	21-Jul-22	2145	430	14:31:24	14:32:25	3.5			FULL	0:01:01
C-GGLS	JEA	LINE	21-Jul-22	2145	440	14:34:11	14:35:05	3.5			FULL	0:00:55
C-GGLS	JEA	LINE	21-Jul-22	2145	450	14:36:49	14:37:48	3.5			FULL	0:00:59
C-GGLS	JEA	LINE	21-Jul-22	2145	460	14:39:33	14:40:27	3.5			FULL	0:00:54
C-GGLS	JEA	LINE	21-Jul-22	2145	470	14:42:13	14:43:14	3.5			FULL	0:01:00
C-GGLS	JEA	LINE	21-Jul-22	2145	480	14:45:06	14:46:00	3.5			FULL	0:00:54
C-GGLS	JEA	LINE	21-Jul-22	2145	490	14:48:02	14:49:03	3.5			FULL	0:01:01
C-GGLS	JEA	LINE	21-Jul-22	2145	500	14:50:47	14:51:41	3.5			FULL	0:00:54
C-GGLS	JEA	LINE	21-Jul-22	2145	510	14:53:27	14:54:27	3.5			FULL	0:01:00
C-GGLS	JEA	LINE	21-Jul-22	2145	520	14:56:07	14:57:02	3.5			FULL	0:00:54
C-GGLS	JEA	LINE	21-Jul-22	2145	530	14:58:55	14:59:55	3.5			FULL	0:01:00
C-GGLS	JEA	LINE	21-Jul-22	2145	540	15:01:57	15:02:52	3.5			FULL	0:00:56
C-GGLS	JEA	LINE	21-Jul-22	2145	550	15:04:44	15:05:37	3.0			FULL	0:00:53
C-GGLS	JEA	LINE	21-Jul-22	2145	560	15:07:15	15:08:03	3.0			FULL	0:00:48
C-GGLS	JEA	LINE	21-Jul-22	2145	570	15:09:55	15:10:49	3.0			FULL	0:00:54
C-GGLS	JEA	LINE	21-Jul-22	2145	580	15:12:31	15:13:18	3.0			FULL	0:00:48
C-GGLS	JEA	LINE	21-Jul-22	2145	590	15:15:09	15:16:02	3.0			FULL	0:00:54
C-GGLS	JEA	LINE	21-Jul-22	2145	600	15:17:41	15:18:12	2.0			FULL	0:00:31
C-GGLS	JEA	LINE	21-Jul-22	2145	610	15:19:59	15:20:33	2.0			FULL	0:00:35
C-GGLS	JEA	LINE	21-Jul-22	2145	620	15:22:13	15:22:45	2.0			FULL	0:00:32
C-GGLS	JEA	LINE	21-Jul-22	2145	630	15:24:35	15:25:09	2.0			FULL	0:00:33
C-GGLS	JEA	LINE	21-Jul-22	2145	640	15:28:28	15:29:01	2.0			FULL	0:00:33
C-GGLS	JEA	LINE	21-Jul-22	2145	650	15:30:29	15:31:00	2.0			FULL	0:00:32
C-GGLS	JEA	LINE	21-Jul-22	2145	660	15:32:45	15:33:19	2.0			FULL	0:00:34
C-GGLS	JEA	LINE	21-Jul-22	2145	670	15:34:38	15:35:09	2.0			FULL	0:00:31
C-GGLS	JEA	LINE	21-Jul-22	2145	680	15:36:44	15:37:17	2.0			FULL	0:00:33
C-GGLS	JEA	LINE	21-Jul-22	2145	690	15:38:36	15:39:06	2.0			FULL	0:00:31
C-GGLS	JEA	LINE	21-Jul-22	2145	700	15:40:51	15:41:26	2.0			FULL	0:00:35
C-GGLS	JEA	LINE	21-Jul-22	2145	710	15:42:49	15:43:20	2.0			FULL	0:00:31
C-GGLS	JEA	LINE	21-Jul-22	2145	720	15:45:00	15:45:36	2.0			FULL	0:00:36

AC	BLK	LTYP	DATE	FLIGHT	FLINE	UTC_START	UTC_END	ACCEPT	IGNORE	REJECT	STATUS	PROD TIME
C-GGLS	JEA	LINE	21-Jul-22	2145	730	15:47:09	15:47:40	2.0			FULL	0:00:31
C-GGLS	JEA	LINE	21-Jul-22	2145	740	15:49:40	15:50:16	2.0			FULL	0:00:36
C-GGLS	JEA	LINE	21-Jul-22	2145	750	15:52:04	15:52:34	2.0			FULL	0:00:30
C-GGLS	JEA	LINE	21-Jul-22	2145	760	15:52:34	15:55:17	2.0			FULL	0:02:43
C-GGLS	JEA	LINE	21-Jul-22	2145	770	15:57:06	15:57:36	2.0			FULL	0:00:30
C-GGLS	JEA	LINE	21-Jul-22	2145	780	15:59:35	16:00:09	2.0			FULL	0:00:34
C-GGLS	JEA	LINE	21-Jul-22	2145	790	16:01:59	16:02:29	2.0			FULL	0:00:30
C-GGLS	JEA	LINE	21-Jul-22	2145	800	16:04:25	16:05:01	2.0			FULL	0:00:36
C-GGLS	JEA	LINE	21-Jul-22	2145	810	16:06:52	16:07:22	2.0			FULL	0:00:30
C-GGLS	JEA	TIE	21-Jul-22	2145	10010	16:20:27	16:21:49	5.6			FULL	0:01:21
C-GGLS	JEA	TIE	21-Jul-22	2145	10020	16:16:22	16:18:57	8.0			FULL	0:02:36
C-GGLS	JEA	TIE	21-Jul-22	2145	10030	16:12:27	16:14:27	8.0			FULL	0:02:00
C-GGLS	JEA	TIE	21-Jul-22	2145	10040	16:08:27	16:10:18	5.9			FULL	0:01:51

9.3 APPENDIX III - FIGURE OF MERIT

B551_MANTRA / SUMMER 2022					
Magnetic Figure of Merit Analysis (SRCDAT: 171911 FLIGHT 2144)					
Job Ref:	B551	Date:	17-Jul-22	Aircraft:	C-GGLS
Location :	Thunder Bay				

Flight Path + Manoevers

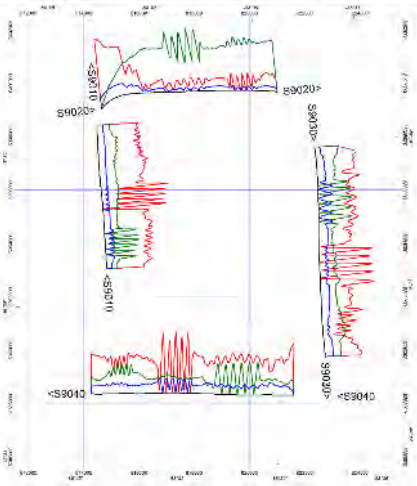

FOM Index : Sensor 1

Calculation note: Residual noise was isolated using a 101 pt Hanning high pass convolution filter with a subsequent low-pass filter (1.0 fid cutoff) applied to reduce non-related HF noise. Individual min-max values determined from the maximum consecutive peak-to-trough residual noise amplitude within each manoevre group

LINE	DIR	TRAV FLG	PITCH		ROLL		YAW			P	R	Y	Σ
			MAX	MIN	MAX	MIN	MAX	MIN					
9010	N		0.0613	-0.1217	0.0959	-0.0700	0.1056	-0.0956		0.1829	0.1659	0.2012	0.5501
9020	E		0.0285	-0.0187	0.0731	-0.0320	0.1262	-0.0854		0.0472	0.1051	0.2115	0.3639
9030	S		0.1436	-0.0791	0.1042	-0.0550	0.0907	-0.1015		0.2228	0.1592	0.1922	0.5741
9040	W		0.1135	-0.0734	0.0610	-0.0381	0.0738	-0.1004		0.1869	0.0991	0.1742	0.4602
									Σ	0.6398	0.5293	0.7792	1.9483
									Full FOM Index :	1.9483			
									Eq. Traverse FOM Index (Σ Trav x 2) :	2.2485			

FOM Index : Sensor 2

LINE	DIR	TRAV FLG	PITCH		ROLL		YAW			P	R	Y	Σ
			MAX	MIN	MAX	MIN	MAX	MIN					
9010	N		0.0742	-0.0953	0.0668	-0.0676	0.0436	-0.0564		0.1694	0.1344	0.1000	0.4038
9020	E		0.0190	-0.0218	0.0638	-0.0375	0.1591	-0.1349		0.0408	0.1013	0.2940	0.4361
9030	S		0.1311	-0.0640	0.0953	-0.0504	0.0870	-0.0936		0.1951	0.1457	0.1806	0.5215
9040	W		0.1184	-0.0713	0.0533	-0.0514	0.0709	-0.0977		0.1897	0.1047	0.1687	0.4631
									Σ	0.5951	0.4861	0.7433	1.8245
									Full FOM Index :	1.8245			
									Eq. Traverse FOM Index (Σ Trav x 2) :	1.8506			

FOM Index : Sensor3

LINE	DIR	TRAV FLG	PITCH		ROLL		YAW			P	R	Y	Σ
			MAX	MIN	MAX	MIN	MAX	MIN					
9010	N		0.0613	-0.0875	-0.0027	-0.0308	0.0296	-0.0295		0.1488	0.0281	0.0591	0.2360
9020	E		0.0092	-0.0102	0.0629	-0.0591	0.0851	-0.0612		0.0193	0.1220	0.1463	0.2876
9030	S		0.0797	-0.0335	0.0360	-0.0068	0.0256	-0.0308		0.1132	0.0428	0.0564	0.2123
9040	W		0.0714	-0.0422	0.0063	-0.0122	0.0537	-0.0353		0.1135	0.0185	0.0891	0.2211
									Σ	0.3948	0.2113	0.3508	0.9570
									Full FOM Index :	0.9570			
									Eq. Traverse FOM Index (Σ Trav x 2) :	0.8965			

9.4 APPENDIX IV - RADAR ALTIMETER CALIBRATION

Terraquest LTD Radar Altimeter Calibration 2022-09-13

C-GGLS: RADAR CALIBRATION DATA SUMMARY
Calibration performed: Sept Iles, PQ (29 June 2021, GLS2022)

					INTERCEPT	-2.8833	
					SLOPE	77.5381	
LINE	**RAW RADAR**	**GPS ALT**	**CORRECTED GPS ALT**	**LASER**	**CALIBRATED RADAR**		**ERROR ***
Ground Ref		52.3	0.0	0.5			
S8010	0.1643	61.0	8.7	10.4			
S8020	0.3863	80.1	27.8	28.8	27.1		-0.7
S8030	0.7650	110.5	58.2	58.4	56.4		-1.8
S8040	1.1468	137.3	85.0	88.4	86.0		1.0
S8050	1.5436	168.8	116.5	119.3	116.8		0.3
S8060	1.9648	201.3	149.0	151.9	149.5		0.5
S8070	2.2031	220.4	168.1	170.5	167.9		-0.2
S8080	2.5404	246.7	194.4	196.6	194.1		-0.3

** Error estimated as (Calibrated Radar) - (Corrected GPS Alt)*

Imperial Units		
LINE	GPS_ALT (ft)	CAL_RAD (ft)
S8010	28.5	0.0
S8020	91.2	88.8
S8030	190.9	185.1
S8040	278.9	282.3
S8050	382.2	383.2
S8060	488.8	490.4
S8070	551.5	551.0
S8080	637.8	636.8

Terraquest LTD Radar Altimeter Calibration 2022-09-13

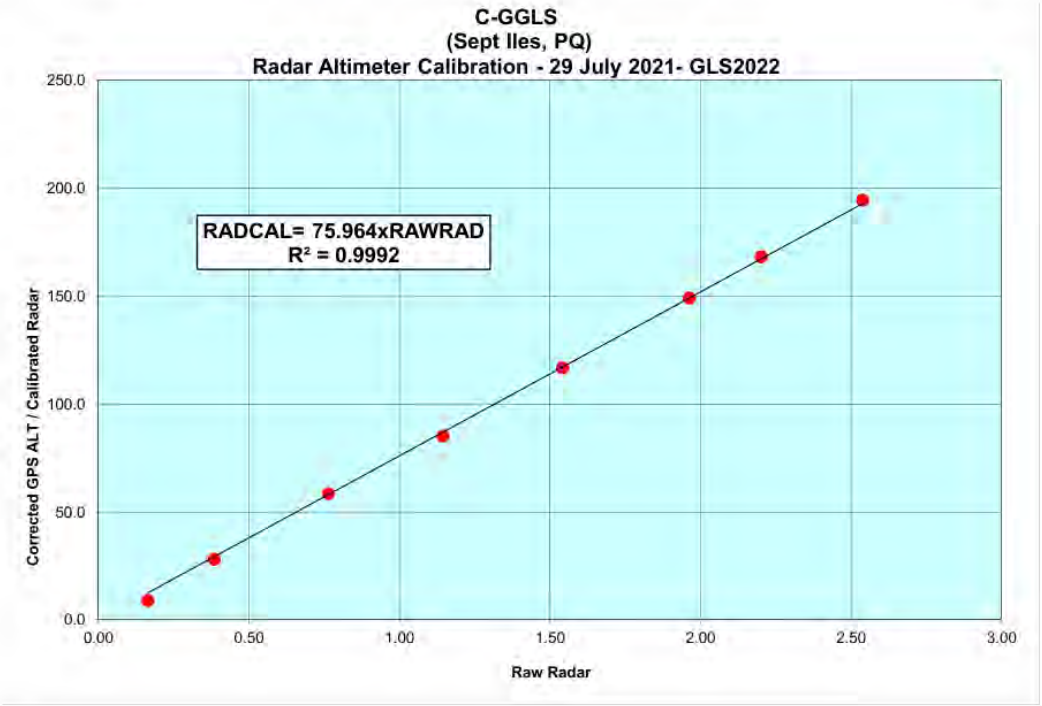

9.5 APPENDIX V – README FILE

TERRAQUEST Final Data Archive Documentation: Part I

==========

```
TERRAQUEST reference : B551

Client: Mantra Exploration Inc.
Project: Jean Project
Type: Aeromagnetic Gradient Survey /w VLF (Fixed Wing)
Operations: Summer, 2022
Survey Base: Thunder Bay, Ontario
Aircraft: Cessna 206, C-GGLS
Archive Version: 20220120
Prepared By: Shane Hefford

1. Data Organisation:

\---B551_MAN_JEAN
    +---DATA
    |       B551_MAN_JEAN_MAG&VLF.gdb
    |       B551_MAN_JEAN_MAG&VLF.gdb.xml
    |
    +---GRIDS
    |       ANSIG.grd
    |       ANSIG.grd.gi
    |       ANSIG.grd.xml
    |       DTMFNL.grd
    |       DTMFNL.grd.gi
    |       DTMFNL.grd.xml
    |       HGEWFNL.grd
    |       HGEWFNL.grd.gi
    |       HGEWFNL.grd.xml
    |       HGNSFNL.grd
    |       HGNSFNL.grd.gi
    |       HGNSFNL.grd.xml
    |       NAAFNL.grd
    |       NAAFNL.grd.gi
    |       NAAFNL.grd.xml
    |       NAAFNL_HP.grd
    |       NAAFNL_HP.grd.gi
    |       NAAFNL_HP.grd.xml
    |       NLKFNL.grd
    |       NLKFNL.grd.gi
    |       NLKFNL.grd.xml
    |       NLKFNL_HP.grd
    |       NLKFNL_HP.grd.gi
    |       NLKFNL_HP.grd.xml
    |       NMLFNL.grd
    |       NMLFNL.grd.gi
    |       NMLFNL.grd.xml
    |       NMLFNL_HP.grd
    |       NMLFNL_HP.grd.gi
    |       NMLFNL_HP.grd.xml
    |       RTF.grd
    |       RTF.grd.gi
    |       RTF.grd.xml
    |       TF3ANM.grd
    |       TF3ANM.grd.gi
    |       TF3ANM.grd.xml
    |       TF3FNL.grd
    |       TF3FNL.grd.gi
    |       TF3FNL.grd.xml
    |       TF3VD1.grd
    |       TF3VD1.grd.gi
    |       TF3VD1.grd.xml
```

```
|
+---MAPS
|   |   B551_MAN_JEAN_M01_DTM.png
|   |   B551_MAN_JEAN_M02_TMI.png
|   |   B551_MAN_JEAN_M03_TMIANM.png
|   |   B551_MAN_JEAN_M04_TMIVD1.png
|   |   B551_MAN_JEAN_M05_ANSIG.png
|   |   B551_MAN_JEAN_M06_HGEW.png
|   |   B551_MAN_JEAN_M07_HGNS.png
|   |   B551_MAN_JEAN_M08_RTF.png
|   |   B551_MAN_JEAN_M09_NAA.png
|   |   B551_MAN_JEAN_M10_NML.png
|   |   B551_MAN_JEAN_M11_NLK.png
|   |
|   \---LORES
|           B551_MAN_JEAN_M01_DTM.JPG
|           B551_MAN_JEAN_M02_TMI.JPG
|           B551_MAN_JEAN_M03_TMIANM.JPG
|           B551_MAN_JEAN_M04_TMIVD1.JPG
|           B551_MAN_JEAN_M05_ANSIG.JPG
|           B551_MAN_JEAN_M06_HGEW.JPG
|           B551_MAN_JEAN_M07_HGNS.JPG
|           B551_MAN_JEAN_M08_RTF.JPG
|           B551_MAN_JEAN_M09_NAA.JPG
|           B551_MAN_JEAN_M10_NML.JPG
|           B551_MAN_JEAN_M11_NLK.JPG
|
+---README
|       B551_MAN_JEAN.ReadMe.txt
|
\---REPORT
```

2. Database Contents: MAG (Geosoft Database [.gdb] format)

"B551_MAN_JEAN_MAG&VLF.gdb"

Data sampled at 10Hz ...

```
X_UTM_WIN  : UTM Easting - WGS84, UTM Zone 15N (metres)
Y_UTM_WIN  : UTM Northing - WGS84, UTM Zone 15N (metres)
Flight     : Flight Number
DATE       : Flight Date (DD/MM/YYYY format - ASCII)
AZIMUTH    : Flight line direction (ranged 0-360 degrees)
FID        : Fiducial (UTC seconds)
TIME       : UTC TIME (hh:mm:ss.ss format)
RADAR      : Radar Altimeter (metres AGL)
RADLAG     : Radar Altimeter, corrected for system lag (metres AGL)
ALT        : WGS84 Altitude (metres AMSL)
DTMFNL     : Final Digital Terrain model (m AMSL)
LAT        : Latitude (degrees)
LON        : Longitude (degrees)
DIURNAL    : Raw Diurnal (nT)
DIUEDIT    : Edited Diurnal (culture removed, nT)
VMX        : Fluxgate X component (nT)
VMY        : Fluxgate Y component (nT)
VMZ        : Fluxgate Z component (nT)
TF1UNC     : Raw measured TMI (nT) - Left Wing
TF2UNC     : Raw measured TMI (nT) - Right Wing
TF3UNC     : Raw measured TMI (nT) - Tail
TF1CMP     : Compensated TMI (nT) - Left Wing
TF2CMP     : Compensated TMI (nT) - Right Wing
TF3CMP     : Compensated TMI (nT) - Tail
TF1CMPEDIT : Edited (spikes removed), Compensated TMI (nT) - Left Wing
TF2CMPEDIT : Edited (spikes removed), Compensated TMI (nT) - Right Wing
TF3CMPEDIT : Edited (spikes removed), Compensated TMI (nT) - Tail
HGEWFNL    : Measured East-West Magnetic gradient (nT/m), lag, level corrected
HGNSFNL    : Measured North-South Magnetic gradient (nT/m), lag, level corrected
TF3DIU     : Diurnal Corrected Total Magnetic Field (Tail TMI, nT)
TF3LVL     : Tie line levelled Total Magnetic Field (Tail TMI, nT)
TF3FNL     : Final, microlevelled Total Magnetic Field (Tail TMI, nT)
```

```
    IGRF_TF    : IGRF Total Field (calculated for July 21 2022, alt = 508 m, 2020 IGRF coefficients)
    TF3ANM     : Anomlaous (IGRF corrected) Total Magnetic Field (nT)
    Ax         : Accelerometer, X component (from MATRIX VLF Receiver)
    Ay         : Accelerometer, Y component (from MATRIX VLF Receiver)
    Az         : Accelerometer, Z component (from MATRIX VLF Receiver)
    Gx         : Gyro, X component (from MATRIX VLF Receiver)
    Gy         : Gyro, Y component (from MATRIX VLF Receiver)
    Gz         : Gyro, Z component (from MATRIX VLF Receiver)
    Mx         : Magnetic Field, X component (from MATRIX VLF Receiver)
    My         : Magnetic Field, Y component (from MATRIX VLF Receiver)
    Mz         : Magnetic Field, Z component (from MATRIX VLF Receiver)
    Ampl_1     : Raw VLF Amplitude (Station NAA, Cutler, Maine)
    Ampl_2     : Raw VLF Amplitude (Station NML, LaMoure, North Dakota)
    Ampl_3     : Raw VLF Amplitude (Station NLK, Jim Creek, Washington)
    Ampl_4     : Raw VLF Amplitude (Station NAU, Aguada, Puerto Rico)
    Azmt_1     : Raw VLF Apparent Station Azimuth (Station NAA, Cutler, Maine)
    Azmt_2     : Raw VLF Apparent Station Azimuth (Station NML, LaMoure, North Dakota)
    Azmt_3     : Raw VLF Apparent Station Azimuth (Station NLK, Jim Creek, Washington)
    Azmt_4     : Raw VLF Apparent Station Azimuth (Station NAU, Aguada, Puerto Rico)
    El_P_1     : Raw VLF Planar Ellipticity (Station NAA, Cutler, Maine)
    El_P_2     : Raw VLF Planar Ellipticity (Station NML, LaMoure, North Dakota)
    El_P_3     : Raw VLF Planar Ellipticity (Station NLK, Jim Creek, Washington)
    El_P_4     : Raw VLF Planar Ellipticity (Station NAU, Aguada, Puerto Rico)
    El_V_1     : Raw VLF Vertical Ellipticity (Station NAA, Cutler, Maine)
    El_V_2     : Raw VLF Vertical Ellipticity (Station NML, LaMoure, North Dakota)
    El_V_3     : Raw VLF Vertical Ellipticity (Station NLK, Jim Creek, Washington)
    El_V_4     : Raw VLF Vertical Ellipticity (Station NAU, Aguada, Puerto Rico)
    Tilt_1     : Raw VLF Tilt Angle (Station NAA, Cutler, Maine)
    Tilt_2     : Raw VLF Tilt Angle (Station NML, LaMoure, North Dakota)
    Tilt_3     : Raw VLF Tilt Angle (Station NLK, Jim Creek, Washington)
    Tilt_4     : Raw VLF Tilt Angle (Station NAU, Aguada, Puerto Rico)
    NAAFNL     : Final, microlevelled VLF Amplitude(mV) (Station NAA, Cutler, Maine)
    NMLFNL     : Final, microlevelled VLF Amplitude(mV) (Station NML, LaMoure, North Dakota)
    NLKFNL     : Final, microlevelled VLF Amplitude(mV) (Station NLK, Jim Creek, Washington)
    NAAFNL_HP  : Final, microlevelled VLF Amplitude High Pass Filtered(mV) (Station NAA, Cutler, Maine)
    NMLFNL_HP  : Final, microlevelled VLF Amplitude High Pass Filtered(mV) (Station NML, LaMoure, North Dakota)
    NLKFNL_HP  : Final, microlevelled VLF Amplitude High Pass Filtered(mV) (Station NLK, Jim Creek, Washington)
    NAA_IP     : VLF In-Phase Component (Station NAA, Cutler, Maine)
    NML_IP     : VLF In-Phase Component (Station NML, LaMoure, North Dakota)
    NLK_IP     : VLF In-Phase Component (Station NLK, Jim Creek, Washington)
    NAA_QD     : VLF Quadrature Component (Station NAA, Cutler, Maine)
    NML_QD     : VLF Quadrature Component (Station NML, LaMoure, North Dakota)
    NLK_QD     : VLF Quadrature Component (Station NLK, Jim Creek, Washington)
```

3. GRIDS

Data grids were prepared using Bi-directional (Akima) spline interpolation, with a grid cell size of 25 metres.

```
    ANSIG.grd        : Analytic Signal
    DTMFNL.grd       : Digital Terrain Model (m AMSL)
    HGEW.grd         : Measured East-West Horizontal Magnetic Gradient (nT/m)
    HGNS.grd         : Measured North-South Horizontal Magnetic Gradient (nT/m)
    RTF.grd          : Reconstructed Total Field (pseudo nT)
    TF3ANM.grd       : Anomalous (IGRF corrected) Total Magnetic Field (nT)
    TF3FNL.grd       : Final, levelled Total Magnetic Field (nT)
    TF3VD1.grd       : Calculated First Vertical Magnetic derivative (nT/m)
    NAAFNL.grd       : Final, levelled VLF Amplitude (mV) (Station NAA, Cutler, Maine)
    NAAFNL_HP.grd    : Final, levelled and high pass filtered VLF Amplitude (mV) (Station NAA, Cutler, Maine)
    NMLFNL.grd       : Final, levelled VLF Amplitude (mV) (Station NML, LaMoure, North Dakota)
    NMLFNL_HP.grd    : Final, levelled and high pass filtered VLF Amplitude (mV) (Station NML, LaMoure, North
Dakota)
    NLKFNL.grd       : Final, levelled VLF Amplitude (mV) (Station NLK, Jim Creek, Washington)
    NLKFNL_HP.grd    : Final, levelled and high pass filtered VLF Amplitude (mV) (Station NLK, Jim Creek, Wash-
ington)
```

```
4.  MAPS

    PNG, JPEG images of the printed 1:10000 map series in full resolution (300 DPI) and low resolution
    (email-able, files in sub folder 'LORES')

        B551_MAN_JEAN_M01_DTM      : Flight Path with DTM grid
        B551_MAN_JEAN_M02_TMI      : Total Magnetic Intensity
        B551_MAN_JEAN_M03_TMIANM   : Anomalous (IGRF corrected) Total Field with contours
        B551_MAN_JEAN_M04_TMIVD1   : Calculated Vertical Magnetic Derivative
        B551_MAN_JEAN_M05_ANSIG    : Calculated Analytic Signal
        B551_MAN_JEAN_M06_HGEW     : Measured East-West Magnetic Gradient
        B551_MAN_JEAN_M07_HGNS     : Measured North-South Magnetic Gradient
        B551_MAN_JEAN_M08_RTF      : Reconstructed Total Field
        B551_MAN_JEAN_M09_NAA      : VLF Amplitude (Station NAA, Cutler, Maine)
        B551_MAN_JEAN_M10_NML      : VLF Amplitude (Station NML, LaMoure, North Dakota)
        B551_MAN_JEAN_M11_NLK      : VLF Amplitude (Station NLK, Jim Creek, Washington)

5. GeoTiff (geo-referenced) VLF Peak Overlays (300 DPI)(set WHITE to "Transparent"):

        B551_MAN_JEAN_FLIGHTPATH     : FLIGHT PATH
        B551_MAN_JEAN_TMIANM_CONTOUR : TMIANM CONTOUR LINES
        B551_MAN_JEAN_PEAKS_NAA      : GRID PEAKS VLF Amplitude (Station NAA, Cutler, Maine)
        B551_MAN_JEAN_PEAKS_NML      : GRID PEAKS VLF Amplitude (Station NML, LaMoure, North Dakota)
        B551_MAN_JEAN_PEAKS_NML      : GRID PEAKS VLF Amplitude (Station NLK, Jim Creek, Washington)


6. README

   Archive documentation: this file ("B551_MAN_JEAN.ReadMe.txt")


7. REPORT

   Project Operational/Logistics Report
```

TERRAQUEST Final Data Archive Documentation: VLF Resistivity, Part II

```
============================================================


TERRAQUEST reference : B551

Client: MANTRA EXPLORATION INC.
Project: JEAN, ON
Type: AEROMAGNETIC HORIZONTAL GRADIENT SURVEY /W VLF (FIXED WING)
Operations: Summer, 2022
Survey Base: Thunder Bay, ON
Aircraft: Cessna U206
Registration: C-GGLS
Archive Version: 221104
Prepared By: Allen Duffy

1. Data Organisation:

\---B551ARC_MANTRA_VLF_INVERSION_221104
    \---VLFRESISTIVITY
        +---NAA
        |   +---GRIDS
        |   |       NAA_RES_005_FNL.grd
        |   |       NAA_RES_005_FNL.grd.gi
        |   |       NAA_RES_005_FNL.grd.xml
        |   |       NAA_RES_010_FNL.grd
        |   |       NAA_RES_010_FNL.grd.gi
```

```
|   |       NAA_RES_010_FNL.grd.xml
|   |       NAA_RES_020_FNL.grd
|   |       NAA_RES_020_FNL.grd.gi
|   |       NAA_RES_020_FNL.grd.xml
|   |       NAA_RES_040_FNL.grd
|   |       NAA_RES_040_FNL.grd.gi
|   |       NAA_RES_040_FNL.grd.xml
|   |       NAA_RES_060_FNL.grd
|   |       NAA_RES_060_FNL.grd.gi
|   |       NAA_RES_060_FNL.grd.xml
|   |       NAA_RES_080_FNL.grd
|   |       NAA_RES_080_FNL.grd.gi
|   |       NAA_RES_080_FNL.grd.xml
|   |       NAA_RES_100_FNL.grd
|   |       NAA_RES_100_FNL.grd.gi
|   |       NAA_RES_100_FNL.grd.xml
|   |
|   +---GRID_GDB
|   |       NAA_RES_GRIDS.gdb
|   |       NAA_RES_GRIDS.gdb.xml
|   |
|   +---MAPS
|   |   |   B551_MAN_JEAN_M12_VLF_RESISTIVITY_NAA.png
|   |   |
|   |   \---LORES
|   |           B551_MAN_JEAN_M12_VLF_RESISTIVITY_NAA.png
|   |
|   +---PROFILE_GDB
|   |       NAA_RES_PROFILE.gdb
|   |       NAA_RES_PROFILE.gdb.xml
|   |
|   \---VOXEL
|           gridvox.var
|           NAA_RES_GRIDS_RESFNL.geosoft_voxel
|           NAA_RES_GRIDS_RESFNL.geosoft_voxel.xml
|
+---NLK
|   +---GRIDS
|   |       NLK_RES_005_FNL.grd
|   |       NLK_RES_005_FNL.grd.gi
|   |       NLK_RES_005_FNL.grd.xml
|   |       NLK_RES_010_FNL.grd
|   |       NLK_RES_010_FNL.grd.gi
|   |       NLK_RES_010_FNL.grd.xml
|   |       NLK_RES_020_FNL.grd
|   |       NLK_RES_020_FNL.grd.gi
|   |       NLK_RES_020_FNL.grd.xml
|   |       NLK_RES_040_FNL.grd
|   |       NLK_RES_040_FNL.grd.gi
|   |       NLK_RES_040_FNL.grd.xml
|   |       NLK_RES_060_FNL.grd
|   |       NLK_RES_060_FNL.grd.gi
|   |       NLK_RES_060_FNL.grd.xml
|   |       NLK_RES_080_FNL.grd
|   |       NLK_RES_080_FNL.grd.gi
|   |       NLK_RES_080_FNL.grd.xml
|   |       NLK_RES_100_FNL.grd
|   |       NLK_RES_100_FNL.grd.gi
|   |       NLK_RES_100_FNL.grd.xml
|   |
|   +---GRID_GDB
|   |       NLK_RES_GRIDS.gdb
|   |       NLK_RES_GRIDS.gdb.xml
|   |
```

```
|   +---MAPS
        |   |   |   B551_MAN_JEAN_M14_VLF_RESISTIVITY_NLK.png
        |   |   |
        |   |   \---LORES
        |   |           B551_MAN_JEAN_M14_VLF_RESISTIVITY_NLK.png
        |   |
        |   +---PROFILE_GDB
        |   |       NLK_RES_PROFILE.gdb
        |   |       NLK_RES_PROFILE.gdb.xml
        |   |
        |   \---VOXEL
        |           gridvox.var
        |           NLK_RES_GRIDS_RESFNL.geosoft_voxel
        |           NLK_RES_GRIDS_RESFNL.geosoft_voxel.xml
        |
        +---NML
        |   +---GRIDS
        |   |       NML_RES_005_FNL.grd
        |   |       NML_RES_005_FNL.grd.gi
        |   |       NML_RES_005_FNL.grd.xml
        |   |       NML_RES_010_FNL.grd
        |   |       NML_RES_010_FNL.grd.gi
        |   |       NML_RES_010_FNL.grd.xml
        |   |       NML_RES_020_FNL.grd
        |   |       NML_RES_020_FNL.grd.gi
        |   |       NML_RES_020_FNL.grd.xml
        |   |       NML_RES_040_FNL.grd
        |   |       NML_RES_040_FNL.grd.gi
        |   |       NML_RES_040_FNL.grd.xml
        |   |       NML_RES_060_FNL.grd
        |   |       NML_RES_060_FNL.grd.gi
        |   |       NML_RES_060_FNL.grd.xml
        |   |       NML_RES_080_FNL.grd
        |   |       NML_RES_080_FNL.grd.gi
        |   |       NML_RES_080_FNL.grd.xml
        |   |       NML_RES_100_FNL.grd
        |   |       NML_RES_100_FNL.grd.gi
        |   |       NML_RES_100_FNL.grd.xml
        |   |
        |   +---GRID_GDB
        |   |       NML_RES_GRIDS.gdb
        |   |       NML_RES_GRIDS.gdb.xml
        |   |
        |   +---MAPS
        |   |   |   B551_MAN_JEAN_M13_VLF_RESISTIVITY_NML.png
        |   |   |
        |   |   \---LORES
        |   |           B551_MAN_JEAN_M13_VLF_RESISTIVITY_NML.png
        |   |
        |   +---PROFILE_GDB
        |   |       NML_RES_PROFILE.gdb
        |   |       NML_RES_PROFILE.gdb.xml
        |   |
        |   \---VOXEL
        |           gridvox.var
        |           NML_RES_GRIDS_RESFNL.geosoft_voxel
        |           NML_RES_GRIDS_RESFNL.geosoft_voxel.xml
        |
        \---README
                B551ARC_MANTRA_VLF_RESISTIVITY.ReadMe.txt
```

1. VLF RESISTIVITY

Resistivity inversion data are grouped in three sub-directories according to the specific VLF Transmitter frequency. Data originating from three VLF Transmitting Stations were processed and presented:

NAA: Cutler, ME (24.0 kHz / 1000 kW)
NML: LaMoure, ND (25.2 kHz / 500 kW)
NLK: Jim Creek, WA (24.8 kHz / 250 kW)

1A. Database Contents: PROFILE_GDB

"NAA_RES_PROFILE.gdb", "NML_RES_PROFILE.gdb" and "NLK_RES_PROFILE.gdb"

Survey line based data archives for each frequency (NAA, NML or NLK), formatted as Geosoft .GDB databases, contain the following data fields :

Data sampled at 10Hz ...

X_UTM_WIN	: UTM Easting - WGS84, UTM Zone 15N (metres)
Y_UTM_WIN	: UTM Easting - WGS84, UTM Zone 15N (metres)
DATE	: Flight Date (DD/MM/YYYY format - ASCII)
Flight	: Flight Number
AZIMUTH	: AZIMUTH (flight line direction, ranged 0-360 deg)
LINE	: Line Number
LTYP	: Line Type (L: Traverse; T: Tie)
ALT	: WGS84 Altitude (metres AMSL)
DTMFNL	: Digital Terrain Model (metres)
LAT	: Latitude (degrees)
LON	: Longitude (degrees)
NAA_RES_005	: Resistivity (model inversion) - depth=5 metres (ohm-m)
NAA_RES_010	: Resistivity (model inversion) - depth=10 metres (ohm-m)
NAA_RES_020	: Resistivity (model inversion) - depth=20 metres (ohm-m)
NAA_RES_040	: Resistivity (model inversion) - depth=40 metres (ohm-m)
NAA_RES_060	: Resistivity (model inversion) - depth=60 metres (ohm-m)
NAA_RES_080	: Resistivity (model inversion) - depth=80 metres (ohm-m)
NAA_RES_100	: Resistivity (model inversion) - depth=100 metres (ohm-m)
NAA_RES_005_FNL	: Resistivity (model inversion) - depth=5 metres (ohm-m) (micro-levelled)
NAA_RES_010_FNL	: Resistivity (model inversion) - depth=10 metres (ohm-m) (micro-levelled)
NAA_RES_020_FNL	: Resistivity (model inversion) - depth=20 metres (ohm-m) (micro-levelled)
NAA_RES_040_FNL	: Resistivity (model inversion) - depth=40 metres (ohm-m) (micro-levelled)
NAA_RES_060_FNL	: Resistivity (model inversion) - depth=60 metres (ohm-m) (micro-levelled)
NAA_RES_080_FNL	: Resistivity (model inversion) - depth=80 metres (ohm-m) (micro-levelled)
NAA_RES_100_FNL	: Resistivity (model inversion) - depth=100 metres (ohm-m) (micro-levelled)

1B. Database Contents: GRID_GDB

"NAA_RES_GRIDS.gdb", "NML_RES_GRIDS.gdb" and "NLK_RES_GRIDS.gdb"

VLF inversion data are also archived organised by depth grid as a series of numerical lattices corresponding to each individual inversion depth (5, 10, 20, 40, 60, 80 and 100 metres depths). This database format is useful for creating 3D data grids. Data are organised into 7 "lines", corresponding to each individual depth plane:

DDEPTH005	: Inversion plane at DEPTH=5m XYZ points
DDEPTH010	: Inversion plane at DEPTH=10m XYZ points
DDEPTH020	: Inversion plane at DEPTH=20m XYZ points
DDEPTH040	: Inversion plane at DEPTH=40m XYZ points
DDEPTH060	: Inversion plane at DEPTH=60m XYZ points
DDEPTH080	: Inversion plane at DEPTH=60m XYZ points
DDEPTH100	: Inversion plane at DEPTH=100m XYZ points

Each line contains the following data fields for each grid vertice:

X	: UTM Easting - WGS84, UTM Zone 15N (metres)
Y	: UTM Easting - WGS84, UTM Zone 15N (metres)

```
RES    : Resistivity (model inversion)
RESFNL : Resistivity (model inversion) (micro-levelled)
DEPTH  : Depth (ranged 0 - -100 metres)
DTMFNL : Digital Terrain Model (metres)


1C.  GRIDS

Grids were prepared using Minimum Curvature interpolation with a 25m grid cell size. Grids
are archived in sub-folders corresponding to frequency (NAA, NML or NLK):

nnn_RES_005_FNL.grd     : final resistivity depth slice (5 metres)
nnn_RES_010_FNL.grd     : final resistivity depth slice (10 metres)
nnn_RES_020_FNL.grd     : final resistivity depth slice (20 metres)
nnn_RES_040_FNL.grd     : final resistivity depth slice (40 metres)
nnn_RES_060_FNL.grd     : final resistivity depth slice (60 metres)
nnn_RES_080_FNL.grd     : final resistivity depth slice (80 metres)
nnn_RES_100_FNL.grd     : final resistivity depth slice (100 metres)

* "nnn" is either "NAA", "NML" or "NLK" according to specific VLF transmitter frequency

1D.  3D (VOXEL) grids :

A 3D grid (Geosoft "voxel" format) was also created using the resistivity inversion
data: the voxel cells are sized at 25x25x5 metres (X, Y, Z dimensions). 3d Voxel grids
were calculated for each VLF Transmitter frequency (NAA, NML and NLK):

nnn_RES_GRIDS_RESFNL.geosoft_voxel

* "nnn" is either "NAA", "NML" or "NLK" according to specific VLF transmitter frequency


1E.  MAPS

"PNG" images of the printed map in full resolution (300 DPI) and low resolution
(email-able, files in sub folder 'LORES') are presented:

B551_MAN_JEAN_M12_VLF_RESISTIVITY_NAA.png
B551_MAN_JEAN_M13_VLF_RESISTIVITY_NML.png
B551_MAN_JEAN_M14_VLF_RESISTIVITY_NLK.png

2. README

Archive documentation: this file ("B551ARC_MANTRA_VLF_RESISTIVITY.ReadMe.txt")
```

Appendix 2. Outcrop Geology Maps

1:5000

MAP1 West

Map2 East

712,000 mE

714,000 mE

5,350,000 mN

5,348,000 mN

Magnetic Declination of 3°77

MAGNETIC TRUE

N

Little Gull Lake

699485 699483 699482 699484 539542

539497 546075 546074 539508 539541 539533 539523

539498 539500 539501 539507 539532 539522 539534

539496 539499 539503 539505 546071 546069 546067 546070 539517

539546 539506 539502 539504 546066 546073 546072 546068 539536

539548 539547 539516

19836 Taconite 39.05

19835 Taconite 23.7

19834 Taconite 26.02

Taconite

Shale

Shale

Shale

Shale

Shale

19831 30.58

Taconite

Mudstone

19830 33.11

19833 Taconite 48.84

19832 Shale 8.03

Legend

JEAN_Outcrops

Sample # % Fe

Grab Sample

July25th Track

August 3rd Track

August 5thTrack

Mantra Exploration Inc

Jean Property

Outcrop Geology and

Iron Assays Map

Date: 2022-10-25

Author: pgeo_tims

Office:

Drawing:

Scale: 1:5000

Projection: UTM Zone 15 (NAD 83)

MAP 1

0 75 150 300

metres

716,000 mE

718,000 mE

5,350,000 mN

5,348,000 mN

18957
14.38

Shale

Shale

Taconite

Taconite

18965
28.63

Shale

Algal mat

Algal cher

18967
19.02

Taconite

18966
31.8

Taconite

Legend

- JEAN_Outcrops
- Sample # / % Fe — Samples_MI
- July 25 track
- Jean August 3rd Tracks
- August 5th track

Magnetic Declination of 3°7

MAGNETIC

TRUE

N

Mantra Exploration Inc

Date: 2022-10-25	Jean Property Outcrop Geology and Iron Assays Map
Author: pgeo_tims	
Office:	
Drawing:	
Scale: 1:5000	Projection: UTM Zone 15 (NAD 83) MAP 2

0 75 150 300

metres

Appendix 3. Assay Certificate

Quality Analysis ... *Innovative Technologies*

Report No.: **A22-11125**
Report Date: **31-Aug-22**
Date Submitted: **08-Aug-22**
Your Reference: **Mantra Jean**

Northern Mineral Exploration
317
Sillesdale Cres
Thunder Bay ON P7C1S7
Canada

ATTN: Andrew Tims

CERTIFICATE OF ANALYSIS

11 Rock samples were submitted for analysis.

The following analytical package(s) were requested:		Testing Date:
8-Iron Ore Analysis XRF	QOP XRF Fusion (Fusion-XRF)	2022-08-29 13:32:07

REPORT **A22-11125**

Notes:

SCC Accredited LAB LAB Accrédité CCN TM

LabID: 266

CERTIFIED BY:

Elitsa Hrischeva, Ph.D.
Quality Control Coordinator

ACTIVATION LABORATORIES LTD.
41 Bittern Street, Ancaster, Ontario, Canada, L9G 4V5
TELEPHONE +905 648-9611 or +1.888.228.5227 FAX +1.905.648.9613
E-MAIL Ancaster@actlabs.com ACTLABS GROUP WEBSITE www.actlabs.com

Analyte Symbol	SiO2	TiO2	Al2O3	Fe2O3(T)	MnO	MgO	CaO	Na2O	K2O	P2O5	Cr2O3	LOI	V2O5	Total
Unit Symbol	%	%	%	%	%	%	%	%	%	%	%	%	%	%
Lower Limit	0.01	0.01	0.01	0.01	0.01	0.01	0.01	0.01	0.01	0.01	0.01		0.003	0.01
Method Code	FUS-XRF	FUS-XRF	FUS-XRF	FUS-XRF	FUS-XRF	FUS-XRF	FUS-XRF	FUS-XRF	FUS-XRF	FUS-XRF	FUS-XRF	GRAV	FUS-XRF	FUS-XRF
18957	84.27	0.01	0.31	14.38	0.03	0.07	0.05	0.06	0.03	0.02	< 0.01	1.33	< 0.003	100.6
18958	87.65	0.03	0.61	8.03	0.15	0.20	1.24	0.05	0.04	0.01	< 0.01	1.80	0.020	99.82
18959	45.04	0.01	0.18	48.84	0.32	0.12	0.09	0.03	0.01	0.02	< 0.01	4.84	< 0.003	99.51
18960	55.72	0.01	0.42	33.11	0.11	0.63	0.10	0.05	0.02	0.02	< 0.01	8.83	< 0.003	99.03
18961	48.28	0.01	0.23	30.58	0.49	1.76	7.02	0.04	0.02	0.03	< 0.01	12.34	0.004	100.8
18962	68.92	0.01	0.12	23.70	0.09	0.17	0.10	0.05	0.01	0.01	< 0.01	5.47	< 0.003	98.65
18963	56.79	0.01	0.29	39.05	0.06	0.12	0.08	0.04	0.04	0.03	< 0.01	2.38	< 0.003	98.88
18964	64.62	0.01	0.28	26.02	0.08	0.38	0.13	0.04	0.02	0.02	< 0.01	7.88	< 0.003	99.48
18965	61.25	0.02	0.27	28.63	0.10	1.00	0.11	0.04	0.01	0.02	< 0.01	7.12	0.004	98.58
18966	59.81	0.01	0.11	31.80	0.21	0.27	1.62	0.04	0.01	0.01	< 0.01	6.32	< 0.003	100.2
18967	76.65	0.02	0.29	19.02	0.12	0.19	0.09	0.08	0.11	0.05	< 0.01	2.47	0.004	99.08

Analyte Symbol	SiO2	TiO2	Al2O3	Fe2O3(T)	MnO	MgO	CaO	Na2O	K2O	P2O5	Cr2O3	V2O5
Unit Symbol	%	%	%	%	%	%	%	%	%	%	%	%
Lower Limit	0.01	0.01	0.01	0.01	0.01	0.01	0.01	0.01	0.01	0.01	0.01	0.003
Method Code	FUS-XRF	FUS-XRF	FUS-XRF	FUS-XRF	FUS-XRF	FUS-XRF	FUS-XRF	FUS-XRF	FUS-XRF	FUS-XRF	FUS-XRF	FUS-XRF
IF-G Meas	40.54	0.01	0.17	55.13	0.04	1.93	1.59	0.04	0.02	0.07		
IF-G Cert	41.2	0.0140	0.150	55.8	0.0420	1.89	1.55	0.0320	0.0120	0.0630		
BE-N Meas	38.76	2.73	10.57	13.16		12.87	14.22	3.27	1.40	1.10	0.06	0.035
BE-N Cert	38.2	2.61	10.1	12.8		13.1	13.9	3.18	1.39	1.05	0.0500	0.042
GS-N Meas	65.89	0.67	14.37	3.72		2.24	2.49	3.88	4.67	0.29		
GS-N Cert	65.80	0.68	14.67	3.75		2.30	2.50	3.77	4.63	0.28		
KH3 Meas	8.76	0.13	2.52	0.89		0.67	47.92	0.09		0.13		
KH3 Cert	8.59	0.130	2.40	0.870		0.650	47.60	0.100		0.1170		
AMIS 0563 (XRF) Meas	8.47	1.36	0.72	37.87		10.50	21.60			7.54		
AMIS 0563 (XRF) Cert	8.46	1.33	0.76	37.09		10.90	21.08			7.44		
AMIS 0577 (XRF) Meas	99.29	0.03	0.38	0.03	< 0.01	0.04	0.06	0.02	0.13		< 0.01	
AMIS 0577 (XRF) Cert	99.00	0.03	0.44	0.04	0.002	0.03	0.05	0.01	0.14		0.002	
AMIS 0461 (XRF) Meas	9.92	0.06	0.96	0.85		0.84	48.06	0.04	< 0.01		0.37	
AMIS 0461 (XRF) Cert	10.1	0.05	0.80	0.782		0.833	48.31	0.02	0.03		0.378	

NORTHERN MINERAL EXPLORATION SERVICES

Transaction ID: 90307 Date: January 8,2023

Assessment Work Report Number: 5264 **Project**: Jean Property

Date (Y/M/D)	Expense Description	Kms	Cost	Airborne	Assays	Equp Rental	Labour	Subtotal	HST	Total
2022-05-16	Terraquest - deposit			16,215.50				16,215.50	2,108.02	18323.52
2022-07-27	Terraquest - flight costs			19,372.40				19,372.40	2,518.41	21890.81
2022-07-31	Andrew Tims May/July Invoice						1,800.00	1,800.00	234.00	2034.00
2022-08-31	Andrew Tims August Invoice	860	473.00				4,200.00	4,673.00	546.00	5219.00
2022-09-02	Actlabs Thunder Bay				567.05			567.05	73.72	640.77
2022-09-30	Andrew Tims Sept. Invoice						7,200.00	7,200.00	936.00	8136.00
2022-07-29	Terraquest - data processing			7,243.10				7,243.10	941.60	8184.70
2022-07-30	Andrew Tims Oct/Nov Invoice						9,600.00	9,600.00	1,248.00	10848.00
Category Totals:		860	$473.00	$42,831.00	$567.05		$22,800.00	$57,071.05	$7,357.75	$75,276.80
									less advance:	
									Balance:	**$75,276.80**